



**MONTCLAIR STATE**  
UNIVERSITY

Montclair State University  
**Montclair State University Digital  
Commons**

---

Theses, Dissertations and Culminating Projects

---

5-2021

## Effect of Abiotic Factors on Enzyme Activity in Brownfield Soils

Diane Hagmann  
*Montclair State University*

Follow this and additional works at: <https://digitalcommons.montclair.edu/etd>



Part of the [Environmental Sciences Commons](#), and the [Soil Science Commons](#)

---

### Recommended Citation

Hagmann, Diane, "Effect of Abiotic Factors on Enzyme Activity in Brownfield Soils" (2021). *Theses, Dissertations and Culminating Projects*. 711.  
<https://digitalcommons.montclair.edu/etd/711>

This Dissertation is brought to you for free and open access by Montclair State University Digital Commons. It has been accepted for inclusion in Theses, Dissertations and Culminating Projects by an authorized administrator of Montclair State University Digital Commons. For more information, please contact [digitalcommons@montclair.edu](mailto:digitalcommons@montclair.edu).

**Effect of Abiotic Factors on Enzyme Activity in Brownfield Soils**

A DISSERTATION

Submitted to the Faculty of

Montclair State University in partial fulfillment

of the requirements

for the degree of Doctor of Philosophy

by

DIANE HAGMANN

Montclair State University

Upper Montclair, NJ

Spring 2021

Dissertation Chair: Dr. Nina Goodey

MONTCLAIR STATE UNIVERSITY

THE GRADUATE SCHOOL

DISSERTATION APPROVAL

We hereby approve the Dissertation

**Effect of Abiotic Factors on Enzyme Activity in Brownfield Soils**

of

Diane Hagmann

Candidate for the Degree:

Doctor of Philosophy

Graduate Program:  
Environmental Science and Management

Dissertation Committee:

Certified by:

[Redacted Signature]

Dr. Scott Hernes  
Vice Provost for Research and  
Dean of the Graduate School

[Redacted Name]

Dr. Nina Goodey  
Dissertation Chair

[Redacted Name]

Dr. Jennifer A. Krumins

[Redacted Name]

Dr. Michael A. Krueger

[Redacted Name]

Dr. Gregory Pope

[Redacted Name]

Dr. José Luis Gallego

May 6, 2021  
Date

Copyright © 2021 by *Diane Hagmann*. All rights reserved.

**ABSTRACT**

## EFFECT OF ABIOTIC FACTORS ON ENZYME ACTIVITY IN BROWNFIELD SOILS

by Diane Hagmann

Several factors can influence soil function, including biotic and abiotic. Biotic factors are those that are living, like microorganisms. Abiotic factors are those that are non-living, and include heavy metals, organic contaminants, pH, and nutrients. Liberty State Park in Jersey City (N.J., U.S.A), is a 100-ha brownfield was once a major rail yard that was restricted public access in 1969. The site without any intervention of humans grew a forest. The primary objective of this dissertation is to understand the impacts of both inorganic and organic contaminants on soil function in addition to provide strategies that can override the negative impacts of these abiotic factors. Several studies were completed in order to attain the primary objective, which included 1) characterizing both organic and inorganic compounds present in Liberty State Park and understand relationship with soil function, 2) further characterize coal particles that abundant in the soil, 3) provide a potential strategy of improving soil function despite the presence of organic and inorganic contaminants by adding different combinations of artificial root exudates on soil enzymatic activities, 4) understand the influence of a gradient of abiotic factors on both soil function and microbial communities. A variety of elevated heavy metals and organic contaminants derived from fossil fuels, like polycyclic aromatic compounds were present in all studied soils. Within Liberty State Park, soils from several vegetated sites within Liberty State Park (43, 146 and 25F) had higher enzyme activities compared to the barren site 25R, which is below detection limit. Optical microscopy analyses revealed bituminous and anthracite coal, coke, tar/pitch, and ash particles were present in all soil samples. Upon further investigation using density separation, pyrolysis gas chromatography confirmed the majority of coal present

are anthracite and higher rank (medium volatile) bituminous. An inoculation with 25F soil into an experimentally created gradient of 25F and 25R soils provided insights into the barren nature of 25R. Some fungal classes decreased while others increased with increasing amounts of 25R soils. One possible strategy of improving soil function is with the addition of artificial exudates, which included sugars, organic acids, and amino acids. The combination of sugars, organic acids, and amino acids, greatly increased phosphatase, cellobiohydrolase, and L-leucine aminopeptidase activity over time in poorly-functioning, barren soil 25R. Phosphatase fold change was the highest compared to the cellobiohydrolase and L-leucine aminopeptidase when artificial exudates were added. The site provides a unique opportunity to understand the impact of abiotic factors, such as inorganic and organic contaminants in the presence or absence of vegetation on soil health. These data can provide a deeper understanding of the chemistry and biochemistry, which can help to inform future remediation efforts in the public interest. These data can also provide a possible strategy to improve soil function within contaminated brownfield soils.

*Keywords:* brownfield, heavy metals, PAHs, industrial barren, artificial root exudates

### ACKNOWLEDGEMENTS

I would like to thank my advisor, Dr. Nina Goodey, for helping shape me as a scientist. I thank her for her considerable amounts of time she has given me over the course of seven years working with her for both my master's and PhD. I appreciate her kindness and hard working values. I have appreciated the discussions with both Dr. Goodey with my other committee members Dr. Jennifer Krumins and Dr. Michael Kruge. I also have appreciated the valuable discussions with my other committee members Dr. Gregory Pope and Dr. José Luis R. Gallego.

Thank you to the National Science Foundation (NSF CBET 1603741) and the PSEG Institute for Sustainability Studies for providing the support for this study. I would like to thank Dr. Frank Gallagher for facilitating access to Liberty State Park. I would like to also thank Dr. Xiaona Li, the analytical instrumentation specialist at Montclair State University. She has been nice and very helpful with analyzing our samples. I would also like to thank Dr. Kevin Olsen also for helping with the ups and downs of the Pyrolysis-GC-MS. I also appreciate Dr. Olsen's time with safety and instrument training. I would also like to thank Laying Wu, Ph.D., for help using the scanning electron microscope. I am grateful to Dr. Maria Mastalerz of Indiana University for the coal petrology and for her guidance in the interpretation of those results. Thank you to Mike Peters for providing beautiful pictures of Liberty State Park.

I would also like to thank my colleagues and friends including Eshariah Dyson, Bhagyashree Vaidya, Dr. Jay Singh, Matthew Cheung, and Cesar Idrovo. I appreciate the trips we have taken to Liberty State Park. I also appreciate the endless hours of discussions we have about research. I have also appreciated learning new things from them as well. I appreciate my other friends I have made along the way at Montclair including Taylor Wiczerak, Anastasia

Figueroa, Kelly Anderson, Yaritza Acosta to name a few. I have appreciated the off-campus trips, game nights and overall support.

I also appreciate my fiancé Brett Florance for being there through this PhD journey. I appreciate my brother and Dad for their love and support. A big shout out to my Mom for encouraging and supporting me through all this. I could not have come this far without the support and love behind me. Thank you again!

**DEDICATION**

*I dedicate this manuscript to my friends and family,  
especially Brett and my Mom who have been there  
through the ups and downs of this journey*

**CONTENTS**

<b>ABSTRACT .....</b>	<b><i>iv</i></b>
<b>ACKNOWLEDGEMENTS .....</b>	<b><i>vi</i></b>
<b>DEDICATION.....</b>	<b><i>viii</i></b>
<b>LIST OF TABLES .....</b>	<b><i>xi</i></b>
<b>LIST OF FIGURES .....</b>	<b><i>xiii</i></b>
<b>CHAPTER 1 .....</b>	<b>1</b>
<b>INTRODUCTION</b>	
INTRODUCTION .....	1
RESEARCH QUESTIONS AND DISSERTATION STRUCTURE .....	3
REFERENCES .....	5
<b>CHAPTER 2 .....</b>	<b>9</b>
<b>ENVIRONMENTAL FORENSIC CHARACTERIZATION OF FORMER RAIL YARD SOILS LOCATED ADJACENT TO THE STATUE OF LIBERTY IN THE NEW YORK/NEW JERSEY HARBOR</b>	
ABSTRACT .....	9
2.1 INTRODUCTION .....	10
2.2 METHODS .....	13
2.3 RESULTS AND DISCUSSION .....	18
2.4 CONCLUSION .....	33
REFERENCES .....	35
<b>CHAPTER 3 .....</b>	<b>59</b>
<b>CHARACTERIZATION OF COAL PARTICLES IN THE SOIL OF A FORMER RAIL YARD AND URBAN BROWNFIELD: LIBERTY STATE PARK, JERSEY CITY (NJ), USA</b>	
ABSTRACT .....	59

3.1 INTRODUCTION .....	60
3.2 METHODS .....	63
3.3 RESULTS AND DISCUSSION .....	66
3.4 CONCLUSION .....	76
REFERENCES .....	78
<b>CHAPTER 4 .....</b>	<b>96</b>
<b>SOIL MICROBIAL FUNCTION AND COMMUNITY COMPOSITION ALONG AN EXPERIMENTALLY CREATED GRADIENT OF TWO CONTAMINATED SOILS</b>	
ABSTRACT .....	96
4.1 INTRODUCTION .....	97
4.2 METHODS .....	100
4.3 RESULTS AND DISCUSSION.....	104
4.4 CONCLUSION .....	113
REFERENCES .....	114
<b>CHAPTER 5 .....</b>	<b>131</b>
<b>REVITALIZING SOIL FUNCTION THROUGH DIFFERENT COMBINATIONS OF ARTIFICIAL ROOT EXUDATES</b>	
ABSTRACT .....	131
5.1 INTRODUCTION .....	132
5.2 METHODS .....	135
5.3 RESULTS .....	139
5.4 DISCUSSION .....	143
5.5 CONCLUSION .....	147
REFERENCES .....	149
<b>DISSERTATION SUMMARY .....</b>	<b>159</b>
REFERENCES.....	162

**APPENDIX-A .....164**  
**APPENDIX-B .....172**  
**APPENDIX-C .....174**

**LIST OF TABLES**

**Table 2-1.** Organic matter content (% , mean  $\pm$  SE; n = 3), extraction and liquid chromatographic results from HMF, 43, 146, 25F and 25R soils. Fraction 1 contains saturated hydrocarbons; fraction 2 – aromatic compounds and long chain ( $> C_{27}$ ) normal alkanes; fraction 3 – polar compounds. The data show that soil from site 146 has the highest percent organic matter. The LC results show the percentage of the total extract as well as yield per kg of dry soil.

**Table 2-2:** Symbols for peak identification used in Figures 1-7.

**Table 2-3.** Carbon preference index (CPI), odd-even predominance (OEP), pristine/phytane (Pr/Ph), Pr/C17, Ph/C18, and weighted average carbon number of HMF, 43, 146, 25F and 25R.

**Table 3-1.** Pyrolysis-GC-MS peak identification for Figures 8-10.

**Table 3-2.** Dry weight percentages of density fractions separated from whole soil of LSP Sites 43 and 25R. See text and Figure 5 for procedural details.

**Table 4-1.** Concentrations of Cd, Cr, Co, As, Cu, Zn, Pb, and Na (mg/kg) in soil from LSP sites 25F and 25R. Concentrations of soils 100% 25F and 100% 25R were reported in Haggmann et al., 2019. The concentrations of the other soil mixtures (25 % 25R, 50 % 25R, and 75 % 25R) were calculated based on experimentally determined amounts of soils that were mixed and were indicated by †.

**Table 5-1.** Composition of artificial root exudates for high and low diversity treatments. Low and high diversity treatments were comprised of a different number of exudate compounds.

These treatments were applied to soil from LSP site 25R.

## LIST OF FIGURES

**Figure 2-1.** Liberty State Park is located in Jersey City, New Jersey (A). Aerial images from: U. S. Geological Survey: 1954 (B, E) and 2014 (C). Study sites within LSP are indicated on the map (43, 146, 25F, 25R). A historical photograph of 25F and 25R from 1951 (D). Sites 25F and 25R are adjacent; 25R is in a strip of land without vegetation (F). Photo credits: D: Andrew Bologovsky, F: Mike Peters Montclair State University

**Figure 2-2.** Flow chart illustrating the experimental design for the experiment.

**Figure 2-3.** Total ion current (TIC) for Py-GC-MS of soil samples from sites HMF (A), 43 (B), 146 (C), 25F (D) and 25R (E). The data for 25R show predominantly mono- and polycyclic aromatic hydrocarbons and aromatic hydrocarbons. See Table 2-2 for compound symbols.

**Figure 2-4.** Total ion current (TIC) for fraction 1 of soil extracts from sites HMF (A), 43 (B), 146 (C), 25F (D), and 25R (E). The data show distributions of alkanes (normal and isoprenoid alkanes ( $m/z$  71) and triterpenoids ( $m/z$  191). See Table 2-2 for compound symbols.

**Figure 2-5.** Mass chromatogram ( $m/z$  191) showing the distribution of hopanes and tricyclic terpanes in the saturated fractions. The  $\beta$ -amyrin derivative is a soil microbe biomarker that was observed in all sites except for 25R. See Table 2-2 for compound symbols.

**Figure 2-6.** Total ion current (TIC) for fraction 2 of soil extracts from the HMF (A), 43 (B), 146 (C), 25F (D), and 25R (E) sites. The \* indicates the peak was taller in the original chromatogram before the top was cut off to reveal more detail for the shorter peaks. The data show fewer polycyclic aromatic hydrocarbons in HMF. Distributions of aromatic compounds are similar for chromatograms B, C, D, and E. See Table 2-2 for compound symbols.

**Figure 2-7.** Total ion current (TIC) for fraction 3 of soil samples from the HMF (A), 43 (B), 146 (C), 25F (D) and 25R (E). The \* indicates the peak was taller in the original chromatogram before the top was cut off to reveal more detail for the shorter peaks. See Table 2-2 for compound symbols.

**Figure 2-8.** Organic petrographic composition (in volume %) of samples 43, 146, 25F, and 25R. The data show that 25F and 25R have more tar/pitch compared to 43 and 146. HMF soil was not analyzed for organic petrography because coal particles were not visible to the naked eye.

**Figure 2-9.** Examples of photomicrographs of anthropogenic particles identified in the samples. Each sample has two photomicrographs. Reflected light, oil immersion.

**Figure 2-10.** Elements listed in order of atomic weight normalized to HMF. The data is arranged from the lowest to the highest (43, 146, 25F and 25R) average metal concentration. The dotted line present in A. and B. is the background HMF.

**Figure 2-11.** Bacterial density (cells/g dry soil, mean and error bars are SE;  $n = 3$ ) and phosphatase activity ( $\text{pmol} \cdot \text{g}^{-1} \cdot \text{hr}^{-1}$ , mean and error bars are SE;  $n = 3$ ) of HMF, 43, 146, 25F, and 25R soils are shown.

**Figure 3-1.** Index map showing location of Liberty State Park (LSP) in Jersey City (NJ), USA, the principal anthracite coal fields of Pennsylvania, and the former Central Railroad of New Jersey main line. Base map: Google Earth; coalfields: Pennsylvania Dept. of Environmental Protection; rail line: Anderson (1984).

**Figure 3-2.** The Central Railroad of New Jersey's rail yard and marine terminal in Jersey City as it appeared in a 1954 aerial image, overprinted with the location of the two soil samples (25R, 43) presented in this study. At the time of the photograph, coal transport operations were largely confined to the zone seen in the lower part of the image, on the tracks leading to Pier 18. Note the locations of the passenger terminal and roundhouse. Base image: U.S. Geological Survey; identification of coal handling facilities: Anderson (1984); pier identification: Brooklyn Historical Society Archives.

**Figure 3-3.** Historical images of CRRNJ coal transport operations in the 1940's. (A) Loaded coal trains in Jim Thorpe, Pennsylvania (Fig. 1; town formerly known as Mauch Chunk). (B) Loaded coal cars approach Pier 18 in the Jersey City rail yard. View to the west showing the yard's track network (Fig. 2). (C) View of Pier 18's two coal dumping towers for transfer of coal from railcar to barge. View is to the west from the eastern end of the pier. (D) View to the

northeast of Pier 18's coal dumpers. Note Ellis Island in the background. Photos: Anderson (1984); used with permission.

**Figure 3-4.** Appearance of Liberty State Park in 2017. (A) Aerial view towards the southwest showing the study area within the park. Note the former passenger rail and ferry terminal, partially restored but non-functioning, and the Liberty Science Center museum, built on the site of the former railroad roundhouse (Fig. 2). Photo: D. Haggmann. (B, C) Dense vegetation covers most of the study area. The top of the Liberty Science Center tower appears in C. (D) Soil sample 25R was collected from this anomalously barren strip within the study area. Photos B-D: M. Peters, Montclair State Univ.; used with permission.

**Figure 3-5.** Experimental flow chart. See section 2 for details. No vegetation detritus was picked from site 25R soil. \* < 2 mm size fraction previously studied in detail (Haggmann et al., 2019).

**Figure 3-6.** Scanning electron micrograph of fragments of a single wet-sieved (> 2 mm) and sonicated LSP 43 coal particle. Note surface encrustations. Scale bar is 300  $\mu\text{m}$ .

**Figure 3-7.** SEM EDS mapping images of a fragment of a single wet-sieved (>2 mm) and sonicated LSP 43 coal particle. Scale bars are 50  $\mu\text{m}$ . (A) SEM image; box shows element mapping area for B-D. (B) Multi-element map (O, Fe, S, Cl, Si, Al) superimposed on SEM image. (C) Element map for aluminum. (D) Element map for silicon. Element mapping images indicate clay mineral platelets adhering to coal.

**Figure 3-8.** Py-GC-MS total ion current chromatograms of materials from the site 43 soil sample: (A) typical soil organic matter (roots & twigs) and (B, C) two coal particles hand-picked from the >2 mm size fraction after wet sieving and sonication. See Table 3-1 for peak identification.

**Figure 3-9.** Py-GC-MS total ion current chromatograms. Forested LSP site 43: (A) whole soil, (B) Fraction 1 floated in DI water, (C) Fraction 2 floated in KI<sub>aq</sub> (1.6 g/mL), and (D) Fraction 3 sank in KI<sub>aq</sub> (1.6 g/mL). See Table 3-1 for peak identification.

**Figure 3-10.** Py-GC-MS total ion current chromatograms. Barren LSP site 25R: (A) whole soil, (B) Fraction 1 floated in DI water, (C) Fraction 2 floated in KI<sub>aq</sub> (1.6 g/mL), and (D) Fraction 3 sank in KI<sub>aq</sub> (1.6 g/mL). See Table 3-1 for peak identification.

**Figure 4-1.** Experimental design for the inoculation of 25F soils into an experimentally created gradient of different soil mixtures. Soil mixtures included 0 % 25R, 25 % 25R, 50 % 25R, 75 % 25R, and 100 % 25R. The non-inoculated treatment were autoclaved soil mixtures with 5 % autoclaved 25F soil. The inoculated treatment were autoclaved soil mixtures that were inoculated with 25F soil. Fresh soils were non-autoclaved 0 % 25R and 100 % 25R soils.

**Figure 4-2.** Moisture (A) and organic matter (B) percentages (w/w) of fresh soils (non-autoclaved) from sites 25F and 25R. Soil samples collected from 25F had higher percentages of

moisture and organic matter. Bars represent the average of five replicates ( $n = 5$ ) with standard errors shown.

**Figure 4-3.** Moisture (A) and organic matter (B) of different percent ratio (w/w) of soils 25F and 25R for non-inoculated (dark gray) and inoculated (light gray) soils after 67 days in a growth chamber. No statistically significant differences in moisture or organic matter were found between non-inoculated and inoculated soils. Increasing percent ratios (w/w) of 25R soil corresponded to decreased percent moisture and organic matter. Bars represent the averages of five replicates ( $n = 5$ ) with standard errors shown. Letters (a-e) over bars indicate significant differences among the means of the different soil mixtures (Tukey test,  $p < 0.05$ ).

**Figure 4-4.** NMDS of fungal genus (A) and bacterial genus (B) across the different treatments (non-inoculated, inoculated and fresh soil). Both soil mixtures and treatments (non-inoculated, inoculated and fresh soils) had a significant impact on fungal and bacterial communities.

**Figure 4-5.** Relative abundances of the top 15 fungal classes (A) and bacterial classes (B) across different soil mixtures for non-inoculated, inoculated and fresh soils.

**Figure 4-6.** Correlations of relative abundance of fungal classes Mortierellomycetes (A) and Sordariomycetes (B) across the ratios of soil mixtures containing increasing percent ratios (w/w) of 25R soil for inoculated soils. There was a significant negative relationship between the relative abundance of Mortierellomycetes and the percent ratio (w/w) of soil mixtures (A) ( $r = -0.976$ ,  $p < 0.01$ , Pearson). There was significant positive relationship between the relative

abundance of Sordariomycetes and the ratios of soil mixtures (B) with increasing amounts of 25R ( $r = 1$ ,  $p < 0.05$ , Spearman).

**Figure 4-7.** Relationship between enzyme activities with the increasing percent ratios (w/w) of 25R soils (0 %, 25 %, 50 %, 75 %, and 100% 25R), for both non-inoculated and inoculated treatments after incubation for 67 days in a growth chamber. The data were fitted to a Linear equation. Phosphatase (A, B), cellobiohydrolase (C, D) and peroxidase (E, F) activities are shown. Phosphatase and cellobiohydrolase activities decreased with increasing percent ratios (w/w) of 25R soil for both non-inoculated and inoculated soils for phosphatase and cellobiohydrolase activities. Peroxidase activity did not decrease with increasing percent ratios (w/w) of 25R soil. However, peroxidase activity did not decrease with increasing percent ratios (w/w) of 25R soil for the non-inoculated soil. The error bars indicate the standard errors with a minimum of 3 replicates ( $n = 3$ ).

**Figure 5-1.** Enzyme activity fold changes of LSP 25R soil are shown for each artificial exudate combinations for phosphatase (A), cellobiohydrolase (B), and L-leucine aminopeptidase (C). The values shown represent the averages of five time points. The data are shown for seven different exudate combinations, (S-, O-, A-, S-O, O-A, S-A, S-O-A). Bars represent the averages of four replicates ( $n=4$ ) with standard errors shown. Significant differences among the means are indicated by letters (Tukey test,  $p < 0.05$ ).

**Figure 5-2.** Effect of low and high diversity treatments added to 25R soil on phosphatase activity ( $\mu\text{mol}\cdot\text{g}^{-1}\cdot\text{hr}^{-1}$ ) for four different combinations of artificial exudates (S-O, O-A, S-A, and

S-O-A) averaged over two times points (30 and 60 days). Dark grey and white bars represent low and high diversity treatments respectively. The difference between phosphatase activities where the soil was treated with low and high diversity treatments were not significant. Bars represent the average of three replicates ( $n = 3$ ) of each enzyme activity with standard errors shown.

## Chapter 1

### Introduction

Both biotic and abiotic factors can impact soil function. Biotic factors are living things like microorganisms, while abiotic factors are non-living factors such as heavy metals, organic contaminants, pH, soil texture, and nutrients. Previous studies have found correlations between soil extracellular enzyme activity and abiotic factors, including soil texture (Sinsabaugh et al., 2008; Šnajdr et al., 2008; Sinsabaugh et al., 2010; Alvarez & Lavado, 1998). Extracellular enzymes can be excreted into the soil by bacteria, fungi and plants (Gadd, 2007; Criquet & Farnet, 2004). Soil microorganisms including bacteria and fungi are important, because it reflects the ability of the soil to degrade organic matter that will provide essential nutrients for vegetation (Sinsabaugh & Follstad, 2012, Haider and Schäffer, 2009).

Extracellular enzymes are involved in the breakdown of different molecules, like cellulose, starch, polypeptides and lignin (Sinsabaugh et al., 2008; Henry et al., 2013; Allison et al., 2007, Jian et al., 2016, Skujiņš, J., & Burns, 1976; Weedon et al., 2014). Measuring phosphatase, cellobiohydrolase and L-leucine aminopeptidase activities serves as proxy measures for nutrient cycling. For example, phosphatase catalyzes the hydrolysis of ester-phosphate bonds found in nucleic acids, phospholipids and other phosphates to yield inorganic phosphate (Jian et al., 2016; Nannipieri et al., 2011; Sinsabaugh et al., 2008). Cellobiohydrolase activity measures the hydrolytic enzyme,  $\beta$ -d-cellobiosidase that is produced by soil microbes, which catalyzes the decomposition of polysaccharides, specifically cellobiose to glucose (Deng & Tabatabai, 1994, Sinsabaugh et al., 2008). L-leucine aminopeptidase hydrolyzes amino acids from the N-terminus (Sinsabaugh et al., 2008). Peroxidase activity is an example of an oxidative enzyme involved in

lignin degradation that use a secondary oxidant, such as  $H_2O_2$ , to degrade aromatic compounds (Sinsabaugh et al., 2010).

Understanding the factors that influence enzyme activity, especially in contaminated soils, is important because it provides understanding of the fundamental chemistry, biochemistry and ecology of these sites. In contaminated soils, the interactions between biotic and abiotic properties of the soil are complex (Krumins et al., 2015). Negative impacts on soil health and function can result from the presence of both heavy metals and organic contaminants (Thavamani et al., 2012; Shen et al., 2005). Such contaminants can decrease soil function and alter the microbial community composition (Alisi et al., 2009b; Buettner and Valentine, 2011a; Hamdi et al., 2007b; Sprocati et al., 2012a). Change in soil function can lead to an alteration of enzyme activity (Baran et al., 2004; Shen et al., 2005). Contaminated soils can even become inhospitable to plant growth if concentrations reach above certain limits (Wong et al., 2006).

Industrial activity can introduce a variety of heavy metals and organic contaminants into soils. Some typical industrial activities that introduce contaminants include mining, smelting, and sewage sludge disposal, as well as activities within rail yards, manufactured gas plants, and petrol stations (Shen et al., 2005, Thavamani et al., 2012; Wang et al., 2008). Parcels of land with high levels of heavy metal and organic contaminants introduced from anthropogenic activities are prevalent across the globe and are referred to as brownfields. According to the U.S. Environmental Protection Agency (EPA), a brownfield is defined as a “property... which may be complicated by the presence or potential presence of a hazardous substance, pollutant, or contaminant” (EPA, 2020). Within the United States there are approximately 450,000 brownfields, with a large number located in New Jersey (EPA, 2020). The contaminants introduced from industrial activity can impede growth of vegetation in these areas and can also

have detrimental impacts on human health. Both inorganic and organic contaminants, such as heavy metals and polycyclic aromatic compounds, are persistent in soils. Additionally, these contaminants can travel to nearby water systems through natural processes such as run off from rain, and negatively impact ecosystem health (Arditsoglou & Samara, 2005; Zota et al., 2009). Thus, characterizing the contaminants present in soils that were once areas of industrial activity is important to promote positive environmental and human health outcomes.

### **RESEARCH QUESTIONS AND DISSERTATION STRUCTURE**

Liberty State Park (LSP) will be used as a case study throughout this dissertation (Chapters 2-5). LSP, located in Jersey City in Northern New Jersey, was an abandoned rail yard, and has been undisturbed by humans since it was abandoned in 1969. The historical use of LSP is discussed in greater detail in Chapters 2 and 3. A forest grew within the 100-ha plot in the core of LSP, despite known levels of heavy metal/loids. The organic contaminants present in LSP have yet to be elucidated. The sites within LSP investigated in this dissertation include several vegetated sites (43, 146, and 25F) and one site barren of vegetation (25R). The vegetated site 25F is adjacent to barren site 25R.

The overall goal of this dissertation work was to understand the impacts of both abiotic properties on soil function and to investigate strategies that can override the negative impacts of these abiotic factors, with aims to meet the following objectives:

**Objective 1:** To characterize both organic and inorganic compounds present in the soils of several sites within LSP. To compare these results to an uncontaminated reference site to identify

compounds that originated from industrial activity at the rail yard. Also, to identify differences between a barren site (25R) and a vegetated site (25F) that are adjacent to each other within LSP.

**Objective 2:** To characterize anthracite and bituminous coals that are abundant in LSP using a simple floatation method to isolate soil organic matter and various coal types.

**Objective 3:** To determine if the inoculation of 25F soil into an experimentally created gradient of two contaminated soils would shift the microbial communities and if abiotic or biotic factors would serve as primary drivers of soil function.

**Objective 4:** To determine if adding different combinations of artificial exudates (sugars, organic acids and amino acids) is a possible strategy to improve soil function of a poorly-functioning, barren soil, such as LSP 25R.

This dissertation was written as a series of individual manuscripts. The second chapter reports the organic and inorganic compounds present in different sites of an urban brownfield in northern New Jersey, Liberty State Park. The third chapter reports a further investigation of the coal that is present in the brownfield to broaden our understanding of the fossil fuel biomarkers. The fourth chapter reports a possible strategy to revitalize a poorly-function soil from LSP through the additions of different combinations of artificial root exudates. The fifth chapter reports studies on the mechanisms by which the abiotic factors within a gradient of soils influence both microbial communities and soil function.

### References

- Alisi, C., Musella, R., Tasso, F., Ubaldi, C., Manzo, S., Cremisini, C., & Sprocati, A. R. (2009). Bioremediation of diesel oil in a co-contaminated soil by bioaugmentation with a microbial formula tailored with native strains selected for heavy metals resistance. *Science of the Total Environment*, 407(8), 3024-3032.
- Allison V.J., Condron L.M., Peltzer D.A., Richardson S.J., Turner B.L., 2007. Changes in enzyme activities and soil microbial community composition along carbon and nutrient gradients at the Franz Josef chronosequence, New Zealand. *Soil Biology and Biochemistry*; 39: 1770-1781.
- Alvarez, R., & Lavado, R. S. (1998). Climate, organic matter and clay content relationships in the Pampa and Chaco soils, Argentina. *Geoderma*, 83(1-2), 127-141.
- Arditsoglou, A., & Samara, C. (2005). Levels of total suspended particulate matter and major trace elements in Kosovo: a source identification and apportionment study. *Chemosphere*, 59(5), 669-678.
- Baran, S., Bielińska, J. E., & Oleszczuk, P. (2004). Enzymatic activity in an airfield soil polluted with polycyclic aromatic hydrocarbons. *Geoderma*, 118(3-4), 221-232.
- Buettner, K. M., & Valentine, A. M. (2012). Bioinorganic chemistry of titanium. *Chemical Reviews*, 112(3), 1863-1881.
- Cuny, D., Denayer, F. O., de Foucault, B., Schumacker, R., Colein, P., & Van Haluwyn, C. (2004). Patterns of metal soil contamination and changes in terrestrial cryptogamic communities. *Environmental Pollution*, 129(2), 289-297.
- Deng, S. P., & Tabatabai, M. A. (1994). Cellulase activity of soils. *Soil Biology and Biochemistry*, 26(10), 1347-1354.

- Hamdi, H., Benzarti, S., Manusadžianas, L., Aoyama, I., & Jedidi, N. (2007). Bioaugmentation and biostimulation effects on PAH dissipation and soil ecotoxicity under controlled conditions. *Soil Biology and Biochemistry*, 39(8), 1926-1935.
- Henry, H. A. (2013). Reprint of "Soil extracellular enzyme dynamics in a changing climate". *Soil Biology and Biochemistry*, 56, 53-59.
- Jian S., Li J., Chen J., Wang G., Mayes M.A., Dzantor K.E., et al., 2016. Soil extracellular enzyme activities, soil carbon and nitrogen storage under nitrogen fertilization: A meta-analysis. *Soil Biology and Biochemistry*; 101: 32-43.
- Krumins, J. A., Goodey, N. M., & Gallagher, F. (2015). Plant–soil interactions in metal contaminated soils. *Soil Biology and Biochemistry*, 80, 224-231.
- Nannipieri P., Giagnoni L., Landi L., Renella G., 2011. Role of Phosphatase Enzymes in Soil. In: Bünemann E, Oberson A, Frossard E, editors. Phosphorus in Action: Biological Processes in Soil Phosphorus Cycling. Springer Berlin Heidelberg, Berlin, Heidelberg, pp. 215-243.
- Shen, G., Lu, Y., Zhou, Q., & Hong, J. (2005). Interaction of polycyclic aromatic hydrocarbons and heavy metals on soil enzyme. *Chemosphere*, 61(8), 1175-1182.
- Singh, J. P., Ojinnaka, E. U., Krumins, J. A., & Goodey, N. M. (2019). Abiotic factors determine functional outcomes of microbial inoculation of soils from a metal contaminated brownfield. *Ecotoxicology and environmental safety*, 168, 450-456.
- Sinsabaugh, R. L., Lauber, C. L., Weintraub, M. N., Ahmed, B., Allison, S. D., Crenshaw, C., Contosta, A.R., Cusack, D., Frey, S., Gallo, M.E., Gartner, T.B., Hobbie, S.E., Holland, K., Keeler, B.L., Powers, J.S., Stursova, M., Takacs-Vesbach, C., Waldrop, M.P.,

- Wallenstein, M.D., Zeglin, L.H. (2008). Stoichiometry of soil enzyme activity at global scale. *Ecology letters*, 11(11), 1252-1264.
- Sinsabaugh, R. L. (2010). Phenol oxidase, peroxidase and organic matter dynamics of soil. *Soil Biology and Biochemistry*, 42(3), 391-404.
- Skujiņš, J., & Burns, R. G. (1976). Extracellular enzymes in soil. *CRC critical reviews in microbiology*, 4(4), 383-421.
- Šnajdr, J., Valášková, V., Merhautová, V., Herinková, J., Cajthaml, T., & Baldrian, P. (2008). Spatial variability of enzyme activities and microbial biomass in the upper layers of *Quercus petraea* forest soil. *Soil Biology and Biochemistry*, 40(9), 2068-2075.
- Thavamani, P., Malik, S., Beer, M., Megharaj, M., & Naidu, R. (2012). Microbial activity and diversity in long-term mixed contaminated soils with respect to polyaromatic hydrocarbons and heavy metals. *Journal of Environmental Management*, 99, 10-17.
- Wang, X., Chen, T., Ge, Y., & Jia, Y. (2008). Studies on land application of sewage sludge and its limiting factors. *Journal of Hazardous Materials*, 160(2-3), 554-558.
- Weedon, J. T., Aerts, R., Kowalchuk, G. A., & van Bodegom, P. M. (2014). No effects of experimental warming but contrasting seasonal patterns for soil peptidase and glycosidase enzymes in a sub-arctic peat bog. *Biogeochemistry*, 117(1), 55-66.
- Wong, C. S., Li, X., & Thornton, I. (2006). Urban environmental geochemistry of trace metals. *Environmental pollution*, 142(1), 1-16.

United States Environmental Protection Agency (EPA). (2020). Overview of EPA's Brownfields Program. Retrieved from <https://www.epa.gov/brownfields/overview-epas-brownfields-program>

Zota, A. R., Willis, R., Jim, R., Norris, G. A., Shine, J. P., Duvall, R. M., Schaidler, L.A., Spengler, J. D. (2009). Impact of mine waste on airborne respirable particulates in northeastern Oklahoma, United States. *Journal of the Air & Waste Management Association*, 59(11), 1347-1357.

## Chapter 2

### **Environmental forensic characterization of former rail yard soils located adjacent to the Statue of Liberty in the New York/New Jersey harbor**

Published as: Hagmann D.F., Kruge M.A., Cheung M., Mastalerz M., Gallego J.L.R., Singh J.P., Krumins J.A., Li X., Goodey N. (2019) Environmental forensic characterization of former rail yard soils located adjacent to the Statue of Liberty in the New York/New Jersey harbor. *Science of the Total Environment* 690:1019-1034. <https://doi.org/10.1016/j.scitotenv.2019.06.495>

#### **Abstract**

Identifying inorganic and organic soil contaminants in urban brownfields can give insights into the adverse effects of industrial activities on soil function, ecological health, and environmental quality. Liberty State Park in Jersey City (N.J., USA) once supported a major rail yard that had dock facilities for both cargo and passenger service; it was later closed off to the public, and a forest developed and spread in the area. The objectives of this study were to: 1) characterize the organic and inorganic compounds in Liberty State Park soils and compare the findings to an uncontaminated reference site (Hutcheson Memorial Forest); and 2) identify differences between the barren low-functioning areas and the forested high-functioning areas of the brownfield. Soil samples were solvent-extracted, fractionated, and analyzed by gas chromatography-mass spectrometry and subjected to loss-on-ignition, pyrolysis-gas chromatography-mass spectrometry, inductively-coupled-plasma mass spectrometry, and optical microscopy analyses. Compared to soil from the reference site, the forested soils in Liberty State Park contained elevated percentages of organic matter (30–45 %) and more contaminants, such as fossil-fuel-derived hydrocarbons and coal particles. Microscopy revealed bituminous and anthracite coal,

coke, tar/pitch, and ash particles. Barren and low-functioning site 25R had a similar organic contaminant profile but contained a higher metal load than other Liberty State Park sites and also lacked higher plant indicators. These can obscure the signatures of contaminants, and data from adjacent barren and vegetated sites are valuable references for soils studies. A deeper understanding of the chemistry, biochemistry, and ecology of barren soils can be leveraged to prevent desertification and land degradation and to restore dysfunctional and phytotoxic soils.

**Keywords:** Brownfield, heavy metals, polycyclic aromatic hydrocarbons, soil forensics, pyrolysis-GC-MS, petrography, industrial barrens

## 2.1. Introduction

Past industries have altered ecosystems by introducing inorganic and organic contaminants into soils (Alker et al., 2000; Gallego et al., 2016; Qian et al., 2017; Thornton et al., 2008).

Specifically, former rail yard soils remain contaminated years after operations have ceased (Jackson, 1997). Loading, unloading, and the train engines themselves can introduce both inorganic compounds such as heavy metals and organic contaminants including polycyclic aromatic hydrocarbons (PAHs) into the soil (Jackson, 1997; Lacey and Cole, 2003; Liu et al., 2008; Malawska and Wilkomirski, 1999; Malawska and Wilkomirski, 2000; Malawska and Wiołkomirski, 2001; Wilkomirski et al., 2011). Organic contaminants can originate from lubricating oils, coal, oil, fertilizers and herbicides (Biache et al., 2017; Wilkomirski et al., 2011). PAHs, many of which are toxic or mutagenic to humans, plants, and animals, (Brooks, 2004; Smith et al., 2006) can originate from incomplete combustion of coal (Haritash and Kaushik, 2009).

Liberty State Park (LSP) in Jersey City, New Jersey is located across the Hudson River from lower Manhattan and the Statue of Liberty and once supported a rail yard (Fig. 1-1A). Originally, LSP consisted of mudflats and salt marsh but was later filled in with New York City construction debris and municipal waste to prepare for the construction of the Central Railroad of New Jersey. The railroad was built between 1860 and 1919, operated until 1967, and was closed in 1970 (Gallagher et al., 2008a). Part of LSP was remediated but a 100-ha un-remediated site, our study area, was fenced to restrict public access. Despite its history of contamination, most areas within our un-remediated study site support a biodiverse and productive forest (Gallagher et al., 2008a). Figure 2-1C shows the locations of our sites within the study area (43, 146, and 25). The organic compounds at LSP had not been previously analysed but coal fragments are visible throughout the site.

We previously discovered high enzyme activities at LSP site 146, which has high heavy metal loads (Hagmann et al., 2015). This finding was surprising because heavy metal and organic contaminants are often thought to decrease soil microbial functioning (Alisi et al., 2009a; Buettner and Valentine, 2011b; Hamdi et al., 2007a; Sprocati et al., 2012b). Because organic contaminants can play a role in soil functioning (Baran et al., 2004; Shen et al., 2005) and display additive effects in combination with heavy metals (Maliszewska-Kordybach and Smreczak, 2003; Shen et al., 2005), we identified organic contaminants at different sites within LSP that might lead to differences in enzymatic activities. It is important to study both inorganic and organic compounds to understand historic industrial activities (Ortiz et al., 2016a).

#### Figure 2-1

The use of pyrolysis gas chromatography – mass spectrometry (Py-GC-MS) is only beginning to see wide application in characterization of brownfield contaminants (Krüge, 2015;

Kruger et al., 2018; Lara-Gonzalo et al., 2015). Here we studied LSP soils via Py-GC-MS and GC-MS combined with organic petrography and determination of soil enzyme activities, major and trace elements, total organic matter, and microbial counts. This unique combination of methods, including the concurrent identification of organic and inorganic pollution with measurements of enzymatic function and microbial counts, provides a multidimensional understanding of the contaminants in LSP soils.

Sites were chosen in LSP and at the reference site at Hutcheson Memorial Forest (HMF). HMF is a non-contaminated site located Franklin Township, New Jersey, which was primarily agricultural and then established as a nature preserve and research station administered by Rutgers University. Comparing LSP and HMF, which are both located within the piedmont region of New Jersey, would allow us to answer questions about the impact of industrial activities and vegetation on organic contaminant profiles in the soils. Soils were characterized at four sites (43, 146, 25F, and 25R) within the un-remediated and closed-off LSP area. Our first hypothesis was that there will be more fossil fuel biomarkers at LSP compared to HMF. According to historic photographs shown in Figure 2-1B, sites 43 and 146 lie along tracks to a coal pier while sites 25F and 25R are located next to each other and along the route to “Pier 11” (Fig. 2-1D). All LSP sites have a history of industrial contamination while the reference site HMF does not. Site 25R lacks plants while the other three LSP sites (43, 146, and 25F) and reference site are vegetated. Our second hypothesis was that the barren site 25R will have more or different contaminants compared to the forested sites at LSP. Our two primary objectives were to: 1.) characterize the organic and inorganic compounds at LSP and compare the findings to a reference site HMF; and 2.) identify differences between the barren site 25R (area with no vegetation) and forested areas at LSP.

## 2.2 Methods

### 2.2.1 Site description

Soil samples were collected from four sites located within an un-remediated, restricted-access, 100-ha plot within LSP, Jersey City, NJ, USA (40° 42' 16 N, 74° 03' 06 W, Fig. 2-1A, B). LSP was formerly a major rail yard and dock facility built on estuarine marshland and was abandoned around 1969 (Gallagher et al., 2008a). In the intervening decades, dense forest cover took over the restricted access plot without human intervention.

Soils for this study were collected from three different vegetated sites within LSP, including 43, 146, and 25F (Fig. 2-1C). A fourth site—25R that is adjacent to 25F—is from a strip of land that remains anomalously barren (Fig. 2-1F). As a reference, soil was also collected from a location within HMF in Franklin Township, N.J.—an abandoned agricultural field with no history of industrial use or contamination about 60 km southwest of LSP—having the same natural successional timeframe.

### 2.2.2 Soil collection and preparation

Soil was collected in July 2016 from LSP sites 25F, 25R, 43, and 146 as well as the reference site HMF. For this study, five samples were collected along a transect at intervals of 4 m for this study into separate bags (depth of 10 cm below the leaf-litter). The samples were stored in a refrigerator (4 °C). At the lab the soils were sieved through a 2-mm sieve and equal amounts of the five samples along a transect were combined into one bag labelled with the transect name and site (e.g., 43A). At each site, five samples were collected along three parallel transects 10 m apart. Thus, fifteen soil subsamples from a 16 by 20 m field grid were combined into three composite samples (one for each transect), as seen in Figure 2-2. For each site, the three

composites samples were submitted separately for laboratory analysis. Figure 2-2 shows an overview of the experimental procedures we used to determine the organic composition of the soils as described in sections 2.4 and 2.5.

Figure 2-2

### 2.2.3 Percent organic matter

The percent organic matter was determined by loss on ignition (LOI). This procedure is described in Hagmann et al. 2015. Briefly, soil was dried at 70°C for 24 hours. The soil was ground using a mortar and pestle and samples were heated to 550°C for 4 hours. The percent organic matter was determined gravimetrically. Results are presented as the mean values of the three composite soil samples taken at each site.

### 2.2.4 Extraction, LC fractionation and GC-MS

For each site, only one analysis was performed, on a global sample combining each of the three transect composites (Section 2.2) in equal measure. Dry soil samples < 2 mm (0.009 - 0.08 g<sub>dry</sub>) underwent solvent extraction as described in Lara-Gonzalo et al. 2015. Briefly, soils were extracted using dichloromethane:methanol (3:1, v/v) in a Soxtherm system (Gerhardt analytical systems: Königswinter, Germany). The extract was concentrated by rotary evaporation. Aliquots of the Soxtherm extract were fractionated and gravimetrically quantified by open column liquid chromatography (LC). First, maltenes and asphaltenes were separated by filtering through 0.45 µm filters using hexane and dichloromethane, respectively; then, maltenes were fractionated into three fractions by LC in columns filled with silica gel and alumina. Fraction 1 (predominantly aliphatic hydrocarbons) was eluted with hexane, Fraction 2 (predominantly aromatic

hydrocarbons) with a mix of dichloromethane:hexane (7:3, v/v) and finally, Fraction 3 (predominantly polar compounds) with dichloromethane:methanol (1:1, v/v).

The analysis of the LC fractions was carried out by GC/MS. The injection of the extracts was performed on a GC/MS QP-2010 Plus (Shimadzu: Kyoto, Japan). A capillary column DB-5ms (5% phenyl 95% dimethylpolysiloxane; 60 m × 0.25 mm i.d. × 0.25 μm film) from Agilent Technologies was used with helium as carried gas at 1 mL/min. The initial oven temperature was 50 °C (held for 2 min) and ramped at 2.5 °C min<sup>-1</sup> up to 310 °C and held for 45 min. The mass spectrometer was operated in electron ionization mode (EI) at 70 eV. It was calibrated daily by autotuning with perfluorotributylamine (PFTBA) and the chromatograms were acquired in full-scan mode (mass range acquisition was performed from 45 to 500 m/z). Compounds were identified using the NIST 2014 Mass Spectral Library (NIST 2014/EPA/NIH) and by reference to the literature.

#### 2.2.5 Pyrolysis-Gas Chromatography-Mass Spectrometry (Py-GC-MS)

For samples HMF, LSP 43, and LSP 146, Py-GC-MS was performed using a CDS Analytical 5000 Pyroprobe (Pennsylvania, USA) coupled to a Thermo Electron DSQ GC/MS (Texas, USA) equipped with an Agilent DB-1MS column (30 m × 0.25 mm i.d. × 0.25 μm film thickness). The GC oven temperature was programmed from 50 °C to 300 °C (at 5 °C min<sup>-1</sup>), with an initial hold of 5 min at 50 °C and a final hold of 15 min at 300 °C. Pyrolysis was performed for 20 s at 610 °C. The MS was operated in full scan mode (50-500 Da, 1.08 scans s<sup>-1</sup>). Quality control was performed by separately analyzing the three composited samples from each site (Section 2.2). For each site, the three yielded very similar results; therefore, only one was used to represent the

site in this paper. Compounds were identified using the NIST MS library and by reference to the literature.

### 2.2.6 Organic petrography

For petrographic analysis, soil samples were mixed with Lucite powder and prepared into pellets in a Leco PR-15 mounting press. A GPX200 grinder/polisher was used to polish the samples according to the standard sample preparation techniques (Taylor et al., 1998). A reflected light microscope Leica DM 2500P linked to a TIDAS PMT IV photometric system was used to determine petrographic composition of the samples by counting 500 points, and the results were recalculated into volume percent. Representative photomicrographs were taken of each sample using the same microscope. Coal, coke, tar and pitch, fly ash/bottom ash, sediments, and other materials were the petrographic categories counted, and each category included several components identified based on their optical characteristics.

### 2.2.7 Elemental analysis

The concentrations of selected elements were determined using a Thermo iCAP Qc inductively coupled plasma mass spectrometry (ICP-MS, Thermo Fisher Scientific, Bremen, Germany). The soil was extracted following EPA method 3050B, which is described in Haggmann et al. (2015). Briefly, 5 mL of 50% HNO<sub>3</sub> was added to a 0.5 g homogenized sample. The solution was heated to 95 ± 5 °C for 15 minutes. After the sample cooled down, 2.5 mL of concentrated HNO<sub>3</sub> was added to the solution and the sample was heated 95 ± 5 °C for 30 minutes. This step was repeated if brown fumes were present. Afterwards, the sample remained at 95 ± 5 °C until the volume was reduced to approximately 2.5 mL. DI (1mL) water was then added to the solution

and drops of 30 % H<sub>2</sub>O<sub>2</sub> (1.5 mL) were added. Further amounts of 30% H<sub>2</sub>O<sub>2</sub> were added until effervescence was minimal. The sample remained at 95 ± 5 °C until the volume dropped to 2.5 mL. The volume was brought up to 50 mL with DI water. The solution was then filtered through a 1 µm filter. Each sample was further diluted to run on the ICP-MS. Samples were diluted to at least 20 times to minimize the matrix effect. An aqueous standard curve was prepared for Li, Mg, Al, P, K, Ca, Sc, V, Cr, Mn, Co, Ni, Cu, Zn, As, Mo, Ag, Cd, Ba and Pb from a stock solution.

#### 2.2.8 Acridine orange direct count (AODC)

Bacterial cell density was measured using epifluorescence microscopy after staining the soil suspensions with acridine orange. Briefly, soil samples were suspended in phosphate buffered saline (PBS) (0.0088 M Na<sub>2</sub>HPO<sub>4</sub>, 0.0013 M NaH<sub>2</sub>PO<sub>4</sub> • H<sub>2</sub>O, 0.15 M NaCl; pH 7.6) and fixed in formalin. The fixed samples were then serially diluted in PBS with a final dilution of 10<sup>-3</sup>. The diluted samples were then stained with 0.1 % acridine orange and transferred on a black polycarbonate 0.2 µm Isopore™ membrane filter (Millipore, Waltham, M.A.) and observed under an epifluorescence microscope with a 100X objective lens (Nikon eclipse Ti-S) (Hobbie et al. 1977, Krumins et al. 2009).

#### 2.2.9 Phosphatase assay

Phosphatase enzyme activity was measured for soil from each site as described in Hagmann et al. 2015. Briefly, moist soil (0.1 g) was added to 100 mL of 0.1 M MES buffer (pH 6.0) and then sonicated for 3 min at 25W. The slurry was stirred continuously, and each sample was added to the well (160 µL). 4-MUB-phosphate was added (40 µL) to three different wells (350 µM in the

well). The concentration was determined by preparing a standard curve using different concentrations of 4-MUB (0, 500, 1000, 1500 and 2500 pmols). Time points were collected on a microplate reader at 30 °C every 20 minutes for 6 hours to measure fluorescence intensity (320 nm ex./450 nm em.).

## 2.3. Results and discussion

### 2.3.1. Bulk organic matter content

The soil from the reference site HMF has an organic matter content of 7.4 % (by LOI), similar to typical forested soils in New Jersey (Table 2-1) (Osman, 2013). It should be noted that the solvent extraction were conducted on soil particles that were less than 2 mm in diameter. In contrast, forested LSP sites 43, 146, and 25F are unusually enriched in organic matter (30 - 45 %) compared to typical New Jersey soils. Compared to the other LSP sites, the barren LSP site 25R has a lower percentage of organic matter (10.8 %). The reference soil from HMF and barren 25R soil have low solvent extract yields (1.3 and 1.2 g/kg<sub>soil</sub>, respectively), compared to the forested LSP sites 43, 146 and 25F, which yielded 7.3 to 9.8 g/kg<sub>soil</sub>. Asphaltenes, higher molecular weight compounds (500 - 1,000 or more Da) (Lewan et al., 2014), are dominant in the soils from HMF and LSP sites 43, 146 and 25F, composing > 70 % of the extracts. Fraction 3 (predominantly polar compounds) is also prevalent (14 – 22 %) in these same soils (Table 2-1). Site 25R is distinctive: in addition to the low extract yield, it contains only 47 % asphaltenes and considerably more saturated hydrocarbons (Fraction 1, 17.6 %) than the other samples.

#### Table 2-1

The forested sites at LSP (43, 146 and 25F) contain both biological materials and contaminants. The additional organic matter and extract yield in soils from these sites is likely

because of augmentation by fossil fuel materials. LOI measurements alone cannot distinguish between coal and natural soil organic matter (Ball, 1964). However, we do indeed commonly see chunks of coal in the LSP soils, which must obviously contribute to the elevated organic matter at LSP. Samples HMF and 25R contain less soil organic matter and extract, but HMF is forested, while 25R is barren (Fig. 2-1). The lower organic matter content and extract yield at 25R likely results from the lack of vegetation because plants provide constant organic inputs into the soil and obviously 25R soil does not receive these inputs. The organic matter content at HMF is normal for a forested soil and simply lacks the supplemental increment because of the contamination found at LSP. We note that the asphaltene contents of the forested LSP sites are high and further work must be done to characterize the asphaltenes, for example, by Py-GC-MS.

### 2.3.2. Py-GC-MS

Pyrolysis-GC-MS results (Table 2-2 and Fig. 2-3) showed that the reference site HMF contains organic compounds found in typical forest soils including lignin [L1], polysaccharide [P1, P2, P3, P4], and protein biomarkers [N2] (Fig. 2-3 A). Reference site HMF also contains low-weight aromatic hydrocarbons [A1, A2, A4] and phenols [F1, F2, F3, F4] (Fig. 2-3 A).

Vegetated LSP sites 43, 146, and 25F contain the compounds present in HMF. These sites also contain PAHs such as naphthalenes and phenanthrenes, where both parent and alkylated forms are present, fluoranthene (Fig. 2-3 B), as well as dibenzofuran [DBF] and methyl dibenzofuran [DBF1]. The chromatogram of barren LSP site 25R shows a notable absence of organic compounds with a biological derivation [e.g., L1, L2 etc.] and thus predominantly aromatic compounds are seen in the trace. The aromatic compounds seen at site 25R are also present in similar proportions at the other LSP sites (Fig. 2-3).

Table 2-2

Figure 2-3

The presence of polysaccharides, lignin, and proteins in HMF was expected because these compounds indicate plants and microorganisms in the soil (*e.g.*, Hempfling & Schulten, 1990). These compounds are also present in vegetated LSP sites 43, 146, and 25F but not at barren site 25R. The pyrolyzates of the LSP sites 43, 146 and 25F soils have similar organic compositions to each other, which is not surprising because they are all vegetated and located within the same brownfield. The PAHs present at LSP sites indicate fossil fuel contamination and include naphthalenes, fluoranthene, and fluorene, and heterocyclic compounds, such as dibenzofuran. One likely source is coal, particles of which are evident to the naked eye in the park soils, and it is known that the presence of coal in the soil can increase the amount of aromatic compounds including PAHs (Kögel-Knabner, 2000; Laumann et al., 2011; Nádudvari et al., 2018; Stout and Emsbo-Mattingly, 2008).

One example of coal indicators include dibenzofuran and methyldibenzofuran (Nádudvari et al., 2018). In contrast to the other sites, 25R pyrolyzate shows a strong predominance of aromatic compounds. These aromatic compounds include monoaromatic hydrocarbons such as BTEX (benzene [A1], toluene [A2], ethylbenzene, xylene [A3]) and polycyclic aromatic hydrocarbons (PAHs) [NAP, PHN, FLA, PYR, CHR, BAN]. Compared to the other LSP sites, the different organic composition at site 25R can be largely attributed to the absence of plants at 25R. Organic compounds at forested LSP soils come from vegetation or industrial sources and compounds originating from plants can obscure signatures of contaminants (Ortiz et al., 2016b). With many of the plant and microbial indicators missing, the PAH indicators are more clearly visible in the 25R total ion current (TIC) trace. Our findings

indicate that the organic contaminant profile of site 25R is similar to the other LSP sites. This suggests that the lack of plants at site 25R is not a result of differences in organic contaminant composition.

### 2.3.3. Solvent extractable organic matter

#### 2.3.3.1. Fraction 1 (saturated hydrocarbons)

The saturated chromatograms (Fig. 2-4) contain two different sub-groups, normal and isoprenoid alkanes ( $m/z$  71) and triterpenoids ( $m/z$  191). The distributions of saturated hydrocarbons indicate that the soil of reference site HMF soil is distinctly different from soils from the four LSP sites (Fig. 2-4, Appendix-A Fig. A1). The HMF samples show a predominance of two higher plant triterpenoid biomarkers, diploptene [B2] and a  $\beta$ -amyryn derivative [B6] as well as the long-chain, odd carbon number alkanes  $n$ -C<sub>29</sub> and  $n$ -C<sub>31</sub> (Figs. 2-4A and 2-5A). For soil samples 43, 146, and 25F, we see a lower relative abundance of the two biomarkers [B2] and [B6] compared to HMF and a broader range of odd-carbon number  $n$ -alkanes (C<sub>24</sub> – C<sub>31</sub>) (Fig. 2-4 B-D, Fig. 2-5 B-D and Appendix-A Fig. A1). The C<sub>27</sub> – C<sub>35</sub> triterpenoid and isoprenoid alkanes are prominent in soils 43 and 146 (Fig. 2-4 B-D). The chromatogram for barren site 25R shows a distinctive “baseline hump”, indicating an unresolved complex mixture (UCM) of hydrocarbons (Fig. 2-4 E). Hopanes are relatively more abundant in site 25R compared to the other sites, however, the biomarkers [B2] and [B6] are not detected (Fig. 2-4 E).

#### Figure 2-4

There is notably more pristane [Pr] than phytane [Ph] at all LSP sites having pristane/phytane (Pr/Ph) ratios of *ca.* 3. In LSP soils, pristane was found more abundant than  $n$ -C<sub>17</sub> and phytane was found to be less abundant than  $n$ -C<sub>18</sub> (Fig. 2-4, Table 2-3, Appendix-A Fig.

A1). Hopanes (m/z 191) are key compounds found in contaminated LSP sites (Fig. 2-5) and were not found in the reference site HMF (Fig. 2-5 A). Soils from 25R do not show the biomarkers [B2] and [B6], likely owing to the absence of plant biomass or low numbers of soil microbes.

Table 2-3

Figure 2-5

The presence of pristane, phytane, hopanes, tricyclic terpanes, sesquiterpanes and steranes in LSP soils indicates fossil fuel contamination (Fig. 2-4, Appendix-A Figs. A2 and A3) (Killops and Killops, 2005; Peters et al., 2005; Wang and Fingas, 2003; Wang and Stout, 2010; Wang et al., 2005). The distribution of these compounds is similar in all samples analyzed, which indicates a similar blend of contaminating hydrocarbons at the four LSP sites. Hopanes, clearly visible in Figures 2-4 and 2-5, suggest the presence of heavy petroleum products such as fuel or lubricating oil in addition to coal (Peters et al., 2005). The reference site HMF does not contain hopanes, consistent with HMF soils containing less contamination compared to LSP. These findings support our first hypothesis that we will find more fossil fuel contaminants in LSP compared to HMF. The reference site HMF also yielded less of Fraction 1 (43.0 mg/kg<sub>soil</sub>) compared to all LSP sites, where yields range from 211-549 mg/kg<sub>soil</sub>. The high Pr/Ph ratios at LSP sites (> 2.7) are consistent with the presence of bituminous coal (Table 2-3) (Peters et al., 2005; Powell and McKirdy, 1973). The main railroad lines through sites 146 and 43 transported coal from Pennsylvania to a coal pier to go to New York City (Fig. 2-1) (Calder, 2010; French, 2002). Other railroad lines were directed to sites 25R and 25F and carried other cargo, however all railroad tracks had locomotives that could spill coal. Our C<sub>27</sub>-C<sub>28</sub>-C<sub>29</sub> sterane ternary diagram pairs sites based on proximity to each other, for example, soils from sites 43 and 146 have higher

abundance of C<sub>29</sub> compared to soils from 25R and 25F (Appendix-A Fig. A4) (Peters et al., 2005). The GC-MS data on the saturated fraction reflects the presence of both coal and petroleum products at LSP.

An odd-even predominance (OEP) is observed for HMF and the forested LSP soils, especially in extracted m/z 71 (Fig. 2-4 and Appendix-A Fig. A1), reflecting the presence of higher plants, specifically plant waxes. The triterpenoid biomarkers [B2] and [B6] are chemical signatures of soil microbes and are seen in HMF and forested LSP soils. Not surprisingly, soils from barren site 25R do not display OEP or biomarkers [B2] or [B6], consistent with the site's lack of vegetation (Fig. 2-4). Within LSP, site 25R has higher isoprenoid to normal alkane ratios (pristane/*n*-C<sub>17</sub> and phytane/*n*-C<sub>18</sub>) compared to the other sites. This can be explained by preferential biodegradation of *n*-alkanes compared to the isoprenoids at some point in the site's history (Table 2-3) (Peters et al., 2005). Biodegradation at site 25R is also supported by the UCM as seen in Figure 2-4E. This is surprising because site 25R supports no vegetation. It is possible that microbial degradation of fossil fuels at site 25R took place at the time of contamination and the signs we observe are from an earlier period of degradation.

#### 2.3.3.2. Fraction 2 (aromatic hydrocarbons)

Soil extract from the reference site HMF had lower amounts of Fraction 2 (predominantly aromatic hydrocarbons) (52.0 mg/kg<sub>soil</sub>) than did LSP soil extracts (Table 2-1). For the forested LSP sites, extract Fraction 2 values ranged from 363 to 506 mg/kg<sub>soil</sub> while LSP soil 25R yielded somewhat less than the other LSP sites, 119 mg/kg<sub>soil</sub> of extract Fraction 2. We intended for the LC separation to segregate saturated hydrocarbons into Fraction 1 and aromatic compounds into Fraction 2 but some long chain aliphatic hydrocarbons (> C<sub>27</sub>) also eluted into Fraction 2 (Fig. 2-

6). We observed only one major aromatic compound in the solvent extract from the uncontaminated reference site HMF (Fig. 2-6 A), which is an abietane derivative [B1]. In the extracts from LSP, the primary aromatic compounds are PAHs (Fig. 2-6 B - E) and include parent and alkylated naphthalenes, phenanthrenes, pyrenes, chrysenes and their isomers [e.g. NAPx, PHN, PYR, CHR]. Also notable in LSP soils are heterocyclic compounds including dibenzofurans and benzonaphthothiophene [DBF, BNT]. Sample 25R's PAH distributions resemble those in the other LSP samples but there is also a noticeable UCM (Fig. 2-6 E).

Figure 2-6

The aromatic fraction data indicate that the chosen reference soil HMF is indeed relatively uncontaminated while all LSP sites have significant PAH contamination. These data also support our hypothesis that there are more fossil fuel biomarkers present at LSP compared to HMF. The overall aromatic hydrocarbon distribution is similar for all LSP soils (Fig. 2-6 B-E), reflecting similar mixtures of contaminants. Fraction 2 data for LSP 25R soil indicated a significant UCM, which suggests weathering and biodegradation, in agreement with Fraction 1 data (Figs. 2-4 E, 6 E). If biodegradation is taking place, we might expect the concentration of low weight molecular PAHs, like naphthalene, to decrease (Biache et al., 2017). We observe PAHs in our data; perhaps these compounds are absorbed in coal particles and thus shielded from biodegradation (Liu et al., 2008). We note that the PAH distributions in the pyrolyzates of the LSP soils and extracted Fraction 2 show a greater predominance of parent PAHs than those of the extract (Fraction 2), as seen by comparison of Figure 2-3E with Figure 2-6E and specifically with PHN in Appendix-A Fig. A5 (Wang and Fingas, 2003). The greater predominance of parent compounds indicates a pyrogenic source, which derives from incomplete

combustion of fossil fuels (Chen et al., 2004; Given, 1987; Micić et al., 2011; Stout and Emsbo-Mattingly, 2008).

#### 2.3.3.3. Fraction 3 (polar compounds)

The soil from the reference site HMF contains ergosterol and stigmasterol derivatives [S2, S3, S4, S5, S6], a diterpenoid tentatively identified as totarol [B13], and octadecanoic acid butyl ester [FA4] (Fig. 2-7 A). This ester and the steroids are also present in the forested soils from LSP (Fig. 2-7 B-D). The plasticizer, diisobutyl phthalate [X1], is present in all soils.

Compounds present in all LSP sites, but not in HMF, include 1-heptacosanol and 1,2-benzenedicarboxylic acid, bis(2-ethylhexyl) ester [B14, X2]. The triterpenoids tentatively identified as 3 $\beta$ -methoxy-D-friedoolean-14-ene and olean-12-en-3-one [B15, B16] were present in LSP 43 and 146 soils, while lupeol and lup-20(29)-ene-3,28-diol [B17, B21] were found in LSP 146 and 25R soils (Fig. 2-7 B-D). LSP site 25R has fewer polar compounds compared to the other sites but includes the steroids stigmasterol and stigmasterol-3-one [S4, S6] (Fig. 2-7 E).

#### Figure 2-7

The soil at HMF contains both ergosterol and stigmasterol derivatives. Ergosterols are generally found in fungi, while stigmasterol typically occurs in higher plants (Peters et al., 2005). HMF also contains totarol [B13], which is a cyclic diterpenoid that is present in resins from higher plants (Tinoco et al., 2006), and a long chain alcohol, 1-heptacosanol, which is present in terrestrial organic matter (Wang et al., 2009; Yunker et al., 1995). All of these compounds are compatible with a normal, temperate forest soil. The vegetation present at HMF is predominantly cedar. The plasticizer diisobutyl phthalate [X1] is present in all the studied soils,

possibly a result of having stored the soil samples in plastic bags. The origin of octadecanoic acid butyl ester in soils is of unknown origin and could be another plasticizer introduced during sample handling (Cahill et al., 2006). The dominant species present at LSP is *Betula populifolia*, which is present at 43, 146 and 25F (Evans et al., 2015; Gallagher et al., 2008b). Lupeol [B8] and lup-20(29)-ene-3,28-diol [B12] are biological indicators of birch (Peters et al., 2005). The microbially and plant-derived steroids and triterpenoids are much less abundant at site 25R, not unexpected since it is void of vegetation. The presence of life in 25R is also apparent in the polar compounds, specifically sitosterol (stigmast-5-en-3-ol) and the degradation product of sitosterol, stigmast-4-en-3-one (Mackenzie et al., 1982; Pautler et al., 2013).

#### 2.3.4. Organic petrography

All samples (soil particles smaller than 2 mm) from LSP had high amount of organic matter and it was represented dominantly by anthropogenic material. Coal particles were prominent in all four samples, accounting for 14.3 to 30.0 vol. %, and they were especially abundant in samples 25R and 43. Coal particles were of various ranks from high volatile bituminous to anthracite, with the latter being the dominant rank in all samples (Fig. 2-8). Carbonization-derived material (coke) is also common and ranges from 6.6 to 12.0 vol. %, with samples 43 and 146 having the largest proportions (Fig. 2-8 and 2-9). Tar and pitch-like material were prominent in samples 25R and 25F (Figs. 2-8 and 2-9), and far less abundant in the other two samples. Combustion-derived material accounted for 7.1 to 23.1%, being most common in sample 146 (Fig. 2-8). The combustion-derived material was represented both by organic material (char) and mineral matter (glass, spinel, etc.) (Fig. 2-9). In total, anthropogenic material accounted for more than 50 vol %

of all the samples with site 25R soil having the largest contribution (Fig. 2-8). Recent organic matter (classified as “other” in Fig. 2-8) was rare and represented by wood fragments.

Figure 2-8

Figure 2-9

Organic petrography was useful in comparing LSP sites in terms of soil organic components, including different ranks of coal, coke, tar and pitch, fly ash/bottom ash, sediments, and other materials (Suárez-Ruiz et al., 2012). The organic petrography profiles of sites close to each other at LSP share similarities; for example, soils from 43 and 146 that are located close in proximity and are along train tracks to a coal pier based on historic aerial photographs (Fig. 2-1B) have the highest abundance of coke. Soils from 25F and 25R, which are adjacent sites, were both prominent in tar and pitch-like material. Site 25R has the largest proportion of non-mineral material (Fig. 2-8), which could be a reason for or the result of a lack of vegetation at this site.

### 2.3.5. Inorganic elemental analysis

The concentrations of several inorganic compounds in HMF and LSP soils were also determined (Appendix-A Table A1). As expected, we found the lowest concentrations of metals (V, Cr, Ni, Cu, Zn, As, and Pb) at the reference site HMF; however, HMF soil showed a high Al concentration ( $20,527 \pm 249$  ppm), which was matched by only one of the LSP sites, 25R (Appendix-A Table A1). There were elevated concentrations of Na, Co, Cu, Zn, As, and Pb at both 25F ([Na]: 873; [Co]: 256; [Cu]: 2256; [Zn] 14435; [As] 630; [Pb] 7145 mg/kg, triplicate measurements, see Appendix-A Table A1 for errors) and 25R ([Na]: 4393; [Co]: 869; [Cu]: 7165; [Zn] 41271; [As]: 1162; [Pb] 20302 mg/kg) compared to the other LSP sites (Appendix-A Table A1).

Sanders (2003) in a survey of New Jersey soils, determined background levels of metals; the HMF metal concentrations closely match his values from northeastern New Jersey (“urban Piedmont”) soils (Appendix-A Table A1) (Sanders, 2003), confirming that HMF is a good reference soil for this study. The high concentrations of Al in HMF relative to LSP soils may suggest a higher abundance of aluminosilicate clay minerals in HMF compared to LSP (Barton et al., 2002; Buettner and Valentine, 2011b). Figure 2-10 shows element concentration anomalies at LSP sites; metal concentrations were normalized to the reference site HMF values.

Specifically, we find anomalously high levels of Na, Co, Cu, Zn, As, and Pb in LSP soils, especially at sites 25F and 25R (Fig. 2-10). For example, As concentrations in 25F and 25R were found to be 119 and 220 times higher compared to HMF, respectively. Although these sites are adjacent, As concentrations are about two times higher at 25R compared to 25F. It is common to find As, Cr, Cu, Pb and Zn in contaminated soil. In particular, As, Cu, Cr, and Zn are associated with chromated copper arsenate, which was used in some rail yards for treating wood used for railroad ties (Kumpiene et al., 2008). Another possible explanation for the anomalously high concentrations is that bulk minerals, perhaps pyrites, sulfides, or oxides, were transported on the railroad lines, possibly supplying not only Fe but also As, Cd, Co, Cu, and Ni (Finkelman, 1995). It is also possible that coal and slag, which can include the trace elements in coal ashes, were transported through LSP (Schweinfurth, 2003).

Figure 2-10

### 2.3.6 Extracellular soil phosphatase activities and bacterial density

Site 146 has the highest bacterial density (cells/g<sub>dry soil</sub>) ( $7.87 (\pm 0.82) \times 10^8$ ) of the sites (Fig. 2-11 A). Soils from HMF ( $4.64 (\pm 0.93) \times 10^8$ ), 43 ( $4.37 (\pm 0.35) \times 10^8$ ), and 25F ( $4.97 (\pm 0.61) \times 10^8$ ) are forested and have similar bacterial densities to each other. The barren site 25R has lower but measurable bacterial density ( $2.09 (\pm 0.76) \times 10^8$  cells/g<sub>dry soil</sub>). The data in Figure 2-11 B show that site 146 has the highest phosphatase activity ( $2.60 (\pm 0.55) \times 10^6$  pmol/g/h) of the soils studied here. This result agrees with previous findings where we found that site 146 has higher phosphatase, cellobiohydrolase and L-leucine-amino peptidase activities compared to three other LSP sites and to HMF (Hagmann et al., 2015). Despite the measurable bacterial density, the phosphatase activity at barren 25R is below the threshold of detection. It is surprising that site 25F, which is located next to site 25R, has high phosphatase activity (pmol/g/h) ( $1.38 (\pm 0.39) \times 10^6$ ). The phosphatase activities at HMF and 43 are ( $0.47 (\pm 0.38) \times 10^6$ ) and ( $0.67 (\pm 0.13) \times 10^6$ ), respectively.

Figure 2-11

The low but measurable bacterial density we found at barren site 25R indicates the presence of bacterial life. Even so, the phosphatase activity in the soil is below the threshold of detection and it is possible the bacteria in 25R soil are dormant, perhaps owing to poor nutrient cycling and availability. In a previous study, Singh and co-workers found via next-generation sequencing that the bacterial community at site 25R is statistically distinct from the other LSP sites (Singh et al., 2019b). The presence of bacteria in 25R soil is consistent with the biodegradation at this site discussed in Section 3.3.1. It is possible that microbial degradation of fossil fuels indicated by the UCM in the 25R GC-MS data took place at some time in the site's history.

Site 146 has high bacterial density and phosphatase activity (Fig. 2-11) and also the highest percent organic matter (44 %) (Table 2-1). We had originally hypothesized that the high function at site 146 is due to differences in organic compound profiles, perhaps because of the absence of specific contaminants that are present at other LSP sites. Conversely, we found that site 146 has an organic composition similar to the other forested sites at LSP as seen in the pyrolysis and GC-MS data (Figs. 2-3, 2-4, 2-5, and 2-6); however, organic composition may not explain the high activity at this site. Site 25R is also distinct from the other LSP sites: it has no plants and no detectable phosphatase activity. If this absence of function is a result of organic contaminants, we would expect to observe differences in the organic contaminant profiles between site 25R and the other LSP sites. Analogously to site 146, we found that the organic composition at site 25R is similar to the other sites at LSP as seen in the pyrolysis and GC-MS data except that compounds associated with higher plants are absent (Figs. 2-3, 2-4, 2-5, and 2-6).

We considered the possibility that the low function at 25R is due not to differences in the identity of organic contaminants but rather the concentration of specific compounds in the soil. This is unlikely because the extract yields from 25R for soil particles less than 2 mm in diameter are significantly lower than for the other LSP sites. These data together suggest that the organic contaminant profile at site 25R is not responsible for the functional differences between this site and other LSP sites. Previous findings by Singh et al. (2019a) showed that abiotic factors are more important than biotic ones for enzymatic function in LSP soils. In light of these findings and having now ruled out a different organic contaminant profile as the reason for the low function at site 25R, our new hypothesis is that the higher concentrations of Na, Co, Cu, Zn, As, and Pb at 25R (discussed in Section 3.5) are responsible for the poor function of the site (Singh

et al., 2019a). The concentrations of these metals are about 2 to 5 times higher than in the forested and high functioning site 25F that is located adjacent to site 25R. We plan to further investigate whether these elevated metal concentrations at 25R affect soil extracellular enzymatic activity and plant production. For example, it is possible that the As concentrations at site 25R are sufficiently high to inhibit phosphatase activity (Lee et al., 2011; Lorenz et al., 2006; Speir et al., 1999).

### 2.3.7 Insights into functional variation between LSP sites

All LSP sites are contaminated with PAHs and other fossil fuel-derived components that are absent or barely detectable at reference site HMF. The presence of the PAHs, hopanes, steranes, and sesquiterpanes supports our first hypothesis that there are more fossil fuel biomarkers at LSP compared to HMF. Vegetated sites at LSP have unnaturally high organic matter content (30 to 45 %), relative to pristine vegetated soils, reflecting large quantities of anthropogenic contaminants in these soils. The distributions of the PAHs and fossil fuel biomarkers are similar for all soils within LSP. However, the yield of extractable organic matter at 25R is lower and thus we suspect that the extraordinarily high content of *inorganic* contaminants rather than organic contaminants explains the barren site's lack of vegetation. We hypothesized that the barren site 25R would have more or different contaminants compared to the forested sites at LSP. This was found to be true for several inorganic contaminants but not for the organic contaminant profiles within LSP.

LSP's history and the soils' chemical and petrographic fingerprints agree with the location of the sites within the rail yard. Sites 43 and 146 are located on what was once a dense array of railroad tracks leading to the coal pier. Their soils contain more coal and less tar and

pitch compared to sites 25F and 25R, which were on different railroad lines carrying other unspecified cargo. We observe wider gaps between tracks in historical photographs of the 25F and 25R area, in which we suspect that dumping activities occurred (Fig. 2-1 D and E). It is possible that 25F is forested and has high phosphatase activity, because it was on an active railroad track whereas 25R was on a gap, where more dumping occurred, and thus has low phosphatase activity. While we did not find evidence that would explain these differences in the nonbiologically-derived organic contaminant profiles, we note significantly higher metal contaminant concentrations in 25R compared to 25F.

#### 2.3.8 Implications for investigating contaminated ecosystems

In this study, we used several experimental methods in conjunction with pyrolysis GC-MS to study soils from three types of sites: an uncontaminated vegetated reference site (HMF), contaminated vegetated sites (LSP 43, 146, 25F) and a contaminated, industrial barren (25R). Our data are consistent with the presence and absence of biologically derived organic matter in the study sites: biological pyrolysis products are not present in the organic chemical fingerprint of soil 25R, which instead shows a predominance of contaminant-derived aromatic compounds. These data serve as a case study or reference set for the differences in data observed for contaminated vegetated and contaminated barren soils, especially because indicators from vegetation can chemically obscure the signatures of contaminants.

Site 25R in LSP is an example of an area that is contaminated and barren as a result of past anthropogenic activities and, possibly, the subsequent environmental and physical conditions. Such “industrial barrens” are present worldwide and are considered “extreme environments” (Kozlov and Zvereva, 2007a). Unfortunately, industrial barrens, and especially

those that have high heavy metal loads, are often unlikely to recover naturally but, even so, they are studied less than other extreme environments. Many studies on industrial barrens focus on evaluation of damage and development of rehabilitation measures while more fundamental studies on soil function and detailed soil characterization are lacking, limiting our understanding of the fundamental chemistry, biochemistry and ecology of these sites. Kozlov and Zvereva suggested that researchers often choose the most contaminated but planted sites within an area for their studies because they are more comparable with less disturbed sites (Kozlov and Zvereva, 2007a).

#### 2.4. Conclusion

Site 25R is an example of an industrial barren and here we have conducted a multifaceted chemical and biochemical analysis of this soil and compared the findings to those in nearby vegetated sites. The phosphatase activity at site 25R is below our limit of detection, yet direct bacterial counts indicate the presence of bacteria. Interestingly, these findings suggest that microbes in 25R soils are present but lying dormant, perhaps as a result of either inorganic contaminant loads or physical abiotic restrictions in the soil. Perhaps fostering plant growth, aerating the soil, or adding root exudates to the contaminated 25R soil will revive some of the microbes and subsequently improve nutrient cycling and overall soil function. The inactive microorganisms may be waiting for an environmental nudge or input to revitalize them and unleash their functional potential in the currently contaminated, poorly functioning, and barren 25R soil. This same story of dormant and abiotically limited microbes, waiting to be revitalized, may be playing out in other industrial barrens throughout the world. It behooves the scientific community to more fully investigate these sites to obtain a deeper and more fundamental

understanding, which can then be leveraged to prevent desertification and land degradation and to restore dysfunctional and phytotoxic soils.

### **Acknowledgements**

We thank the National Science Foundation (NSF CBET 1603741) and the PSEG Institute for Sustainability Studies for the support for this study. We thank Gregory Pope for valuable discussions during the project. Finally, we thank Frank Gallagher for facilitating access to Liberty State Park.

### References

- Alisi C., Musella R., Tasso F., Ubaldi C., Manzo S., Cremisini C., et al., 2009. Bioremediation of diesel oil in a co-contaminated soil by bioaugmentation with a microbial formula tailored with native strains selected for heavy metals resistance. *Sci. Total Environ.*; 407: 3024-3032.
- Alker S., Joy V., Roberts P., Smith N., 2000. The Definition of Brownfield. *J. Environ. Plann. Man.*; 43: 49-69.
- Ball D., 1964. Loss-on-ignition as an estimate of organic matter and organic carbon in non-calcareous soils. *J. Soil Sci.*; 15: 84-92.
- Baran S., Bielińska J.E., Oleszczuk P., 2004. Enzymatic activity in an airfield soil polluted with polycyclic aromatic hydrocarbons. *Geoderma*; 118: 221-232.
- Biache C., Ouali S., Cébron A., Lorgeoux C., Colombano S., Faure P., 2017. Bioremediation of PAH-contaminated soils: Consequences on formation and degradation of polar-polycyclic aromatic compounds and microbial community abundance. *J. Hazard Mater.*; 329: 1-10.
- Brooks K.M., 2004 Polycyclic aromatic hydrocarbon migration from creosote-treated railway ties into ballast and adjacent wetlands. Madison, WI: U.S. Department of Agriculture, Forest Service, Forest Products Laboratory.
- Buettner K.M., Valentine A.M., 2011. Bioinorganic chemistry of titanium. *Chem. Rev.*; 112: 1863-1881.
- Cahill T.M., Seaman V.Y., Charles M.J., Holzinger R., Goldstein A.H., 2006. Secondary organic aerosols formed from oxidation of biogenic volatile organic compounds in the Sierra Nevada Mountains of California. *J. Geophys Res Atmos*; 111.

- Caldes C., 2010 Jersey City's Hudson River Waterfront Book Two: Lehigh Valley, Central Railroad of New Jersey, Erie, DL&W, Erie-Lackawanna 1941-1964. Vol 2: Journal Square Publishing.
- Chen Y., Bi X., Mai B., Sheng G., Fu J., 2004. Emission characterization of particulate/gaseous phases and size association for polycyclic aromatic hydrocarbons from residential coal combustion. *Fuel*; 83: 781-790.
- Evans J.M., Parker A., Gallagher F., Krumins J.A., 2015. Plant Productivity, Ectomycorrhizae, and Metal Contamination in Urban Brownfield Soils. *Soil Sci.*; 180: 198-206.
- Finkelman R.B., 1995. Modes of Occurrence of Environmentally-Sensitive Trace Elements in Coal. In: Swaine DJ, Goodarzi F, editors. *Environmental Aspects of Trace Elements in Coal*. Springer Netherlands, Dordrecht, pp. 24-50.
- French K., 2002 Railroads of Hoboken and Jersey City. Charleston, SC: Arcadia Publishing.
- Gallagher F.J., Pechmann I., Bogden J.D., Grabosky J., Weis P., 2008a. Soil metal concentrations and productivity of *Betula populifolia* (gray birch) as measured by field spectrometry and incremental annual growth in an abandoned urban Brownfield in New Jersey. *Environ. Pollut.*; 156: 699-706.
- Gallagher F.J., Pechmann I., Bogden J.D., Grabosky J., Weis P., 2008b. Soil metal concentrations and vegetative assemblage structure in an urban brownfield. *Environ. Pollut.*; 153: 351-361.
- Gallego J., Rodríguez-Valdés E., Esquinas N., Fernández-Braña A., Afif E., 2016. Insights into a 20-ha multi-contaminated brownfield megasite: an environmental forensics approach. *Sci. Total Environ.*; 563: 683-692.

- Given P., 1987. The mobile phase in coals: its nature and modes of release. Final report–Part 2. Efforts to Better Define the Nature and Magnitude of the Mobile Phase. Prepared for the US Department of Energy. DOE-PC-60911-F2., pp. 42.
- Hagmann D.F., Goodey N.M., Mathieu C., Evans J., Aronson M.F.J., Gallagher F., et al., 2015. Effect of metal contamination on microbial enzymatic activity in soil. *Soil Biol. Biochem.*; 91: 291-297.
- Hamdi H., Benzarti S., Manusadžianas L., Aoyama I., Jedidi N., 2007. Bioaugmentation and biostimulation effects on PAH dissipation and soil ecotoxicity under controlled conditions. *Soil Biol. Biochem.*; 39: 1926-1935.
- Haritash A., Kaushik C., 2009. Biodegradation aspects of polycyclic aromatic hydrocarbons (PAHs): a review. *J. Hazard. Mater.*; 169: 1-15.
- Jackson D.P., 1997. Evaluation of ex-situ soil washing as a remedial strategy for heavy metal removal from railyard ballast. *Hazardous and Industrial Wastes*; 29: 158-164.
- Killops S., Killops V., 2005 *Introduction to Organic Geochemistry*. Oxford: Blackwell Publishing.
- Kögel-Knabner I., 2000. Analytical approaches for characterizing soil organic matter. *Org. Geochem.*; 31: 609-625.
- Kozlov M.V., Zvereva E.L., 2007. Industrial barrens: extreme habitats created by non-ferrous metallurgy. *Rev. Environ. Sci. Bio.*; 6: 231-259.
- Kruege M., 2015. *Analytical pyrolysis principles and applications to environmental science*. Environmental Applications of Instrumental Chemical Analysis, CRC Press, Boca Raton, FL: 533-569.

- Kruger M.A., Gallego J.L.R., Lara-Gonzalo A., Esquinas N., 2018. Chapter 7 - Environmental Forensics Study of Crude Oil and Petroleum Product Spills in Coastal and Oilfield Settings: Combined Insights From Conventional GC–MS, Thermodesorption–GC–MS, and Pyrolysis–GC–MS. In: Stout SA, Wang Z, editors. Oil Spill Environmental Forensics Case Studies. Butterworth-Heinemann, pp. 131-155.
- Kumpiene J., Lagerkvist A., Maurice C., 2008. Stabilization of As, Cr, Cu, Pb and Zn in soil using amendments – A review. *Waste Manag.*; 28: 215-225.
- Lacey R.F., Cole J.A., 2003. Estimating water pollution risks arising from road and railway accidents. *Q. J. Eng. Geol. Hydroge.*; 36: 185.
- Lara-Gonzalo A., Kruger M.A., Lores I., Gutiérrez B., Gallego J.R., 2015. Pyrolysis GC–MS for the rapid environmental forensic screening of contaminated brownfield soil. *Org. Geochem.*; 87: 9-20.
- Laumann S., Micić V., Kruger M.A., Achten C., Sachsenhofer R.F., Schwarzbauer J., et al., 2011. Variations in concentrations and compositions of polycyclic aromatic hydrocarbons (PAHs) in coals related to the coal rank and origin. *Environ. Pollut.*; 159: 2690-2697.
- Lee S.-H., Kim E.Y., Park H., Yun J., Kim J.-G., 2011. In situ stabilization of arsenic and metal-contaminated agricultural soil using industrial by-products. *Geoderma*; 161: 1-7.
- Lewan M.D., Warden A., Dias R.F., Lowry Z.K., Hannah T.L., Lillis P.G., et al., 2014. Asphaltene content and composition as a measure of Deepwater Horizon oil spill losses within the first 80days. *Org. Geochem.*; 75: 54-60.
- Liu H., Chen L.-P., Ai Y.-W., Yang X., Yu Y.-H., Zuo Y.-B., et al., 2008. Heavy metal contamination in soil alongside mountain railway in Sichuan, China. *Environ. Monit. and Assess*; 152: 25.

Lorenz N., Hintemann T., Kramarewa T., Katayama A., Yasuta T., Marschner P., et al., 2006.

Response of microbial activity and microbial community composition in soils to long-term arsenic and cadmium exposure. *Soil Biol. Biochem.*; 38: 1430-1437.

Mackenzie A.S., Brassell S.C., Eglinton G., Maxwell J.R., 1982. Chemical Fossils: The

Geological Fate of Steroids. *Science*; 217: 491.

Malawska M., Wilkomirski B., 1999. An analysis of polychlorinated biphenyls (PCBs) content

in soil and plant leaves (*taraxacum officinale*) in the area of the railway junction Iława

Główna AU -. *Toxicol. Environ. Chem.*; 70: 509-515.

Malawska M., Wilkomirski B., 2000. Soil and plant contamination with heavy metals in the area

of the old railway junction Tarnowskie Góry and near two main railway routes. *Rocz*

*Panstw Zakł Hig*; 51: 259-267.

Malawska M., Wiołkomirski B., 2001. An Analysis of Soil and Plant (*Taraxacum Officinale*)

Contamination with Heavy Metals and Polycyclic Aromatic Hydrocarbons (PAHs) In the

Area of the Railway Junction Iława Główna, Poland. *Water Air Soil Pollut.*; 127: 339-

349.

Maliszewska-Kordybach B., Smreczak B., 2003. Habitat function of agricultural soils as affected

by heavy metals and polycyclic aromatic hydrocarbons contamination. *Environ. Int.*; 28:

719-728.

Micić V., Krüge M.A., Köster J., Hofmann T., 2011. Natural, anthropogenic and fossil organic

matter in river sediments and suspended particulate matter: A multi-molecular marker

approach. *Sci. Total Environ.*; 409: 905-919.

Nádudvari Á., Fabiańska M.J., Marynowski L., Kozielska B., Koniecznyński J., Smółka-

Danielowska D., et al., 2018. Distribution of coal and coal combustion related organic

- pollutants in the environment of the Upper Silesian Industrial Region. *Sci. Total Environ.*; 628-629: 1462-1488.
- Ortiz J.E., Borrego Á.G., Gallego J.L.R., Sánchez-Palencia Y., Urbanczyk J., Torres T., et al., 2016a. Biomarkers and inorganic proxies in the paleoenvironmental reconstruction of mires: The importance of landscape in Las Conchas (Asturias, Northern Spain). *Org. Geochem.*; 95: 41-54.
- Ortiz J.E., Sánchez-Palencia Y., Torres T., Domingo L., Mata M.P., Vegas J., et al., 2016b. Lipid biomarkers in Lake Enol (Asturias, Northern Spain): Coupled natural and human induced environmental history. *Org. Geochem.*; 92: 70-83.
- Osman K.T., 2013. Organic Matter of Forest Soils. *Forest Soils: Properties and Management*. Springer International Publishing, Cham, pp. 63-76.
- Pautler B.G., Sanborn P.T., Simpson A.J., Simpson M.J., 2013. Molecular characterization of organic matter in Canadian Arctic paleosols for paleoecological applications. *Org. Geochem.*; 63: 122-138.
- Peters K.E., Peters K.E., Walters C.C., Moldowan J., 2005 *The biomarker guide*. Vol 1: Cambridge University Press.
- Powell T.G., McKirdy D.M., 1973. Relationship between Ratio of Pristane to Phytane, Crude Oil Composition and Geological Environment in Australia. *Nature-Phys Sci.*; 243: 37.
- Qian Y., Gallagher F., Deng Y., Wu M., Feng H., 2017. Risk assessment and interpretation of heavy metal contaminated soils on an urban brownfield site in New York metropolitan area. *Environ. Sci. Pollut. R.*; 24: 23549-23558.

- Sanders P.F., 2003. Ambient levels of metals in New Jersey soils. Environmental Assessment and Risk Analysis Element Research Project Summary. New Jersey Dept. of Environmental Protection, Division of Science, Research & Technology, Trenton, N.J.
- Schweinfurth S.P., 2003 Coal--a Complex Natural Resource: An Overview of Factors Affecting Coal Quality and Use in the United States. Vol 1143: US Department of the Interior, US Geological Survey.
- Shen G., Lu Y., Zhou Q., Hong J., 2005. Interaction of polycyclic aromatic hydrocarbons and heavy metals on soil enzyme. *Chemosphere*; 61: 1175-1182.
- Singh J.P., Ojinnaka E.U., Krumins J.A., Goodey N.M., 2019a. Abiotic factors determine functional outcomes of microbial inoculation of soils from a metal contaminated brownfield. *Ecotoxicol. Environ. Saf.*; 168: 450-456.
- Singh J.P., Vaidya B.P., Goodey N.M., Krumins J.A., 2019b. Soil microbial response to metal contamination in a vegetated and urban brownfield. *J. Environ. Manage.*; 244: 313-319.
- Smith M.J., Flowers T.H., Duncan H.J., Alder J., 2006. Effects of polycyclic aromatic hydrocarbons on germination and subsequent growth of grasses and legumes in freshly contaminated soil and soil with aged PAHs residues. *Environ. Pollut.*; 141: 519-525.
- Speir T.W., Kettles H.A., Parshotam A., Searle P.L., Vlaar L.N.C., 1999. Simple kinetic approach to determine the toxicity of AS[V] to soil biological properties. *Soil Biol. Biochem.*; 31: 705-713.
- Sprocati A.R., Alisi C., Tasso F., Marconi P., Sciullo A., Pinto V., et al., 2012. Effectiveness of a microbial formula, as a bioaugmentation agent, tailored for bioremediation of diesel oil and heavy metal co-contaminated soil. *Process Biochem.*; 47: 1649-1655.

- Stout S.A., Emsbo-Mattingly S.D., 2008. Concentration and character of PAHs and other hydrocarbons in coals of varying rank – Implications for environmental studies of soils and sediments containing particulate coal. *Org. Geochem.*; 39: 801-819.
- Suárez-Ruiz I., Flores D., Mendonça Filho J.G., Hackley P.C., 2012. Review and update of the applications of organic petrology: Part 1, geological applications. *Int. J. Coal Geol.*; 99: 54-112.
- Taylor G.H., Teichmüller M., Davis A., Diessel C., Littke R., Robert P., 1998 *Organic petrology*. Gebrüder Borntraeger, Berlin.
- Thornton I., Farago M.E., Thums C.R., Parrish R.R., McGill R.A.R., Breward N., et al., 2008. Urban geochemistry: research strategies to assist risk assessment and remediation of brownfield sites in urban areas. *Environ. Geochem. and Health*; 30: 565-576.
- Tinoco P., Almendros G., Sanz J., González-Vázquez R., González-Vila F.J., 2006. Molecular descriptors of the effect of fire on soils under pine forest in two continental Mediterranean soils. *Org. Geochem.*; 37: 1995-2018.
- Wang Z., Fingas M.F., 2003. Development of oil hydrocarbon fingerprinting and identification techniques. *Mar. Pollut. Bull.*; 47: 423-452.
- Wang Z., Stout S., 2010 *Oil spill environmental forensics: fingerprinting and source identification*: Elsevier.
- Wang Z., Yang C., Fingas M., Hollebone B., Peng X., Hansen A.B., et al., 2005. Characterization, Weathering, and Application of Sesquiterpanes to Source Identification of Spilled Lighter Petroleum Products. *Environ. Sci. Technol.*; 39: 8700-8707.
- Wang Z., Yang C., Kelly-Hooper F., Hollebone B.P., Peng X., Brown C.E., et al., 2009. Forensic differentiation of biogenic organic compounds from petroleum hydrocarbons in biogenic

and petrogenic compounds cross-contaminated soils and sediments. *J. Chromatogr. A*; 1216: 1174-1191.

Wiłkomirski B., Sudnik-Wójcikowska B., Galera H., Wierzbicka M., Malawska M., 2011.

Railway transportation as a serious source of organic and inorganic pollution. *Water Air Soil Pollut.*; 218: 333-345.

Yunker M.B., Macdonald R.W., Veltkamp D.J., Cretney W.J., 1995. Terrestrial and marine

biomarkers in a seasonally ice-covered Arctic estuary — integration of multivariate and biomarker approaches. *Mar. Chem.*; 49: 1-50.

## TABLES

**Table 2-1.** Organic matter content (% , mean  $\pm$  SE; n = 3), extraction and liquid chromatographic results from HMF, 43, 146, 25F and 25R soils. Fraction 1 contains saturated hydrocarbons; fraction 2 – aromatic compounds and long chain ( $> C_{27}$ ) normal alkanes; fraction 3 – polar compounds. The data show that soil from site 146 has the highest percent organic matter. The LC results show the percentage of the total extract as well as yield per kg of dry soil.

Sample	Organic Matter (% of soil)	Extract yield (g/kg <sub>soil</sub> )	Fraction 1 mg/kg <sub>soil</sub> (% of extract)	Fraction 2 mg/kg <sub>soil</sub> (% of extract)	Fraction 3 mg/kg <sub>soil</sub> (% of extract)	Asphaltenes mg/kg <sub>soil</sub> (% of extract)
HMF	7.43 $\pm$ 0.63	1.28	43.0 (3.3)	52.0 (4.0)	287 (22.1)	918 (70.6)
LSP 43	29.8 $\pm$ 0.86	9.21	451 (4.9)	506 (5.5)	929 (10.1)	7,314 (79.5)
LSP 146	44.8 $\pm$ 2.18	9.83	549 (5.6)	451 (4.6)	1421 (14.5)	7,379 (75.3)
LSP 25F	31.6 $\pm$ 4.79	7.38	429 (5.8)	363 (4.9)	1,095 (14.8)	5,513 (74.5)
LSP 25R	10.8 $\pm$ 1.94	1.21	211 (17.6)	119 (9.9)	307 (25.6)	563 (46.9)

**Table 2-2:** Symbols for peak identification used in Figures 2-1 through 2-7.

Aliphatic Hydrocarbons	
Numerals	normal alkanes
Pr	pristane
Ph	phytane
Hx	hopanes (x is the carbon number)
Ts	18 $\alpha$ (H)-22,29,30-trisnorhopane
Tm	17 $\alpha$ (H)-22,29,30-trisnorhopane
TRx	tricyclic terpane
Aromatic Compounds	
Alkylated aromatic compounds, "x" is degree of substitution	
A1	benzene
A2	toluene
A3	m-xylene & p-xylene
A4	styrene
A5	biphenyl
NAP	naphthalene
NAPx	alkylnaphthalene isomers
PHN	phenanthrene
PHNx	alkylphenanthrene isomers
ANT	anthracene
FLA	fluoranthene
FLU	fluorene
FLON	9H-fluoren-9-one
PYR	pyrene
PYRx	alkypyrene isomers
CHR	chrysene
CHRx	alkylchrysene isomers
BAN	benzo[a]anthracene
BNT	benzonaphthothiophene
BFLA	benzofluorene
DBF	dibenzofuran
DBFx	alkyldibenzofuran isomers
DBT	dibenzothiophene
Polysaccharide Marker Compounds	
P1	cyclopentenone
P2	furfural
P3	3-methylcyclopentenone
P4	methylfurfural
P5	levoglucosan
Phenolic Compounds	
F1	phenol
F2	2-methylphenol
F3	3-methylphenol & 4-methylphenol
F4	vinylphenol
Lignin Marker Compound	
L1	guaiacol
L2	methylguaiacol
L3	ethylguaiacol

L4	vinylguaiacol
L5	syringol
L6	vanillin
L7	trans iso-eugenol
L8	acetovanillone
L9	vinylsyringol
L10	prop-1-enyl syringol
L11	prop-2-enyl syringol (trans)
L12	acetosyringone
<hr/>	
Fatty Acid	
FA1	<i>n</i> -hexadecanoic acid
FA2	<i>n</i> -octadecanoic acid
FA3	methyl ester (E) 9-octadecanoic acid
FA4	octadecanoic acid, butyl ester
<hr/>	
Nitrogen Compounds	
N1	benzonitrile
N2	benzeneacetonitrile
N3	indole
N4	diketodipyrrole
<hr/>	
Steroid	
S1	C29 steradiene
S2	cholest-5-en-3-ol
S2	ergost-5-en-3-ol
S3	$\gamma$ -stigmasterol
S4	stigmast-5-en-3-ol
S5	stigmastanol
S6	stigmast-4-en-3-one
<hr/>	
Plasticizer	
X1	diisobutyl phthalate
X2	1,2-benzenedicarboxylic acid, bis(2-ethylhexyl) ester
<hr/>	
Other Compounds	
B1	abietane derivative
B2	$\beta$ -amyrin derivative
B3	diploptene
B4	totarol
B5	1-heptacosanol
B6	3 $\beta$ -methoxy-D-friedoolean-14-ene
B7	olean-12-en-3-one
B8	lupeol
B9, B10	dammarane isomers
B11	cyclolaudenol
B12	lup-20(29)-ene-3,28-diol

**Table 2-3.** Carbon preference index (CPI), odd-even predominance (OEP), pristane/phytane (Pr/Ph), Pr/C17, Ph/C18, and weighted average carbon number of HMF, 43, 146, 25F and 25R.

Sample	CPI	OEP	Pr/Ph	Pr/C17	Ph/C18	weighted average carbon number
HMF	2.573	2.782	0.634	2.464	2.137	26.33
43	4.726	4.480	3.533	2.667	0.539	23.82
146	6.770	6.689	2.720	2.430	0.635	25.23
25F	4.067	4.877	2.960	3.576	0.689	24.53
25R	1.533	1.225	3.148	11.853	1.264	23.80

## FIGURES

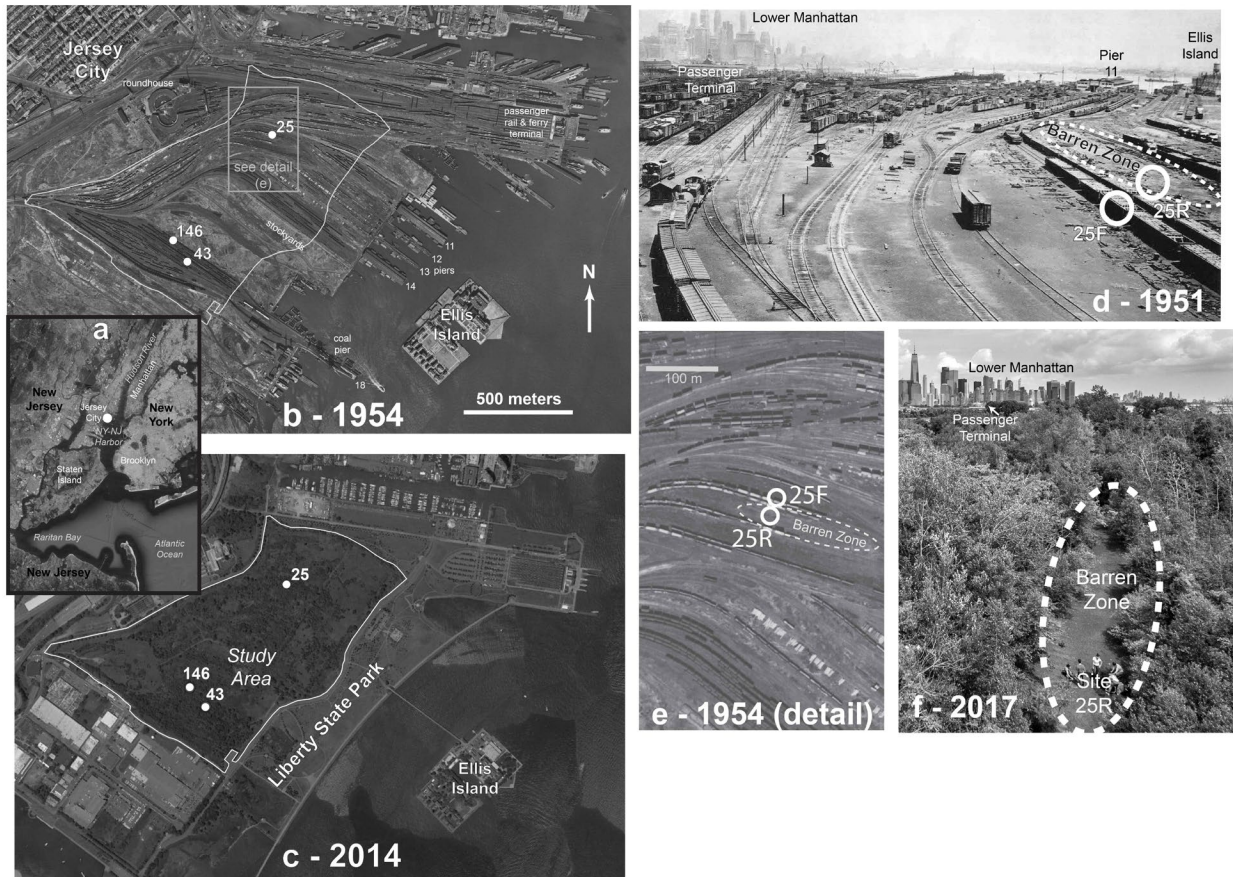


**Figure 2-1.** Liberty State Park is located in Jersey City, New Jersey (A). Aerial images from: U. S. Geological Survey: 1954 (B, E) and 2014 (C). Study sites within LSP are indicated on the map (43, 146, 25F, 25R). A historical photograph of 25F and 25R from 1951 (D). Sites 25F and 25R are adjacent; 25R is in a strip of land without vegetation (F). Photo credits: D: Andrew Bologovsky, F: Mike Peters Montclair State University

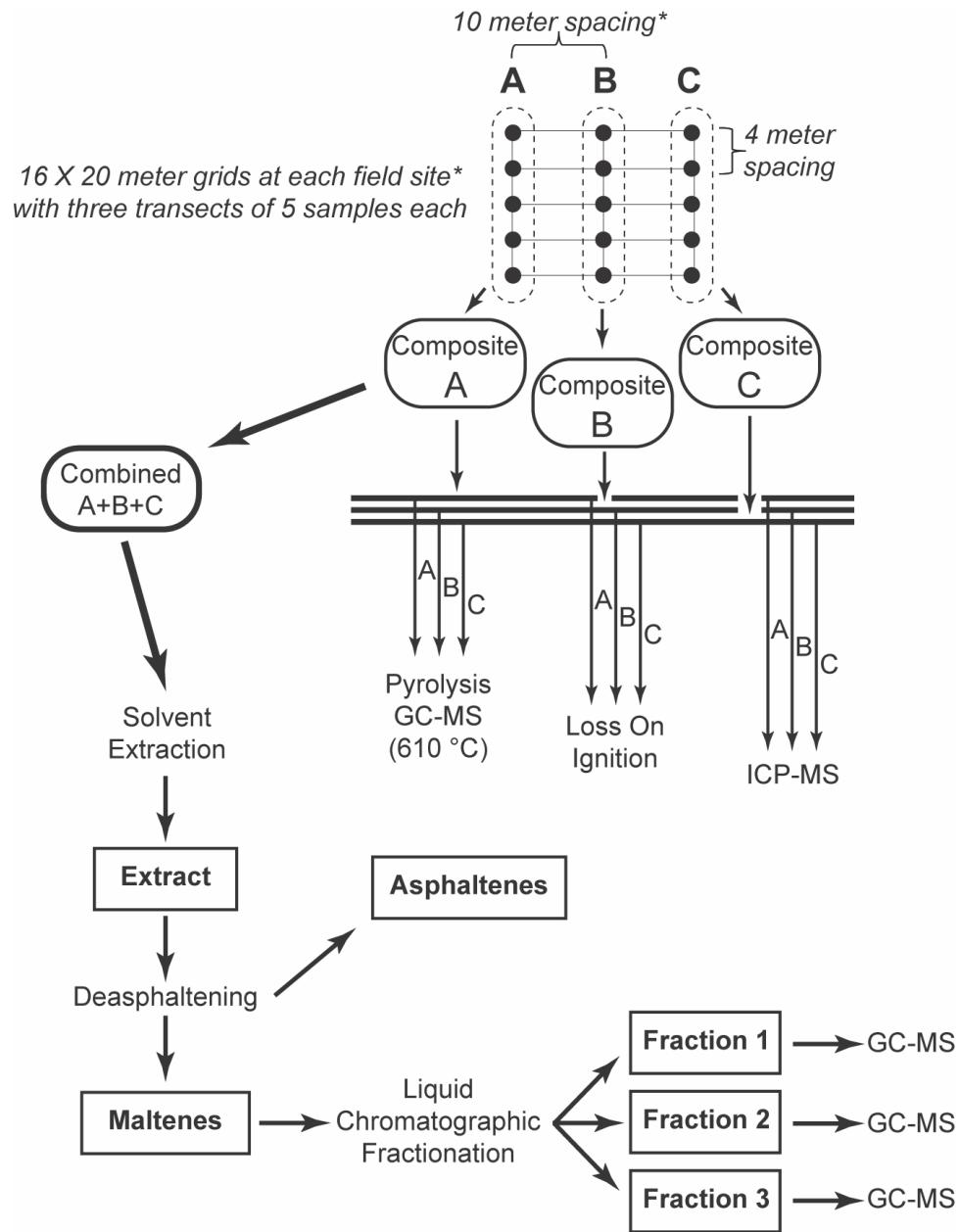


**Figure 2-2.** Flow chart illustrating the experimental design for the experiment.

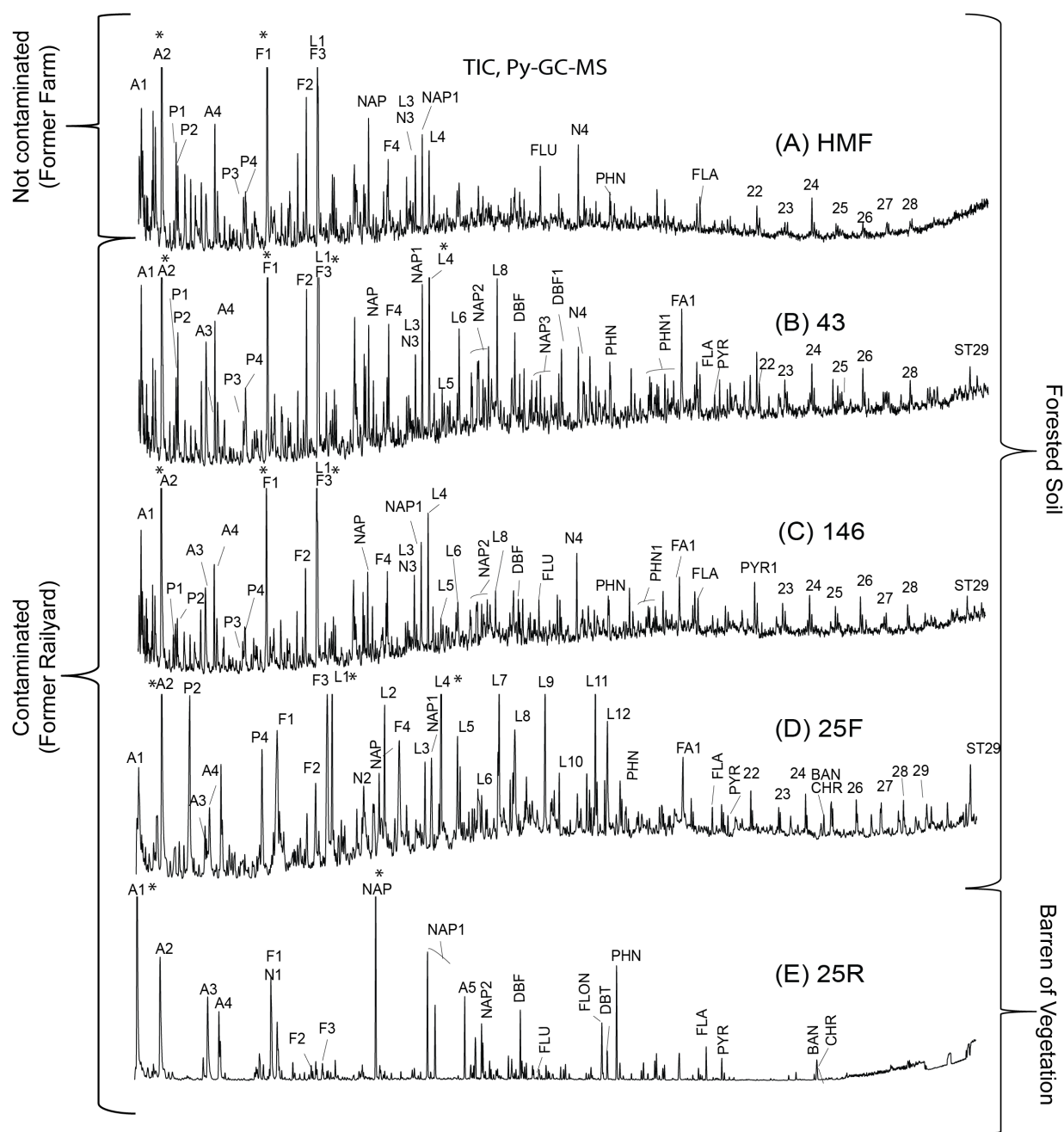


**Figure 2-3.** Total ion current (TIC) for Py-GC-MS of soil samples from sites HMF (A), 43 (B), 146 (C), 25F (D) and 25R (E). The data for 25R show predominantly mono- and polycyclic aromatic hydrocarbons and aromatic hydrocarbons. See Table 2-2 for compound symbols.

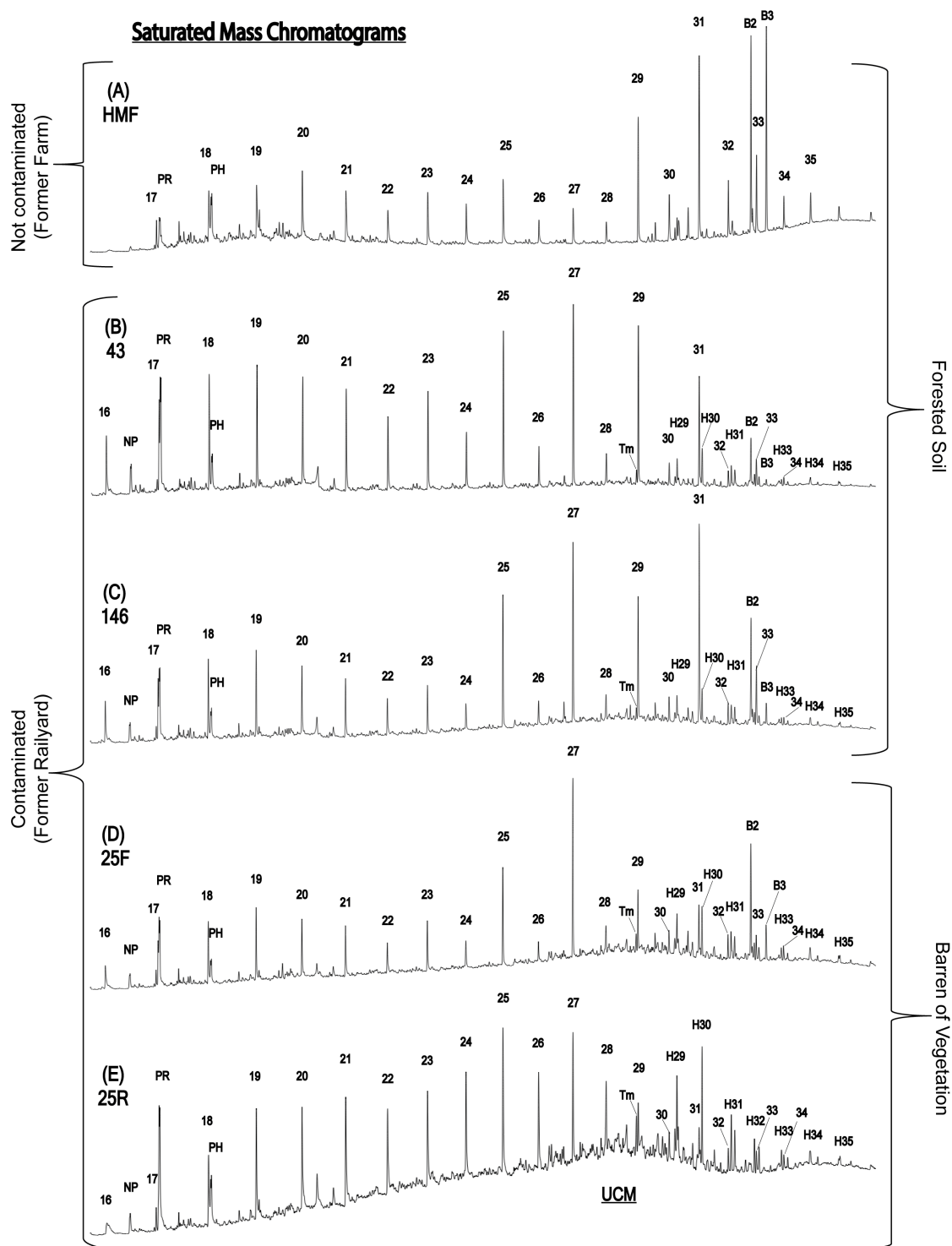


**Figure 2-4.** Total ion current (TIC) for fraction 1 of soil extracts from sites HMF (A), 43 (B), 146 (C), 25F (D), and 25R (E). The data show distributions of alkanes (normal and isoprenoid alkanes ( $m/z$  71) and triterpenoids ( $m/z$  191). See Table 2-2 for compound symbols.

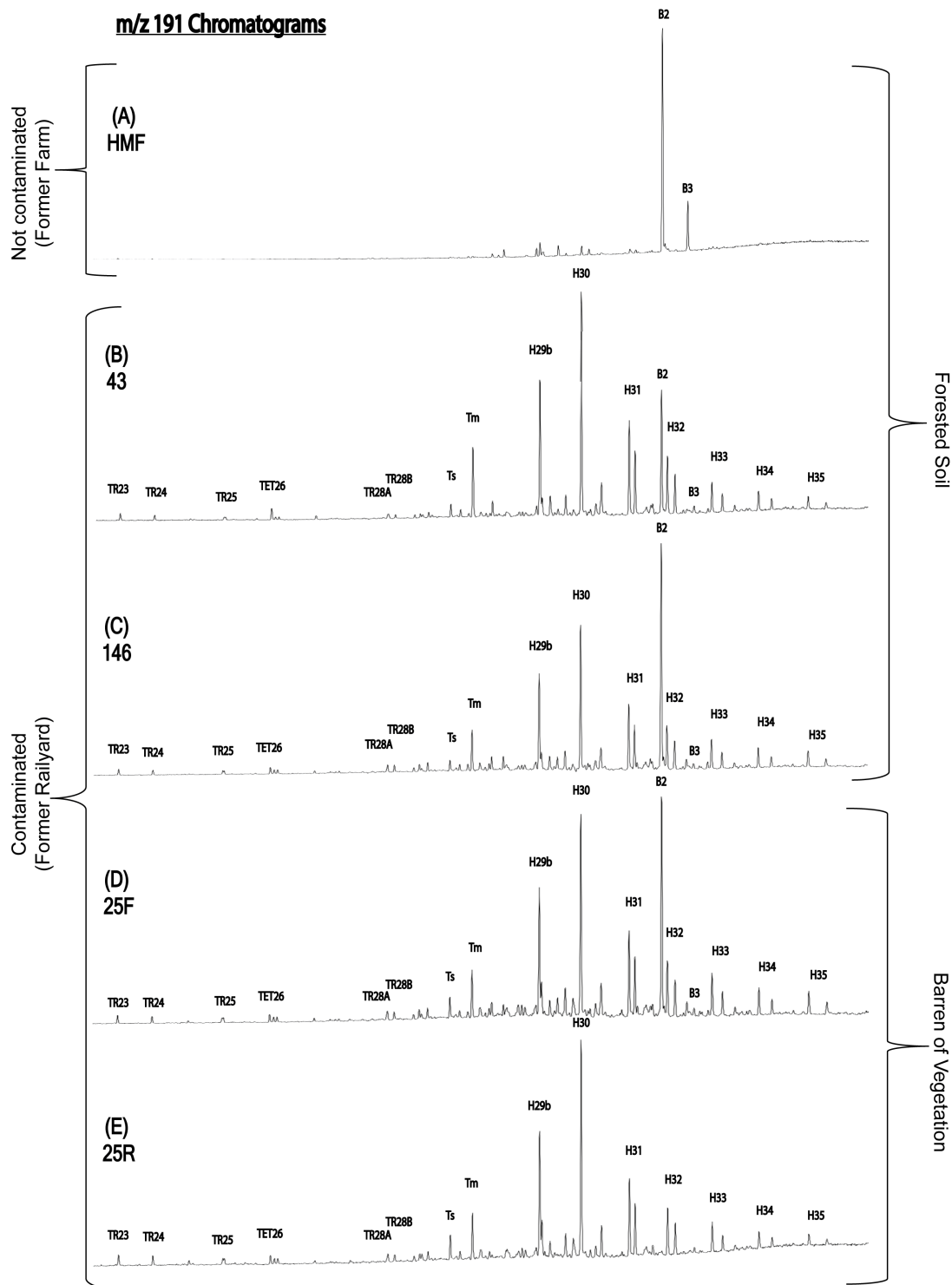


**Figure 2-5.** Mass chromatogram (m/z 191) showing the distribution of hopanes and tricyclic terpanes in the saturated fractions. The  $\beta$ -amyrin derivative is a soil microbe biomarker that was observed in all sites except for 25R. See Table 2-2 for compound symbols.

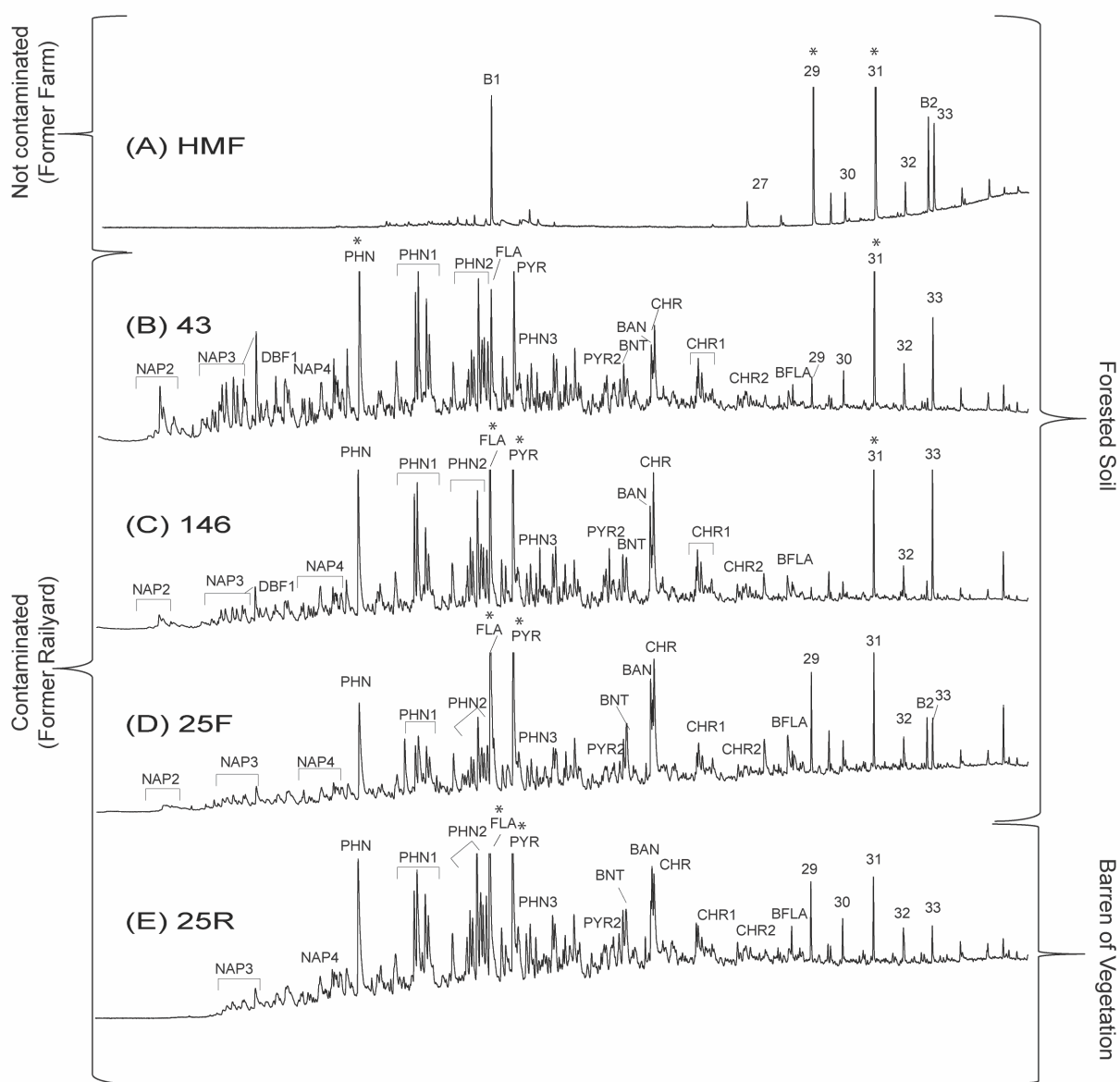


**Figure 2-6.** Total ion current (TIC) for fraction 2 of soil extracts from the HMF (A), 43 (B), 146 (C), 25F (D), and 25R (E) sites. The \* indicates the peak was taller in the original chromatogram before the top was cut off to reveal more detail for the shorter peaks. The data show fewer polycyclic aromatic hydrocarbons in HMF. Distributions of aromatic compounds are similar for chromatograms B, C, D, and E. See Table 2-2 for compound symbols.

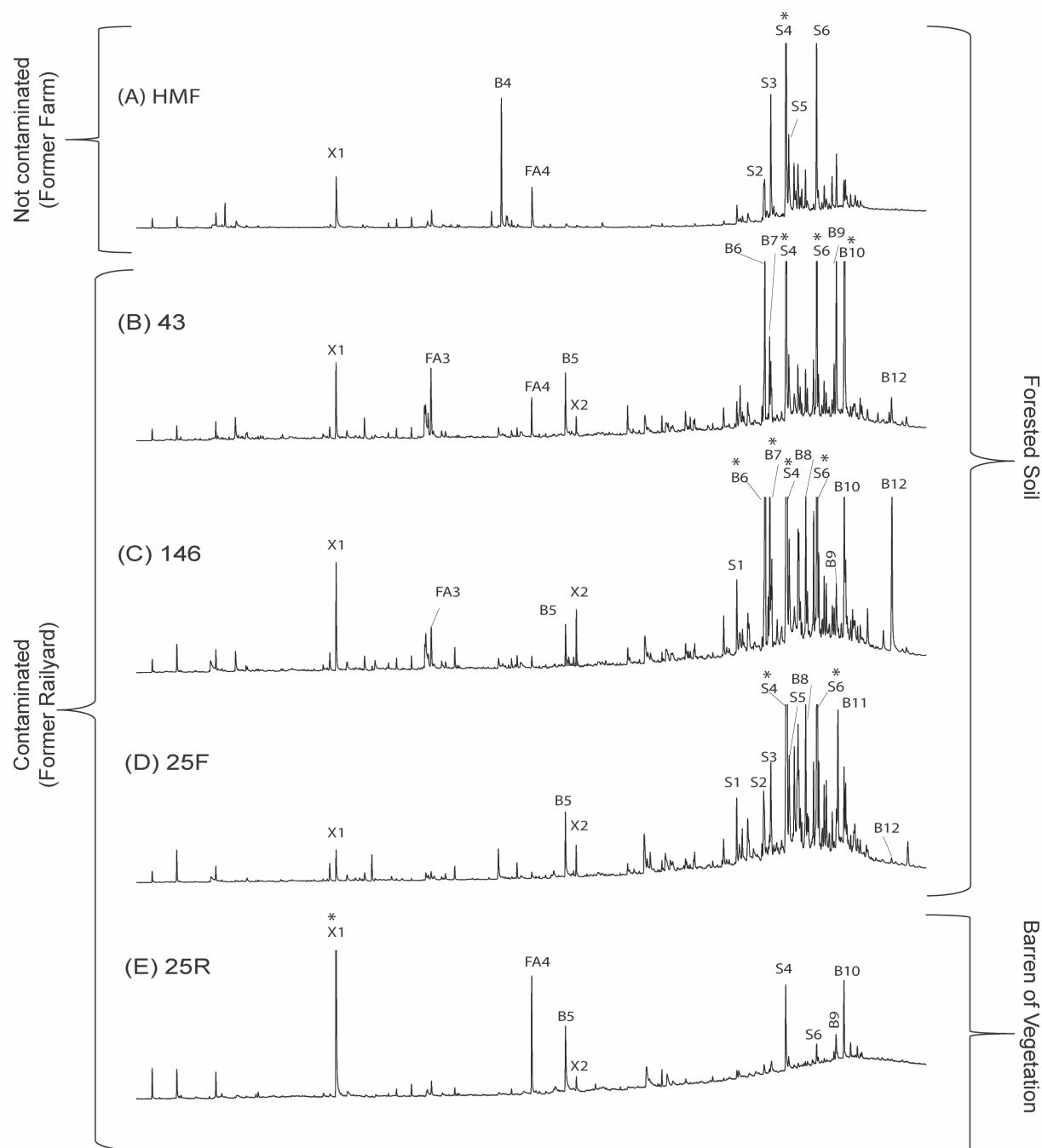


**Figure 2-7.** Total ion current (TIC) for fraction 3 of soil samples from the HMF (A), 43 (B), 146 (C), 25F (D) and 25R (E). The \* indicates the peak was taller in the original chromatogram before the top was cut off to reveal more detail for the shorter peaks. See Table 2-2 for compound symbols.

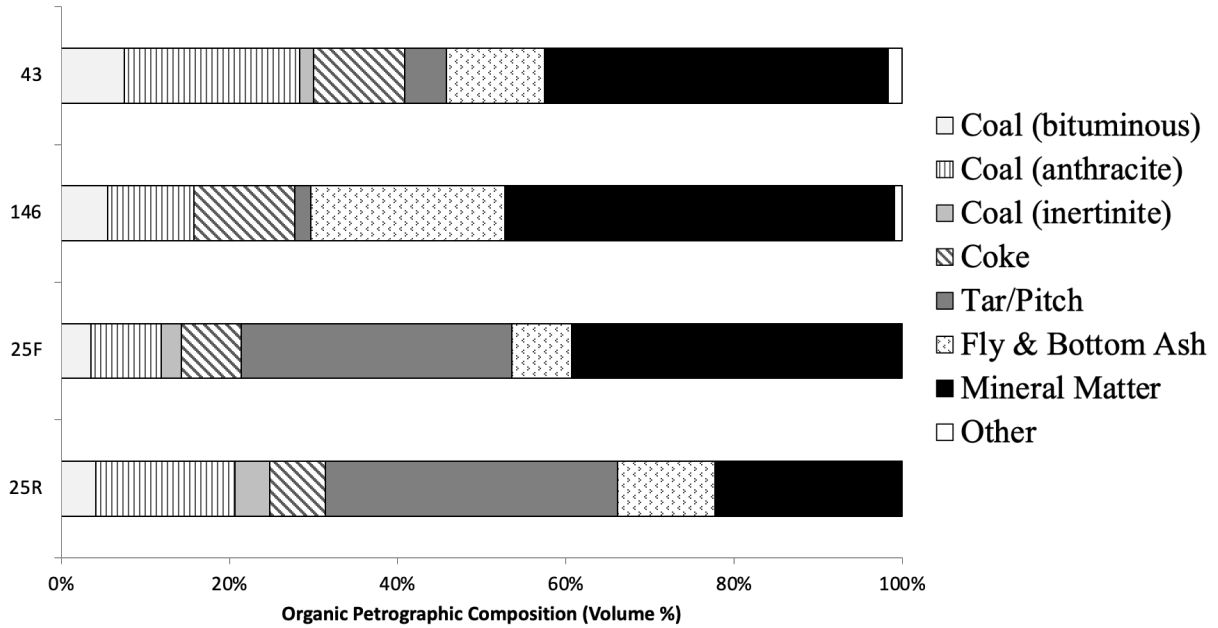


**Figure 2-8.** Organic petrographic composition (in volume %) of samples 43, 146, 25F, and 25R. The data show that 25F and 25R have more tar/pitch compared to 43 and 146. HMF soil was not analyzed for organic petrography because coal particles were not visible to the naked eye.

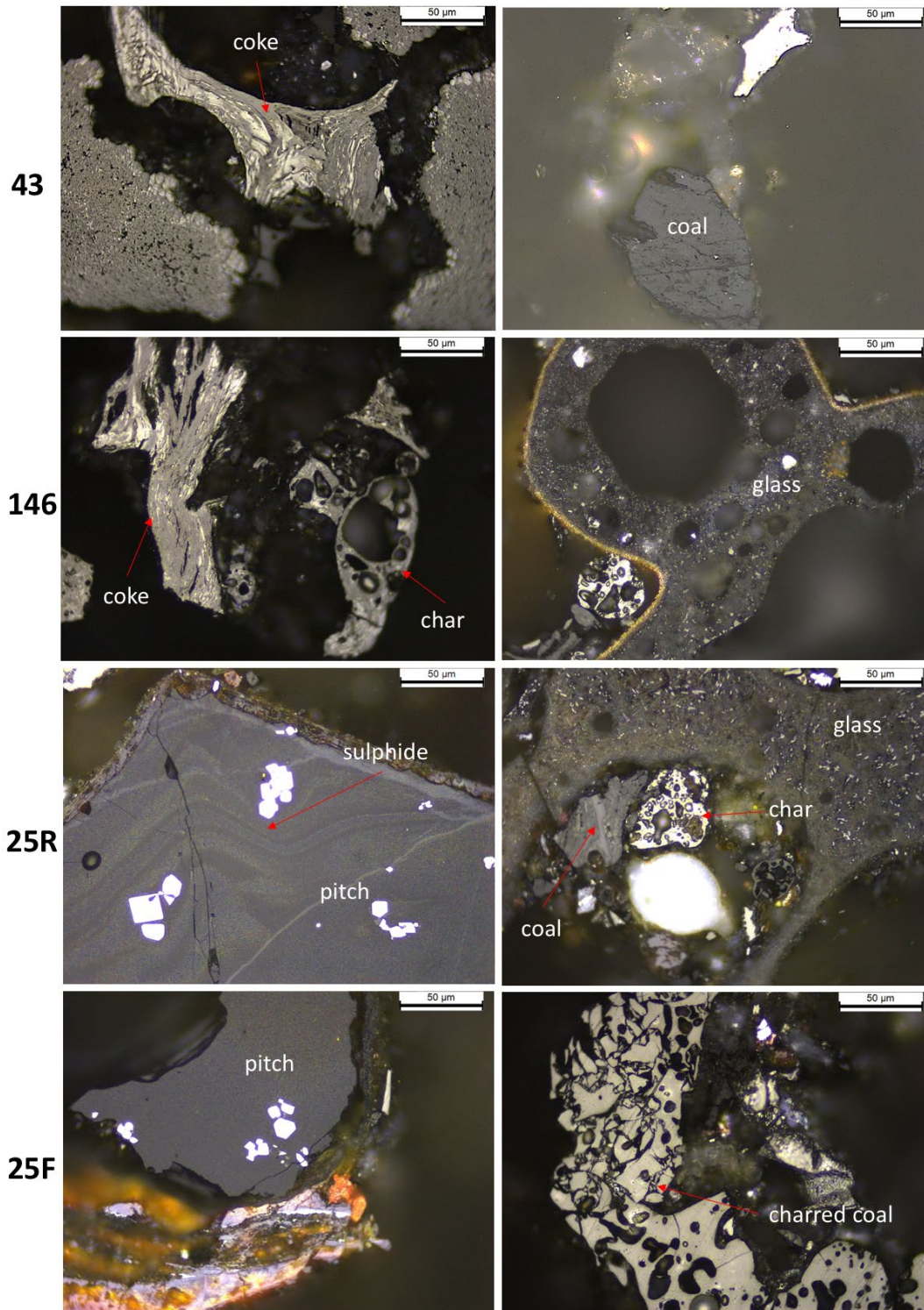


**Figure 2-9.** Examples of photomicrographs of anthropogenic particles identified in the samples. Each sample has two photomicrographs. Reflected light, oil immersion.

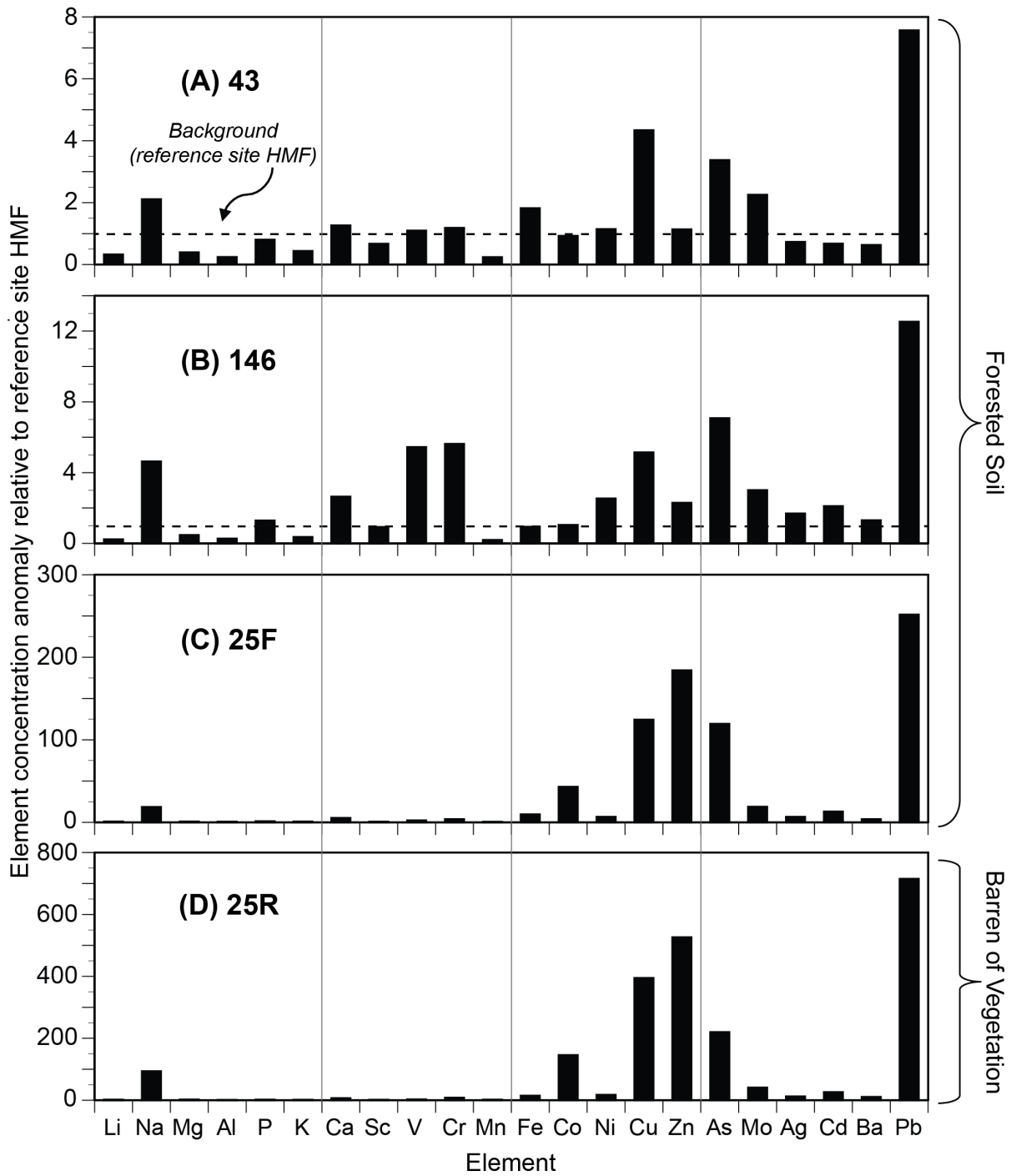


**Figure 2-10.** Elements listed in order of atomic weight normalized to HMF. The data are arranged from the lowest to the highest (43, 146, 25F and 25R) average metal concentration.

The dotted line present in A. and B. is the background HMF.

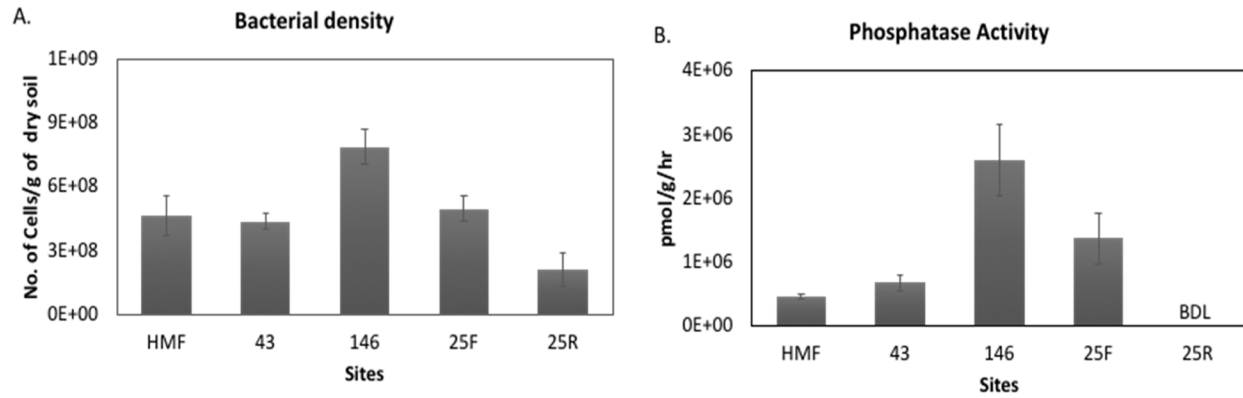


**Figure 2-11.** Bacterial density (cells/g dry soil, mean and error bars are SE;  $n = 3$ ) and phosphatase activity ( $\text{pmol} \cdot \text{g}^{-1} \cdot \text{hr}^{-1}$ , mean and error bars are SE;  $n = 3$ ) of HMF, 43, 146, 25F, and 25R soils are shown.

### Chapter 3

#### **Characterization of coal particles in the soil of a former rail yard and urban brownfield:**

##### **Liberty State Park, Jersey City (NJ), USA**

Published as: Haggmann D.F., Krüge M.A., Goodey N.M., Krumins J.A. (2020) Characterization of coal particles in the soil of a former rail yard and urban brownfield: Liberty State Park, Jersey City (NJ), USA. *International Journal of Coal Geology* 217:103328.

<https://doi.org/10.1016/j.coal.2019.103328>

#### **Abstract**

From the 1850's until the 1960's, the Central Railroad of New Jersey was among several major railways shipping anthracite and bituminous coal to the New York City area, transferring coal from railcar to barge at its extensive rail yard and port facility in Jersey City. The 490 ha Liberty State Park was developed on the site after the rail yard closed, but a ca. 100 ha brownfield zone within the park remains off limits to visitors pending future remediation. As part of an environmental forensic and industrial archeological investigation of this zone, the present study characterizes anthracite and bituminous coal particles present in abundance in the soil by scanning electron microscopy (SEM) and pyrolysis-gas chromatography-mass spectrometry (Py-GC-MS). A simple pretreatment procedure employing density separation improved the analytical results. This detailed information about the nature of contaminants at the site will help to inform the remediation effort in the public interest.

## Keywords

environmental forensics, coal, Liberty State Park, brownfield remediation, pyrolysis-gas chromatography-mass spectrometry (Py-GC-MS), density separation

### 3.1. Introduction

The Central Railroad of New Jersey (CRRNJ) was one of several major private railways operating from the mid-19th to the mid-20th century with an eastern terminus on New York Harbor and the Hudson River in the U.S. state of New Jersey (Figs. 3-1, 3-2). Typical of these intermodal operations, the CRRNJ transported freight and passengers from the interior to a vast rail yard along the shore for transfer to barges and ferries, respectively, for connection across the water to nearby New York City and points east (Anderson, 1984). Due to unfavorable economic conditions, including competition from highway transportation, all of these private railways ceased operations during the mid-20th century. Some of the lines were subsequently incorporated into the New Jersey Transit regional system, which still maintains a rail-to-ferry passenger service out of the historic station in Hoboken (NJ). CRRNJ's Jersey City station was restored as a tourist attraction but no longer operates, as the tracks were removed when the rail yard was abandoned in the late 1960's and subsequently converted into Liberty State Park (LSP) (Gallagher et al., 2008a; b). The park takes its name from the iconic Statue of Liberty, situated about 600 m across the water at its closest point, allowing park visitors a dramatic view of the rear of the colossus.

Figure 3-1

Figure 3-2

Coal transport was a major component of CRRNJ operations, for example, producing about 26 % of the company's total revenue in 1943, with 28 % of the coal moving via Pier 18 and its dedicated network of tracks at that time (Figs. 3-2, 3-3). The railroad conveyed anthracite coal (Fig. 3-3A) from its own mines in eastern Pennsylvania and also hauled bituminous coal trains originating further west belonging to other companies. Relative tonnages of anthracite and bituminous coals were roughly the same, varying over time with market demand. Arriving at Pier 18, massive coal dumping structures transferred the cargo to waiting coal barges (Figs. 3-3B-D) (Anderson, 1984).

Figure 3-3

After the rail yard and its piers were closed and dismantled, the state of New Jersey acquired the land and created the 490 ha LSP. About 100 ha of the park remains an unremediated brownfield site, off limits to the public and constituting the study area of this project (Fig. 3-4A). In recent years, the site's botanical succession, soil microbiology, and contaminant geochemistry have been extensively studied (e.g., Gallagher et al., 2008a; b; 2018; Hagmann et al., 2015; Hagmann et al., 2019 *see Ch. 2*; Krumins et al., 2015; Singh et al., 2019a; b). In spite of evident inorganic and organic contamination, including abundant visible coal fragments in the soil, most of the restricted zone supports lush plant life, the product of natural, passive revegetation over a half century (Figs. 3-4B, C).

Figure 3-4

Unburned coal, particularly of high volatile bituminous rank, contains high concentrations of polycyclic aromatic hydrocarbons (PAHs) among other compounds (Stout and Emsbo-Mattingly, 2008; Laumann et al., 2011). While PAHs in soils may affect plant health (Brooks, 2004; Smith et al., 2006), the extent to which this is an environmental concern in this

case is linked to the degree of PAH bioavailability and biodegradability if sequestered within coal particles in soil (Stout and Emsbo-Mattingly, 2008; Yang et al., 2008a; b; Achten and Hofmann, 2009; Achten et al., 2011; Fabiańska et al., 2016; Hindersmann and Achten, 2018; Nádudvari et al., 2018a; b). Haggmann et al. (2019; *see Ch. 2*) undertook an environmental forensic investigation of coal-contaminated soils from the LSP brownfield site, describing in detail the distribution of saturated and aromatic hydrocarbons, heavy metals, and coal macerals. However, they used only the < 2 mm particle size fraction, to the exclusion of the visible coal particles evident during field sampling. The present study re-examines soils from two of the investigated sampling locales within LSP (Fig. 3-2), this time considering the full particle size range with emphasis on coal, to aid in future remediation of the brownfield.

Micro-scale analytical pyrolysis-gas chromatography-mass spectrometry (Py-GC-MS) has been shown to provide a rapid, reproducible means of chemically characterizing a wide variety of solid organic matter types with minimal sample preparation (Wampler, 2007). Py-GC-MS has increasingly been applied to environmental investigation of soils and sediments (summarized in Krüge, 2015), specifically including brownfield studies (Lara-Gonzalo et al., 2015) and environmental forensics (Krüge et al., 2018). It is utilized here for the direct, qualitative characterization of coal particles and coal-contaminated soil.

Sedimentary petrologists have long favored density separation for isolating heavy minerals from sandstones for microscopic evaluation (e.g., Boggs, 2009). It has also been employed extensively in coal studies, evolving into the use of the sophisticated analytical technique of density gradient centrifugation for the separation of coal and kerogen macerals (e.g., Dyrkacz and Horwitz, 1982; Crelling, 1988; 1989; Stankiewicz et al., 1994a;b; Krüge et al.,

1997). In the present study, a simple floatation method was employed to isolate soil organic matter and various coal types to improve the chemical characterization results.

The restricted zone of LSP is slated for gradual remediation into managed wetland, grassland, and forest with public access (McDonald, 2018). The environmental forensic and industrial archeological approach of the present study will help to inform the remediation effort in the public interest.

## **3.2. Methods**

### **3.2.1. Site description**

Soils for this study were collected within LSP in Jersey City (NJ, USA) include soil from vegetated Site 43, formerly beneath a railroad track, and soil from Site 25R taken on what remains an anomalously barren strip of land formerly between railroad tracks (Figs. 3-1 thru 3-4). These sites are inside the unremediated, restricted-access 100-ha zone of the park. The railroad tracks and their crossties were removed around the time the railyard was abandoned in the late 1960s. Since the railyard was abandoned, a dense forest consisting mostly of hardwood and herbaceous assemblages naturally grew within the restricted-access area (Gallagher et al., 2008a; b) (Figs. 3-4A-C).

### **3.2.2. Soil collection**

Soil was collected from LSP sites 43 and 25R from below the leaf litter to a depth of 10 cm and stored in at 4 °C. Sample coordinates were determined by reference to Global Positioning System (GPS) satellite signals in the field, transferred to aerial imagery using the Google Earth application, and carefully matched by graphical overlay to the 1954 aerial image

(Fig. 3-2) in the U.S. Geological Survey archives ([earthexplorer.usgs.gov](http://earthexplorer.usgs.gov)) as previously detailed (Hagmann et al., 2019; *see Ch.2 Fig. 2-1*).

### 3.2.3. Hand-picked coal and plant material

Vegetation detritus from LSP site 43 was hand-picked from whole soil. This plant material, which consisted of roots and twigs, were rinsed in deionized (DI) water and dried (40 °C overnight). In another procedure, soil samples from sites 25R and 43 were wet-sieved through a 2 mm sieve and sonicated in DI water. The > 2 mm fraction was further separated into the following categories based on visual inspection under a binocular microscope: coal, coke, and combustion spherules. Coal particles from both sites (2 to 10 mm in size) were designated for further processing, as described in Sections 2.4 and 2.6 (Fig. 3-5).

Figure 3-5.

### 3.2.4. Scanning electron microscopy (SEM)

Before SEM, the hand-picked coal particles were individually air-dried and gently crushed using a mortar and pestle. Fragments of a single coal particle were spread on the carbon tape and then loaded on the SEM sample stub. After applying a thin layer of carbon film under a Denton Desk 4 coater, the fragments were observed by the Hitachi S-3400N SEM and with Bruker –AXS Energy Dispersive X-Ray Spectroscopy (EDS) detector.

### 3.2.5. Soil separation by density

Soils from both sites were also separated based on density (Fig. 3-5). First, dried whole soil (40 °C overnight) was ground using a mortar and pestle to pass through a 1 mm sieve. A 5 g aliquot was placed in 10 mL of DI water (1.0 g/mL) and the floating material after centrifugation was collected (Fraction 1). An aqueous potassium iodide (ACS Reagent Grade, Ricca Chemical, Fisher Scientific) solution (1.6 g/mL in DI water, 10 mL) was added to the remaining soil (i.e., the sink material after Fraction 1 was removed). The particles that were floating after centrifugation were collected in filter paper and rinsed with DI water (Fraction 2). Finally, the remaining residue was rinsed with DI water and collected (Fraction 3). For each fraction, the suspension was thoroughly mixed and then centrifuged at 4,000 rpm for 15 minutes. Aliquots of Fraction 3 residues were analyzed by SEM, following the procedure outlined in Section 2.4. Fraction 1 was predicted to contain the natural biomass that floats in water, Fraction 2 was expected to include the coal particles that float in the dense aqueous KI solution, while Fraction 3 should include the soil mineral matter that is too dense to float in either liquid.

### 3.2.6. Pyrolysis-Gas Chromatography-Mass Spectrometry (Py-GC-MS)

The hand-selected vegetation detritus was crushed using a mortar and pestle and analyzed by Py-GC-MS (Fig. 3-5). Several of the hand-picked coal particles were individually crushed using a mortar and pestle and separately analyzed by Py-GC-MS. These included ten individual coal particles from site 43 and three coal particles from site 25R. Whole soil samples and each of the three fractions separated by density from LSP sites 43 and 25R were also pyrolyzed. For quality control, Py-GC-MS of the 25R whole soil was performed twice. Py-GC-MS was accomplished using a CDS 5150 Pyroprobe (CDS Analytical Inc., Oxford, PA) coupled to a

Thermo Finnigan Focus DSQ GC/MS (Thermo Electron Corporation, Madison, WI) equipped with an Agilent DB-1MS column (30 m × 0.25 mm i.d. × 0.25 μm film thickness). The GC oven temperature was programmed from 50 °C to 300 °C (at 5 °C min<sup>-1</sup>), with an initial hold of 5 min at 50 °C and a final hold of 15 min at 300 °C. Pyrolysis was performed for 20 s at 610 °C. The MS was operated in full scan mode (50-500 Da, 1.08 scans s<sup>-1</sup>). The MS was calibrated by autotuning with PFTBA and blanks were run each day before samples were analyzed. Compounds were identified using the W8N08 mass spectral library (John Wiley and Sons, Inc., New York, NY), the online NIST Standard Reference Database Number 69 ([webbook.nist.gov/chemistry/](http://webbook.nist.gov/chemistry/)), and by reference to the literature. For this study, no internal or external standards were employed, thus no attempts at quantitative determination were made.

### 3.3. Results and discussion

#### 3.3.1. SEM of coal particles

Hand-selected coal particles from the > 2 mm fraction of soil from LSP site 43 were imaged using SEM, revealing surface encrustations that had resisted sonication (Fig. 3-6). The EDS mapping indicated that the encrustations like those imaged in Figure 3-7 are aluminosilicate phases (strong Si, Al, and O spectral signals) adhering to the coal. The overlapping spectral signals (Fig. 3-7B) can more clearly be seen in the individual mapping of Al and Si (Figs. 3-7C, D). Other hand-picked coal particles from LSP sites 43 and 25R produced similar SEM images. EDS also detected Fe and S in molar abundances roughly the same as those of Si and Al.

Figure 3-6

Figure 3-7

Using organic petrography, Hagemann and co-workers demonstrated that the < 2 mm size fraction of the site 43 soil contained about 32 % detrital clay by volume (Hagemann et al., 2019; *see Ch. 2 Fig. 2-8*). It is likely therefore that the aluminosilicate phases observed by SEM are clays. EDS spectra show approximately equal molar amounts of Si and Al, as well as an absence of K and Na. This suggests that the observed clays are most likely kaolinite (Welton, 1984). The iron and sulfur might be present as pyrite or a weathered derivative, however this was not confirmed petrographically.

The aluminosilicate clay encrustations present on the site 43 and 25R coal particles, such as those seen in Figures 3-6 and 3-7, have been interpreted as hallmarks of coal weathering in that oxidation allows clay minerals to better adhere to the coal surface (Xia et al., 2014, Xia & Yang, 2014). The LSP samples are from the top 10 cm of the soil profile. Thus the coal particles were likely subjected to weathering over a half century or more, having been exposed to atmospheric O<sub>2</sub> in soil pore spaces, infiltrating meteoric water, seasonal temperature swings, and action by resident soil microbes. If the coal particles had been weathered chemically as well as physically, their composition would obviously have been affected. The particles were therefore subjected to chemical analysis in part to determine if this indeed had been the case (Sec. 3.2).

### 3.3.2. Py-GC-MS of coal particles and plant material

The pyrolysis products of the vegetation detritus from site 43 included lignin marker compounds [methoxyphenols, labeled as chromatographic peaks L1-L15], polysaccharide derivatives [P1-P6], phenols [F1-F3], long-chain aliphatic hydrocarbons [^], steroids [S1, S2], and triterpenoids similar to  $\beta$ -amyrone [BAM] (Fig. 3-8A, Table 3-1). Ten coal particles were analyzed by Py-GC-MS. Nine of them had pyrograms resembling the one in Figure 3-8B,

essentially showing only the simple monoaromatic hydrocarbons benzene [A1], toluene [A2], and alkylated benzenes [A3-A6]. Only one out of ten site 43 coal particles had a distinctly different pyrogram (Fig. 3-8C). This much more complex pyrolyzate, in addition to the monoaromatics [A1-A7], contained phenol and alkylated phenols [F1-F8], dibenzofuran [DBF], alkylated dibenzofurans [DBFx], parent and alkylated PAHs including naphthalenes [Nx], phenanthrenes [PHNx], fluorene [FLU], pyrenes [PYRx], and chrysenes [CHRx]. The alkylated PAHs were relatively more abundant than the parent compounds, and pristane predominated over phytane.

Figure 3-8

Table 3-1

The lignin and polysaccharide marker compounds present in the pyrolyzate of the plant material (Fig. 3-8A), which is comprised of roots and twigs, are those typical of vegetation and forest soil biomass (e.g., Saiz-Jiménez & de Leeuw, 1986; Hempfling & Schulten, 1990; Kuder & Krüge, 1998; Kuroda & Nakagawa-izumi, 2006). The steroids and triterpenoids likely derive from the plant matter and/or soil microbes (Hagmann et al., 2019, *see Ch. 2*). Fresh and degraded plant materials obviously constitute important, non-contaminant soil components, which furthermore produce strong pyrolytic signatures. In their prior study, Hagmann and co-workers (2019) pyrolyzed whole LSP soils, yielding results in which the contaminant signals were mixed with those of the natural vegetation present (Hagmann et al., 2019, *see Ch. 2*). One objective of the present study is the isolation of the coal contaminant signatures from that of the plant material, for which the first step is the characterization of the individual components. The

next step (Section 3.3) is the experimental attempt to isolate these soil constituents by density separation.

It was assumed that the coal particles hand-picked from the soil samples (Sec. 2.3) would include coals of different ranks since the historical record documents bulk transport of bituminous and anthracite by coal-fired locomotives (Anderson, 1984). One coal particle (Fig. 3-8B) produced simple alkylated benzenes nearly exclusively upon pyrolysis, consistent with previously documented anthracite coal pyrolyzates (Xu et al., 2017). Organic petrography indicated the presence of inertinite-dominant coal particles in soil samples from Site 43 (Hagmann et al., 2019, *see Ch. 2 Fig. 2-8*) but inertinite pyrolysis products are considerably more complex (Stankiewicz et al., 1994a). Therefore, this coal particle and the other eight yielding similar pyrograms are all deemed to be anthracite by their distinctive pyrolytic fingerprint (although in the absence of confirmation by organic petrology or proximate and ultimate analysis). The sample shown in the SEM images (Figs. 3-6, 3-7) is one of these eight particles. About 70% of the coal at this site was previously determined to be anthracite by petrographic examination (Hagmann et al., 2019, *see Ch. 2 Fig. 2-8*), so it would not be surprising that most of the hand-picked coal particles in the present study would be anthracite.

Pyrolysis products from the remaining coal particle (Fig. 3-8C) closely resemble those of bituminous coal (Hatcher et al., 1992; Kruege & Bensley, 1994; Stankiewicz et al., 1994a; b; Laumann et al., 2011). These authors attest to the singular importance of oxygenated compounds in high-volatile bituminous coal pyrolyzates, in particular the phenols, as well as secondary amounts of dibenzofurans. These compounds are clearly evident in this particle's pyrolyzate [F1-F7, DBF1, DBF2]. Alkyl naphthalenes are also important components of bituminous coal pyrolyzates (Hatcher et al., 1992; Kruege & Bensley, 1994; Stankiewicz et al.,

1994a) and are among the most abundant [N0-N3] in the present example (Fig. 3-8C). These same authors also demonstrated that pyrolytic phenols predominate when analyzing vitrinite of lower rank high volatile bituminous coals. However, in pyrolyzates of coals of increasing rank, the relative importance of the phenols is progressively reduced, while both parent and alkylated PAHs become more evident (Kruge & Bensley, 1994; Laumann et al., 2011). Although phenols [F1-F7] are very significant components in the present case (Fig. 3-8C), the prevalence of naphthalenes [N0-N3], and larger parent and alkyl-PAHs including the phenanthrenes [PAHx], pyrenes [PYRx], and chrysenes [CHRx] suggest that this is likely to be a higher rank bituminous coal. Previous petrographic examination (Hagmann et al., 2019, *see Ch. 2 Fig. 2-8*) indicated that 17% of the coal in the site 43 soil was medium volatile bituminous while only 8% was high volatile. The particle in this case (Fig. 3-8C) is likely to be medium volatile based on its pyrolytic signature. Pyrolysis did not reveal marked evidence of chemical weathering, such as oxygenated PAHs.

### 3.3.3. Density separation of soil

Whole soils from vegetated site 43 and barren site 25R were separated into three fractions based on density (Fig. 3-5, Table 3-2). To achieve a clean signal for the coal Py-GC-MS fingerprints, the plant material, predicted to be Fraction 1, needed to be separated from the coal particles, expected in Fraction 2, as explained in Section 3.3.2. The residue material anticipated in Fraction 3 was anticipated to confirm that the coal particles had been successfully isolated in Fraction 2. The site 25R soil yielded only 0.06 % by weight of light Fraction 1 while site 43 yielded 0.39 %. LSP site 43 had more of the intermediate Fraction 2 (3.10 %) compared to site

25R (0.89 %). For both sites, most of the material remained in the heavy third fraction (92.6 and 95.9 %, respectively, for 43 and 25R).

Table 3-2

Previous work (on the < 2 mm size fraction) indicated that the LSP soil samples were rich in organic matter (soil biomass plus coal, coke and char). Site 43 soil was found to consist of about 30 % by weight of organic matter, while 25R had about 11 % (Hagmann et al., 2019, *see Ch. 2 Table 2-1*). Therefore the low Fraction 1 and 2 yields (Table 3-2) appear incongruous at first glance. With bituminous coal and anthracite having specific densities of 1.32 and 1.47 g/mL, respectively (Flores, 2013; Wood et al., 1983), the KI solution with a density of 1.6 g/mL employed in the present experiment was expected to be adequate for the floatation of both types of coal. However, based on the SEM observations (Figs. 3-6, 3-7), stubbornly adhering mineral phases evidently precluded a complete isolation of coal fragments by density, relegating most of the material to the third (residual) fraction (Table 3-2). Adhering or embedded minerals increase the bulk density of the coal particles, perturbing the outcome of float-sink procedures (Garcia et al., 1991; Stankiewicz et al., 1994b; Suárez-Ruiz & Crelling, 2008). SEM examination of the residual fraction did indeed reveal abundant, widely-distributed mineral matter for both soil samples. A more rigorous attempt to isolate the organic materials from the minerals by a micronization pretreatment was beyond the scope of this project.

#### 3.3.4. Py-GC-MS of soil density fractions

To investigate their organic chemical composition in detail, whole soil and each density fraction were subjected to Py-GC-MS (Fig. 3-5). Results from the two field sites are presented separately.

#### 3.3.4.1. Forested site 43 soil

Upon pyrolysis, forested site 43's whole soil revealed a predominance of simple alkylbenzenes and naphthalenes [A1-A7, N0-N3] (Fig. 3-9A). Notable minor components include polysaccharide and lignin marker compounds [P1-P3, L1], phenols [F1-F5], dibenzofurans [DBFx], PAHs [FLUx, PHNx, FLA, PYR, CHR], diketodipyrrole [DKDP] and long-chain *n*-alkanes [+]. Haggmann and co-workers (2019) noted a greater prevalence of polysaccharide and lignin markers, as well as phenols in site 43 soil pyrolyzates, but it must be kept in mind that they analyzed only the < 2 mm soil size fraction (Haggmann et al., 2019; *see Ch. 2 Fig. 2-3*). The site 43 density Fraction 1 pyrolyzate is distinctly different from the whole soil, with lignin and polysaccharide markers dominant [L1-L15, P1-P6], along with phenols [F1-F8], diketodipyrrole [DKDP], fatty acids [FA1-FA3], long-chain *n*-alkenes [^], and sterols [S1, S2] (Fig. 3-9B).

#### Figure 3-9

The complex pyrolyzate of Site 43's Fraction 2 has an overwhelmingly aromatic signature (Fig. 3-9C). Significant compounds include monoaromatic hydrocarbons [A1-A7], phenols [F1-F8], naphthalenes [N0-N3], dibenzofurans [DBFx], and parent and alkylated PAHs [FLU1, PHNx, PYRx, CHRx, BeP]. *n*-Alkanes [+] and triterpenoids [BAM] are also noteworthy. In contradistinction, Fraction 3 produced mostly monoaromatic hydrocarbons [A1-A7] upon pyrolysis, accompanied by naphthalenes [N0-N2] with relatively minor phenols [F1-F3] and aliphatics [+] (Fig. 3-9D).

#### 3.3.4.2. Barren site 25R soil

Site 25R is anomalously free of plant life (Fig. 3-4D), standing in stark contrast to its lushly vegetated surroundings (Fig. 3-4B, C). Hagemann et al. (2019), *see Ch. 2*, concluded that this is primarily due to the extraordinarily high heavy metal contamination of this narrow strip of land, formerly between train tracks (Fig. 3-2) which were removed when the railyard was closed in the 1960's (Gallagher et al., 2008a). The abundant coal particles in its soil are the subject of the present study.

Simple monoaromatic [A1-A9] and diaromatic [N0-N2, BB0] compounds with a trace of phenanthrene [PHN] comprise nearly all of site 25R's whole soil pyrolyzate (Fig. 3-10A). This site's < 2 mm soil size fraction previously pyrolyzed (Hagemann et al., 2019, *see Ch. 2*) yielded similar results but with a distinct shift towards the heavier aromatics. The first density fraction (Fig. 3-10B) produced a contrastingly complex distribution of pyrolysis products, in particular, monoaromatics [A1-A5], polysaccharide and lignin markers [P1-P6, L1-L15], phenols [F1-F8], diketodipyrrole [DKDP], fatty acids [FA1-FA3], and steroids [S1-S3].

#### Figure 3-10

The second density fraction's pyrogram is also complex, but indicates a very different distribution of compounds (Fig. 3-10C). Monoaromatic [A1-A7] and diaromatic [N0-N3, BB1] hydrocarbons predominate, along with phenols [F1-F8]. Three to five-ring aromatic compounds are also in evidence, notably dibenzofurans [DBFx], phenanthrenes [PHNx], pyrenes [PYRx], chrysenes [CHRx], and benzo[*e*]pyrene [BeP]. Pristane [Pr] and *n*-alkanes [+] attest to a minor aliphatic component. The third, residual density fraction offered a very limited yield upon pyrolysis, mostly benzene [A1], a few other monoaromatics [A2-A5] and naphthalene [N0] (Fig. 3-10D).

### 3.3.4.3. Coal contamination in soil: Insights from Py-GC-MS of density fractions

A temperate forest soil is naturally rich in organic material, with roots, leaf litter, humus, fungi, and soil microbes. Forested soils in LSP have an anomalously high organic matter content: 30 % by weight in the case of site 43 compared to a natural background value of about 7.5 %, attributed to the additional burden of coal, coke and char contamination therein (Hagmann et al., 2019, *see Ch. 2 Table 2-1*). Pyrolysis of the whole soil should therefore yield a complex mixture of products from all organic materials present, in proportion to the relative amounts of each type. Pyrolysis proneness should also be considered as wood and coal would yield abundant pyrolysis products, whereas coke and char would not. The combined effect can be seen in Figure 3-9A, showing aromatic hydrocarbons together with polysaccharide and lignin marker compounds in site 43's whole soil pyrolyzate.

The soil density fractionation experiment was undertaken in an attempt to separate the soil's organic components to improve the specificity of the subsequent chemical analyses. A critical factor was the isolation of the soil biomass from the fossil fuel contaminants present. The pyrolysis products of the first density fractions of both soils (Figs. 3-9B, 3-10B) closely resemble those of the soil vegetation detritus (Fig. 3-8A) in the predominance of lignin and polysaccharide markers and steroids. Therefore, plant matter is evidently the main component of the light fraction in both cases. The presence of diketodipyrrole [DKDP] – a known protein pyrolysis product (Orsini et al., 2017) – and relatively more fatty acids in the density fractions is most likely due to soil microbial contributions. Although site 25R is barren of plant life, trace amounts of biomass were detected in its soil (Fig. 3-10B, Table 3-2), likely derived from the adjacent vegetated areas (Fig. 3-4D).

The second density fractions of both soils also produced very similar pyrolyzates (Figs. 3-9C, 3-10C). As described above, their pyrograms both show a predominance of mono- and diaromatic hydrocarbons, and phenols, along with parent and alkylated PAHs. The polysaccharide and lignin markers compounds characteristic of the vegetation debris are not detected. These distributions in turn closely resemble those derived from the medium volatile bituminous coal particle (Fig. 3-8C). It can be concluded that the second density fractions are predominantly bituminous coal. The triterpenoids [BAM] evident in soil 43's pyrogram likely indicate some, perhaps degraded, biomass contribution (Fig. 3-9C).

The third density fractions are alike in that their pyrolyzates contain predominantly simple monoaromatic hydrocarbons (Figs. 3-9D, 3-10D). They bear a strong resemblance to the anthracite pyrolysis products (Fig. 3-8B), indicating that anthracite is the primary pyrolyzable component therein. The presence of anthracite in this residual density fraction is likely due to the added mass of adhering mineral phases, as observed by SEM (Figs. 3-6, 3-7), precluding floatation in the 1.6 g/mL fluid employed. The site 43 pyrogram shows more of the alkylbenzenes and naphthalenes, along with trace amounts of phenols, suggesting that some bituminous coal is also present in this fraction, similarly burdened with mineral matter. The minor C<sub>11</sub>-C<sub>26</sub> *n*-alkanes detected (Fig. 3-9D) may arise from petroleum or coal tar-derived contamination in the soil adhering to mineral phases. Solvent extraction to test this supposition was beyond the scope of this project, but it is compatible with the conclusions of the prior study which did employ extraction and subsequent GC-MS (Hagmann et al., 2019, *see Ch. 2*). This prior work also documented the presence of coke and char in these soils, confirmed during the hand-picking procedure of the present study (Sec. 2.3), but these materials yield little upon pyrolysis and thus escape detection by Py-GC-MS.

### 3.4. Conclusions

Analytical pyrolysis provided compelling evidence for the presence of biomass and bituminous and anthracite coal in the LSP soil density fractions. These insights should ideally be checked by organic petrography. The simple density separation experiment undertaken in this soil contamination study is shown to offer a helpful preparative technique, although not a rigorously quantitative one. The procedure could be improved by a micronization pretreatment step to more effectively permit separation of mineral components from the organic ones and by organic petrographic confirmation of the fraction compositions.

Of primary concern with the presence of coal at Liberty State Park is the potential environmental risk, principally due to coal's constituent PAHs. The abundant coal particles in LSP soils are the legacy of the park's past as major rail yard and port for the large-scale commercial transport and transfer of coal, powered by coal-fired steam locomotives, riding on rails supported by wooden crossties likely treated with coal tar-derived creosote. However, much of the LSP coal is anthracite and higher rank (medium volatile) bituminous. Extractable PAH content in coal decreases markedly with increasing coal rank (Stout and Emsbo-Mattingly, 2008; Laumann et al., 2011), therefore high rank coal particles in soil should pose less of an environmental concern on this basis. While the PAH-rich high volatile bituminous coal is proportionately less abundant at LSP, the extent to which it might be toxic or mutagenic to humans, plants, and animals is nonetheless linked to its degree of bioavailability. With the evidently flourishing plant communities in great majority of the LSP brownfield zone, limited hot spots of acute contamination therein (Hagmann et al., 2019, *see Ch. 2*) likely demand the most intensive remediation efforts. Analysis of soil components by Py-GC-MS, particularly

after a preparative density separation procedure, is shown to be effective in the environmental forensic and industrial archeological investigation of this urban brownfield. This detailed information about the nature of contaminants will help to inform future remediation efforts in the public interest.

#### Acknowledgements

We thank the National Science Foundation (NSF CBET 1603741) and the PSEG Institute for Sustainability Studies for the support for this study. We would also like to thank Laying Wu, Ph.D., for help using the scanning electron microscope, Matthew Cheung for assistance with historical research, and Mike Peters for field site photography. We sincerely thank Frank Gallagher, Ph.D. for facilitating access to Liberty State Park. One of us (MK) acknowledges the memory of his longtime friend and colleague, the late Professor Jack Crelling, coal petrographer and density separation pioneer.

### References

- Achten, C., Hofmann, T., 2009. Native polycyclic aromatic hydrocarbons (PAH) in coals – A hardly recognized source of environmental contamination. *Sci. Total Environ.* 407, 2461-2473.
- Achten, C., Cheng, S., Straub, K.L., Hofmann T., 2011. The lack of microbial degradation of polycyclic aromatic hydrocarbons from coal-rich soils, *Environ. Pollut.* 159, 623-629.
- Anderson, E., 1984. *The Central Railroad of New Jersey's First 100 Years, 1849-1949.* Center for Canal History and Technology, Canal Museum, Easton (PA).
- Boggs, S., 2009. *Petrology of Sedimentary Rocks*, 2nd ed. Cambridge University Press, Cambridge.
- Brooks, K.M., 2004. Polycyclic aromatic hydrocarbon migration from creosote-treated railway ties into ballast and adjacent wetlands. Madison, WI: U.S. Department of Agriculture, Forest Service, Forest Products Laboratory.
- Crelling J.C., 1988. Separation and characterization of coal macerals including pseudovitrinite. 1988 Ironmaking Conference Proceedings.
- Crelling J. C., 1989. Separation and characterization of coal macerals: accomplishments and future possibilities. *Am. Chem. Soc. Div. Fuel Chem. Prepr.* 34, 1, 249-255.
- Dyrkacz G.R., Horwitz E.P., 1982. Separation of coal macerals. *Fuel* 61, 3-12.
- Flores, R.M., 2014. *Coal and coalbed gas: fueling the future.* Elsevier, Waltham, MA.
- Fabiańska M.J., Ciesielczuk, J., Misz-Kennan, M., Kruszewski, L., Kowalski, A., 2016. Preservation of coal-waste geochemical markers in vegetation and soil on self-heating coal-waste dumps in Silesia, Poland. *Geochemistry* 76, 211-226.

- Gallagher, F.J., Pechmann, I., Bogden, J.D., Grabosky, J., Weis, P., 2008a. Soil metal concentrations and vegetative assemblage structure in an urban brownfield. *Environ. Pollut.*, 153, 351-361.
- Gallagher, F.J., Pechmann, I., Bogden, J.D., Grabosky, J., Weis, P., 2008b. Soil metal concentrations and productivity of *Betula populifolia* (gray birch) as measured by field spectrometry and incremental annual growth in an abandoned urban Brownfield in New Jersey. *Environ. Pollut.* 156, 699–706.
- Gallagher, F.J., Goodey, N.M., Haggmann, D.F., Singh, J.P., Holzapfel, C., Litwhiler, M., Krumins, J.A., 2018. Urban re-greening: A case study in multi-trophic biodiversity and ecosystem functioning in a post-industrial landscape. *Diversity* 10, 119.
- Garcia, A.B., Moineiro, S.R., Martinez-Tarazona, M.R., Tascón, J.M., 1991. Influence of weathering process on the flotation response of coal. *Fuel* 70, 1391-1397.
- Haggmann, D.F., Goodey, N.M., Mathieu, C., Evans, J., Aronson, M.F.J., Gallagher, F.J., Krumins, J.A., 2015. Effect of metal contamination on microbial enzymatic activity in soil. *Soil Biol. Biochem.* 91, 291-297.
- Haggmann, D.F., Kruege, M.A., Cheung, M., Mastalerz, M., Gallego, J.L.R., Singh, J.P., Krumins, J.A., Li, X., Goodey, N.M., 2019. Environmental forensic characterization of former rail yard soils located adjacent to the Statue of Liberty in the New York/New Jersey harbor. *Sci. Total Environ.* 690, 1019-1034. <https://doi.org/10.1016/j.scitotenv.2019.06.495>.
- Hatcher, P.G., Faulon, J.L., Wenzel, K.A., Cody, G.D., 1992. A structural model for lignin-derived vitrinite from high-volatile bituminous coal (coalified wood). *Energy Fuels* 6, 813-820.

- Hempfling R., Schulten H.R., 1990. Chemical characterization of the organic matter in forest soils by Curie point pyrolysis-GC/MS and pyrolysis-field ionization mass spectrometry. *Org. Geochem.* 15, 131-145.
- Hindersmann, B., Achten, C., 2018. Urban soils impacted by tailings from coal mining: PAH source identification by 59 PAHs, BPCA and alkylated PAHs. *Environ. Pollut.* 242, 1217-1225.
- Kruger M.A., 2015. Analytical pyrolysis principles and applications to environmental science, in: Barbooti, M. (Ed.), *Environmental Applications of Instrumental Chemical Analysis*. CRC Press, Boca Raton (FL), p. 533-569.
- Kruger, M.A., Bensley, D.F., 1994. Flash pyrolysis-gas chromatography/mass spectrometry of Lower Kittanning vitrinites: Changes in the distributions of polyaromatic hydrocarbons as a function of coal rank, in: Mukhopadhyay, P. K., Dow, W.G. (Eds.), *Vitrinite Reflectance as a Maturity Parameter: Applications and Limitations*. Amer. Chem. Soc. Symp. Series 570, p. 136-148.
- Kruger M. A., Landais P., Bensley D. F., Stankiewicz B. A., Elie M., Ruau O., 1997. Separation and artificial maturation of macerals from Type II kerogen. *Energy Fuels* 11, 503-514.
- Kruger M.A., Gallego J.L.R., Lara-Gonzalo A., Esquinas N., 2018. Environmental forensics study of crude oil and petroleum product spills in coastal and oilfield settings: Combined insights from conventional GC-MS, thermodesorption-GC-MS and pyrolysis-GC-MS, in: Stout S., Wang Z. (Eds.), *Oil Spill Environmental Forensics Case Studies*. Butterworth-Heinemann (Elsevier), Oxford (UK), pp. 131-156.
- Krumins, J.A., Goodey, N.M., Gallagher, F.J., 2015. Plant–soil interactions in metal contaminated soils. *Soil Biol. Biochem.* 80, 224-231.

- Kuder, T., Kruge, M.A., 1998. Preservation of biomolecules in sub-fossil plants from raised peat bogs - A potential paleoenvironmental proxy. *Org. Geochem.* 29, 1355-1368.
- Kuroda, K., Nakagawa-izumi, A., 2006. Analytical pyrolysis of lignin: Products stemming from  $\beta$ -5 substructures. *Org. Geochem.* 37, 665-673.
- Lara-Gonzalo A., Kruge M.A., Lores I., Gutiérrez B., Gallego J.L.R., 2015. Pyrolysis-GC-MS for the rapid environmental forensic screening of contaminated brownfield soil. *Org. Geochem.* 87, 9-20.
- Laumann, S., Micić, V., Kruge, M.A., Achten, C., Sachsenhofer, R.F., Schwarzbauer, J., Hofmann, T., 2011. Variations in concentrations and compositions of polycyclic aromatic hydrocarbons (PAHs) in coals related to the coal rank and origin. *Environ. Pollut.* 159, 2690-2697.
- McDonald, T.T., 2018. N.J. to turn 240 acres of Liberty State Park into wildlife oasis. *The Jersey Journal*, January 11, 2018.  
[https://www.nj.com/hudson/2018/01/nj\\_announces\\_massive\\_plan\\_to\\_restore\\_240\\_acres\\_of.html](https://www.nj.com/hudson/2018/01/nj_announces_massive_plan_to_restore_240_acres_of.html). Retrieved June 8, 2019.
- Nádudvari Á., Fabiańska M.J., Marynowski L., Kozielska B., Koniecznyński J., Smółka-Danielowska D., Ćmiel, S., 2018a. Distribution of coal and coal combustion related organic pollutants in the environment of the Upper Silesian Industrial Region. *Sci. Total Environ.* 628-629, 1462-1488.
- Nádudvari, A., Marynowski, L., Fabiańska, M.J., 2018b. Application of organic environmental markers in the assessment of recent and fossil organic matter input in coal wastes and river sediments: A case study from the Upper Silesia Coal Basin (Poland). *Int. J. Coal Geol.* 196, 302-316.

- Orsini, S., Parlanti, F, Bonaduce, I., 2017. Analytical pyrolysis of proteins in samples from artistic and archaeological objects. *J. Anal. Appl. Pyrol.* 124, 643-657.
- Saiz-Jiménez, C., de Leeuw, J.W., 1986, Lignin pyrolysis productions: Their structures and their significance as biomarkers. *Org. Geochem.* 10, 869-876.
- Singh, J.P., Ojinnaka, E.U., Krumins, J.A., Goodey, N.M., 2019a. Abiotic factors determine functional outcomes of microbial inoculation of soils from a metal contaminated brownfield. *Ecotox. Environ. Safe.* 168, 450-456.
- Singh, J.P., Vaidya, B.P., Goodey, N.M., Krumins, J.A., 2019b. Soil microbial response to metal contamination in a vegetated and urban brownfield. *J. Environ. Manage.* 244, 313-319.
- Smith, M.J., Flowers, T.H., Duncan, H.J., Alder, J., 2006. Effects of polycyclic aromatic hydrocarbons on germination and subsequent growth of grasses and legumes in freshly contaminated soil and soil with aged PAHs residues. *Environ. Pollut.* 141, 519-525.
- Stankiewicz, B. A., Kruge M. A., Crelling, J. C., 1994a. Geochemical characterization of maceral concentrates from Herrin No. 6 coal (Illinois Basin) and Lower Toarcian shale kerogen (Paris Basin), in: Curnelle, R., Sévérac, J.-P. (Eds.), *Pétrologie Organique, Recueil des Communications, Colloque International des Pétrographes Organiciens Francophones, Publ. Spéc., Bull. Centres Rech. Explor.-Prod. Elf Aquitaine, Vol. 18, p. 237-251.*
- Stankiewicz B.A., Kruge M.A., Crelling J.C., Salmon G.L., 1994b. Density gradient centrifugation: application to the separation of macerals of Type I, II and III sedimentary organic matter. *Energy Fuels* 8,1513-1521.

- Stout, S.A., Emsbo-Mattingly, S.D., 2008. Concentration and character of PAHs and other hydrocarbons in coals of varying rank – Implications for environmental studies of soils and sediments containing particulate coal. *Org. Geochem.* 39, 801-819.
- Suárez-Ruiz, I., & Crelling, J.C. (Eds.), 2008. *Applied coal petrology: the role of petrology in coal utilization*. Elsevier, Amsterdam. 398 p.
- Wampler, T.P., 2007. Analytical pyrolysis: An overview, in: Wampler, T.P. (Ed.), *Applied Pyrolysis Handbook*, 2nd ed., CRC Press, Boca Raton (FL, USA), pp. 1–26.
- Welton, J.E., 1984. *SEM Petrology Atlas. Methods in Exploration Series No. 4*, American Association of Petroleum Geologists, Tulsa (OK) USA. 240 p.
- Wood, G.H., Kehn, T.M., Carter, M.D., Culbertson, W.C., 1983. *Coal Resource Classification System of the US Geological Survey. Geological Survey Circular 891*, U.S. Geological Survey, Denver (CO). 65 p.
- Xia, W., Yang, J., & Liang, C., 2014. Investigation of changes in surface properties of bituminous coal during natural weathering processes by XPS and SEM. *Appl. Surf. Sci.* 293, 293-298.
- Xia, W., Yang, J., 2014. Changes in surface properties of anthracite coal before and after inside/outside weathering processes. *Appl. Surf. Sci.* 313, 320-324.
- Xu, J., Zhuo, J., Zhu, Y., Pan, Y., Yao, Q., 2017. Analysis of volatile organic pyrolysis products of bituminous and anthracite coals with single-photon ionization time-of-flight mass spectrometry and gas chromatography/mass spectrometry. *Energy Fuels* 31:730-737.
- Yang, Y., Ligouis, B., Pies, C., Grathwohl, P., Hofmann, T., 2008a. Occurrence of coal and coal-derived particle-bound polycyclic aromatic hydrocarbons (PAHs) in a river floodplain soil. *Environ. Pollut.* 151, 121-129.

Yang, Y., Ligouis, B., Pies, C., Achten, C., Hofmann, T., 2008b. Identification of carbonaceous geosorbents for PAHs by organic petrography in river floodplain soils. *Chemosphere* 71, 2158-2167.

**Table 3-1.** Pyrolysis-GC-MS peak identification for Figures 3-8 thru 3-10

<u>Aliphatic Hydrocarbons</u>		<u>Polysaccharide markers</u>	
+	n-alkanes	P1	furan-3-one
^	n-alk-1-enes	P2	2-furancarboxaldehyde
pr	pristane	P3	3-furancarboxaldehyde
<u>Monoaromatic Compounds</u>		P4	methylfuranone
A1	benzene	P5	methylfuranocarboxaldehyde
A2	toluene	P6	benzenediol
A3	ethylbenzene	<u>Lignin markers</u>	
A4	meta- & para-xylene	L1	guaiacol
A5	styrene	L2	methylguaiacol
A6	ortho-xylene	L3	ethylguaiacol
A7	C3-alkylbenzene	L4	vinylguaiacol
A8	benzaldehyde	L5	eugenol
A9	benzonitrile	L6	vanillin
<u>Polycyclic aromatic compounds</u>		L7	cis iso-eugenol
Nx	naphthalenes	L8	trans iso-eugenol
BBx	biphenyls	L9	acetovanillone
DBFx	dibenzofurans	L10	vinylsyringol
PHNx	phenanthrenes	L11	prop-1-enyl syringol
FLUx	fluorenes	L12	prop-2-enyl syringol (cis)
FLA	fluoranthene	L13	syringaldehyde
PYRx	pyrenes	L14	prop-2-enyl syringol (trans)
BAN	benzo[a]anthracene	L15	acetosyringone
CHRx	chrysenes	<u>Fatty acids</u>	
BeP	benzo[e]pyrene	FA1	n-hexadecanoic acid
(x indicates extent of alkyl substitution)		FA2	n-octadec-9-enoic acid
<u>Phenols</u>		FA3	n-octadecanoic acid
F1	phenol	<u>Steroids</u>	
F2	2-methylphenol	S1	stigmastan-3,5-diene
F3	3-methylphenol & 4-methylphenol	S2	stigmasta-5-en-3-ol
F4	2-ethylphenol	S3	stigmasta-3,5-dien-7-one
F5	2,4-dimethylphenol	S4	stigmasta-4-en-one
F6	4-ethylphenol	S5	stigmasta-4,22-dien-3one
F7	3-ethylphenol & 3,5-dimethylphenol	<u>Other</u>	
F8	vinylphenol	BAM	terpenoids similar to $\beta$ -amyrone (C <sub>30</sub> H <sub>48</sub> O) or derivative
F9	trimethylphenol isomers	DKDP	diketodipyrrole
		X	contaminant introduced during processing

**Table 3-2.** Dry weight percentages of density fractions separated from whole soil of LSP Sites 43 and 25R. See text and Figure 3-5 for procedural details.

Soil	Total soil dry weight	Fraction 1 (floated in DI water)	Fraction 2 (floated in 1.6 g/mL KI <sub>aq</sub> )	Fraction 3 (sank in 1.6 g/mL KI <sub>aq</sub> )
43	5.007 g	0.39 %	3.10 %	92.58 %
25R	5.046 g	0.06 %	0.89 %	95.94 %

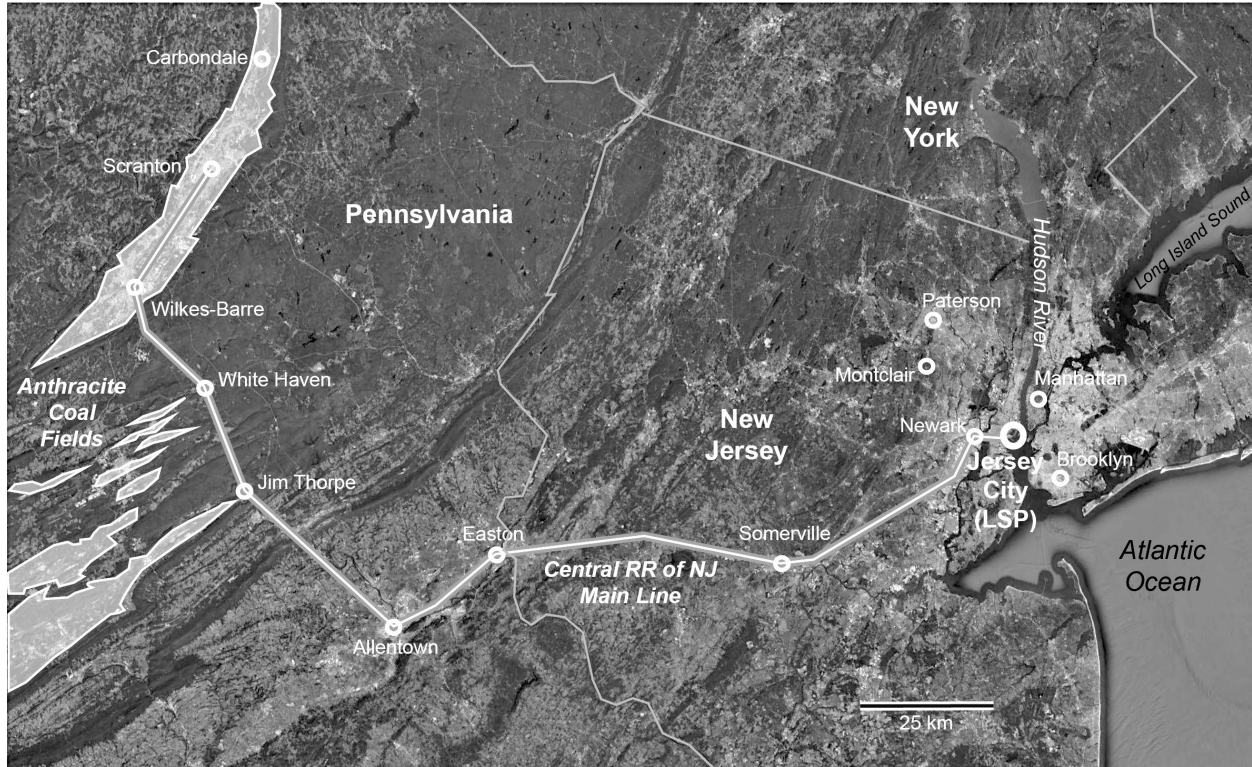


**Figure 3-1.** Index map showing location of Liberty State Park (LSP) in Jersey City (NJ), USA, the principal anthracite coal fields of Pennsylvania, and the former Central Railroad of New Jersey main line. Base map: Google Earth; coalfields: Pennsylvania Dept. of Environmental Protection; rail line: Anderson (1984).

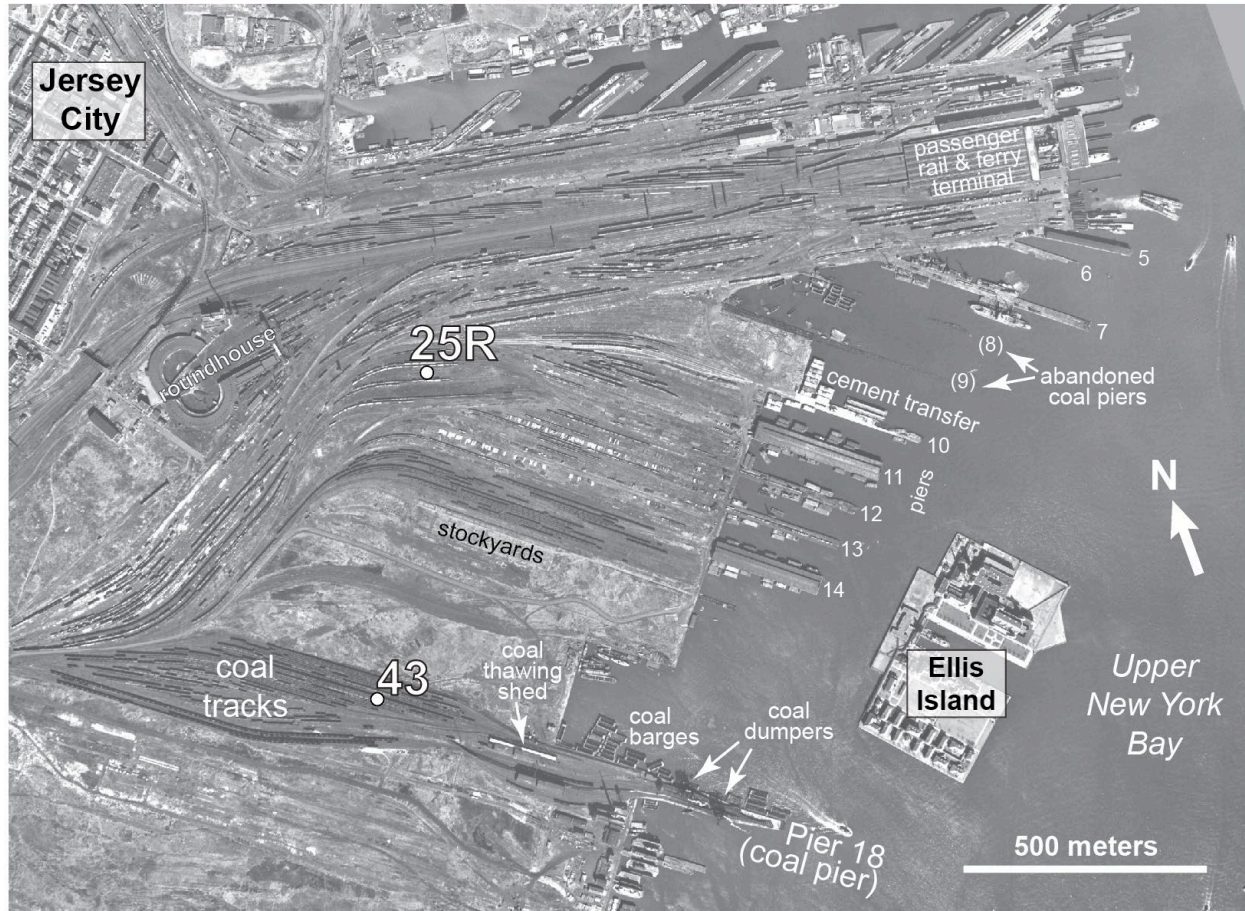


**Figure 3-2.** The Central Railroad of New Jersey's rail yard and marine terminal in Jersey City as it appeared in a 1954 aerial image, overprinted with the location of the two soil samples (25R, 43) presented in this study. At the time of the photograph, coal transport operations were largely confined to the zone seen in the lower part of the image, on the tracks leading to Pier 18. Note the locations of the passenger terminal and roundhouse. Base image: U.S. Geological Survey; identification of coal handling facilities: Anderson (1984); pier identification: Brooklyn Historical Society Archives.

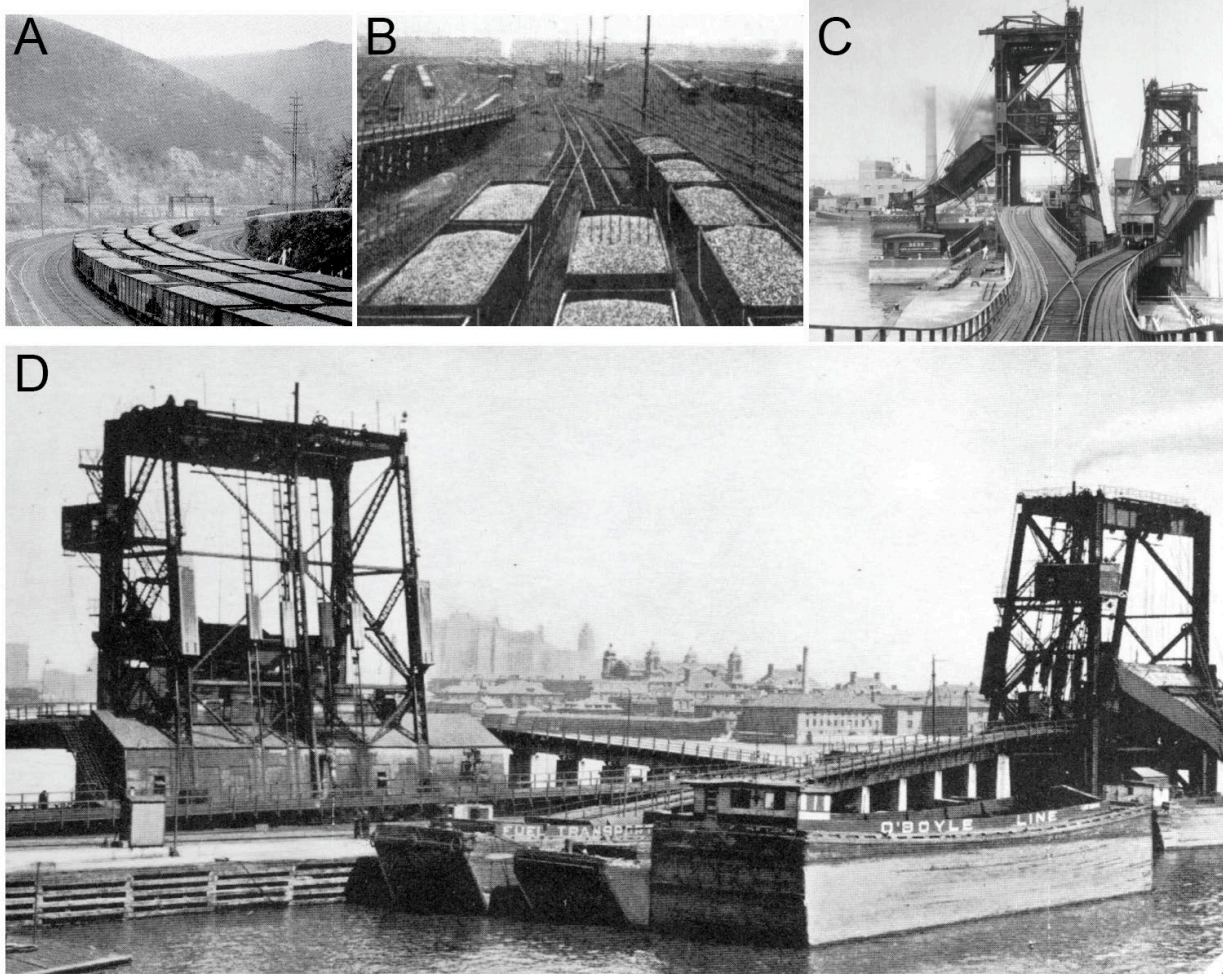


**Figure 3-3.** Historical images of CRRNJ coal transport operations in the 1940's. (A) Loaded coal trains in Jim Thorpe, Pennsylvania (Fig. 1; town formerly known as Mauch Chunk). (B) Loaded coal cars approach Pier 18 in the Jersey City rail yard. View to the west showing the yard's track network (Fig. 2). (C) View of Pier 18's two coal dumping towers for transfer of coal from railcar to barge. View is to the west from the eastern end of the pier. (D) View to the northeast of Pier 18's coal dumpers. Note Ellis Island in the background. Photos: Anderson (1984); used with permission.

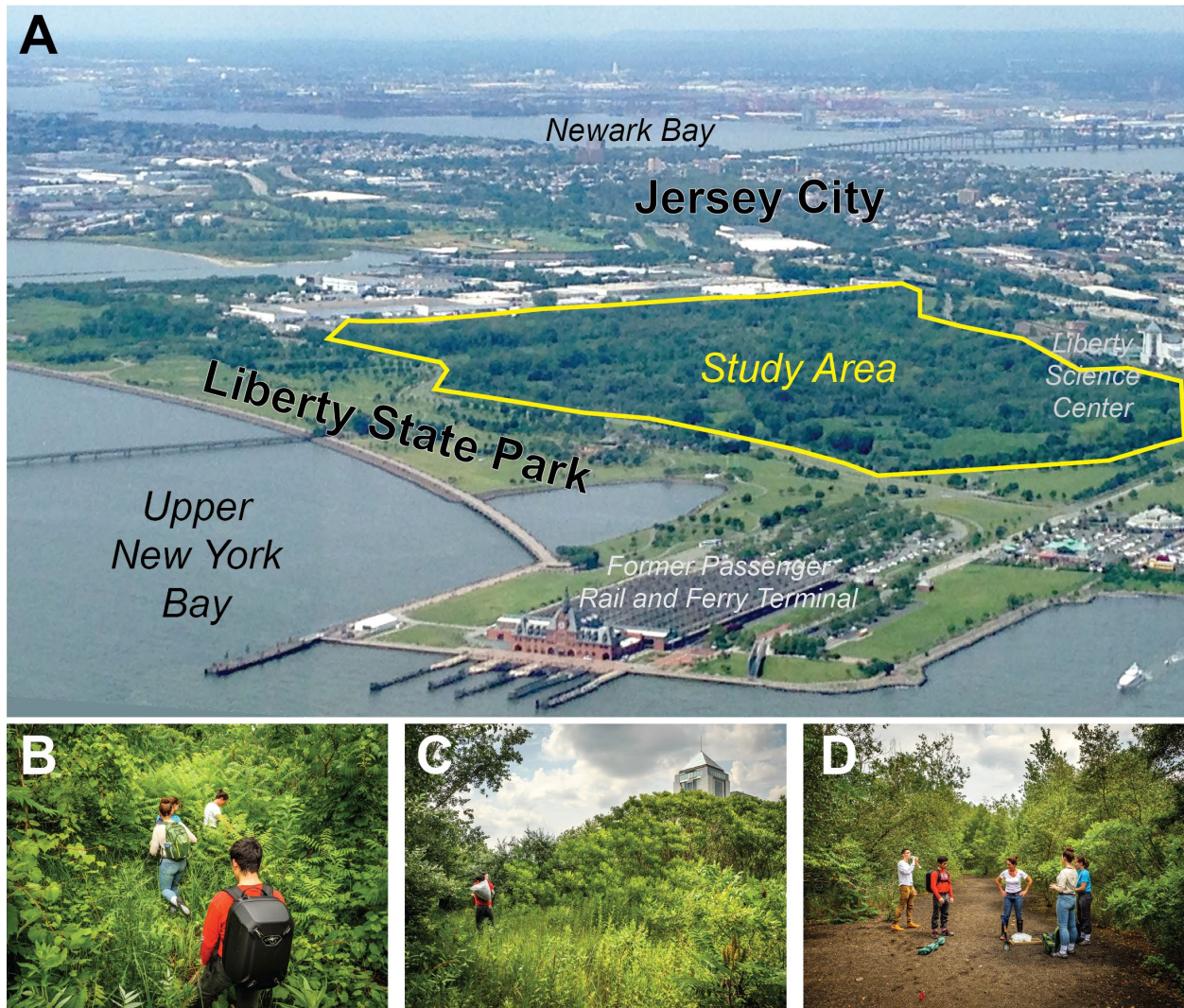


**Figure 3-4.** Appearance of Liberty State Park in 2017. (A) Aerial view towards the southwest showing the study area within the park. Note the former passenger rail and ferry terminal, partially restored but non-functioning, and the Liberty Science Center museum, built on the site of the former railroad roundhouse (Fig. 2). Photo: D. Haggmann. (B, C) Dense vegetation covers most of the study area. The top of the Liberty Science Center tower appears in C. (D) Soil sample 25R was collected from this anomalously barren strip within the study area. Photos B-D: M. Peters, Montclair State Univ.; used with permission.

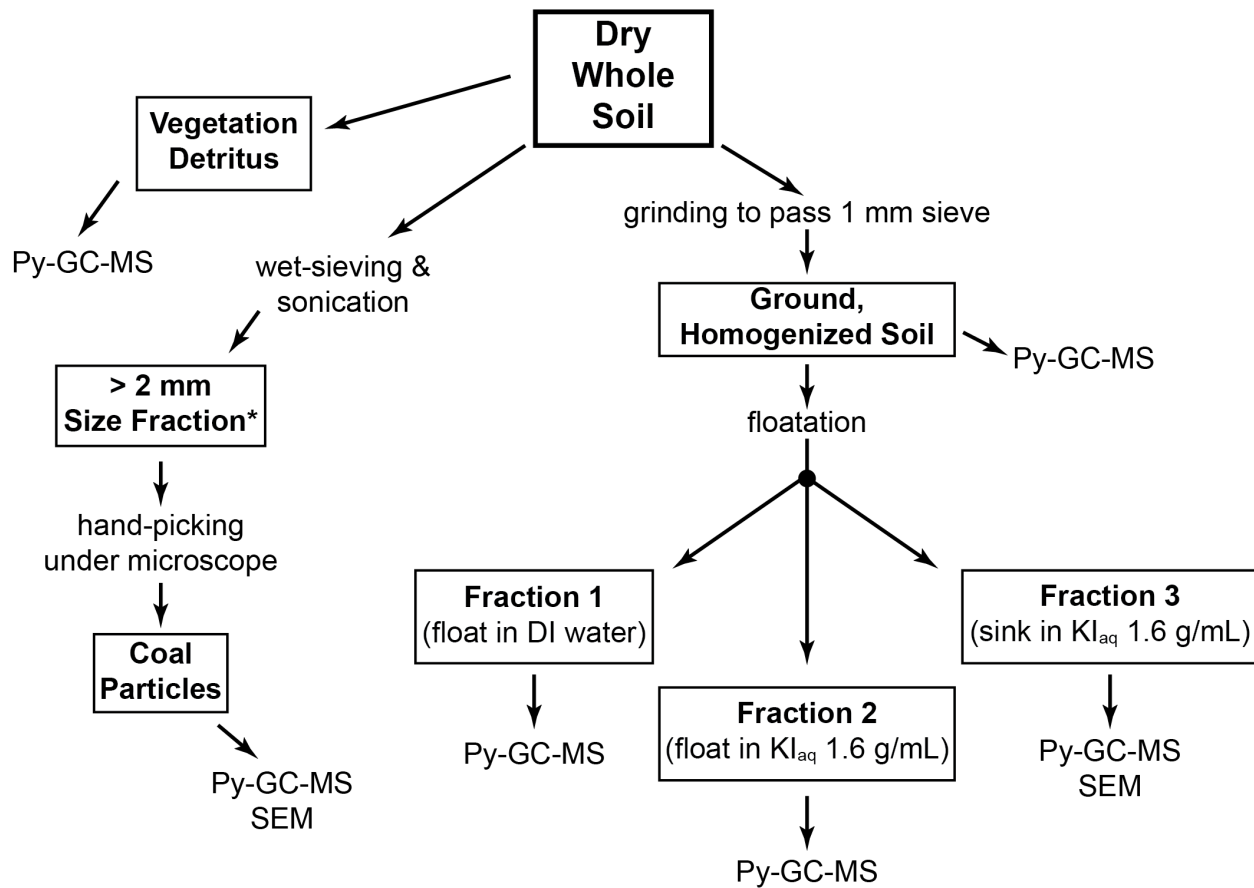


**Figure 3-5.** Experimental flow chart. See section 2 for details. No vegetation detritus was picked from barren site 25R soil. \* < 2 mm size fraction previously studied in detail (Hagmann et al., 2019, *see Ch. 2*).



**Figure 3-6.** Scanning electron micrograph of fragments of a single wet-sieved ( $> 2$  mm) and sonicated LSP 43 coal particle. Note surface encrustations. Scale bar is 300  $\mu\text{m}$ .

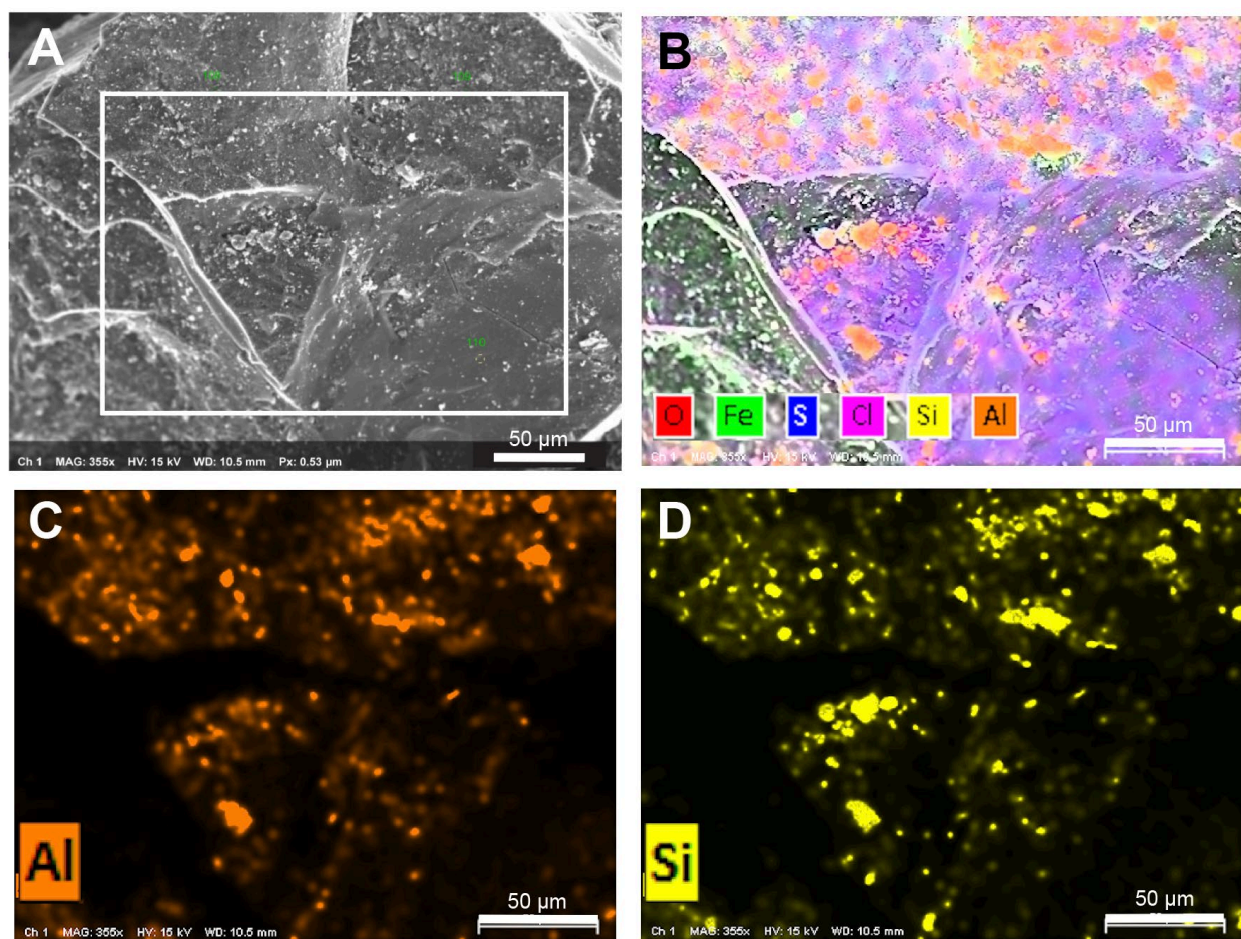


**Figure 3-7.** SEM EDS mapping images of a fragment of a single wet-sieved (>2 mm) and sonicated LSP 43 coal particle. Scale bars are 50 μm. (A) SEM image; box shows element mapping area for B-D. (B) Multi-element map (O, Fe, S, Cl, Si, Al) superimposed on SEM image. (C) Element map for aluminum. (D) Element map for silicon. Element mapping images indicate clay mineral platelets adhering to coal.

**Forested Site 43**  
**Py-GC-MS Total Ion Current**

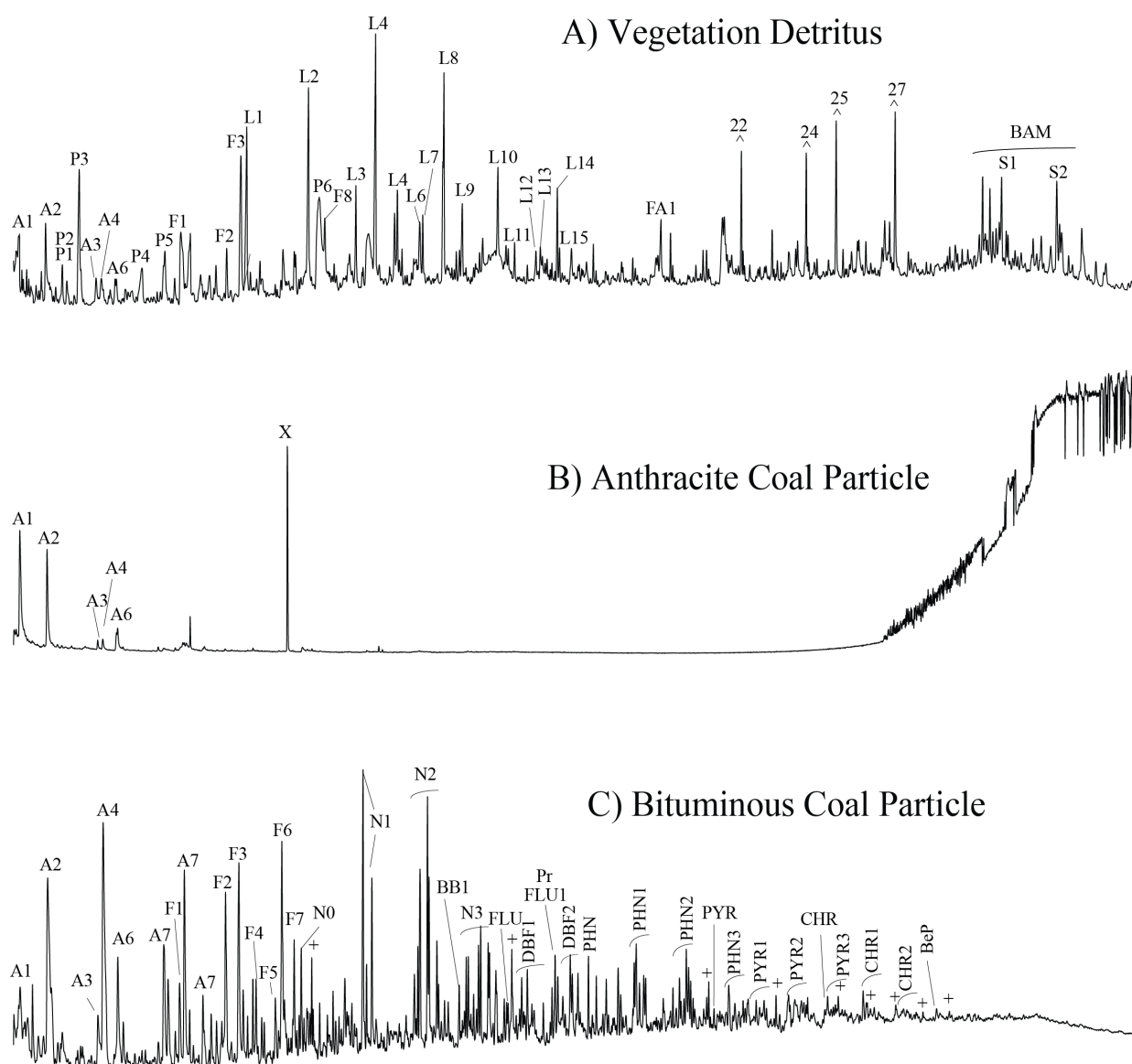


**Figure 3-8.** Py-GC-MS total ion current chromatograms of materials from the site 43 soil sample: (A) typical soil organic matter (roots & twigs) and (B, C) two coal particles hand-picked from the >2 mm size fraction after wet sieving and sonication. See Table 3-1 for peak identification.

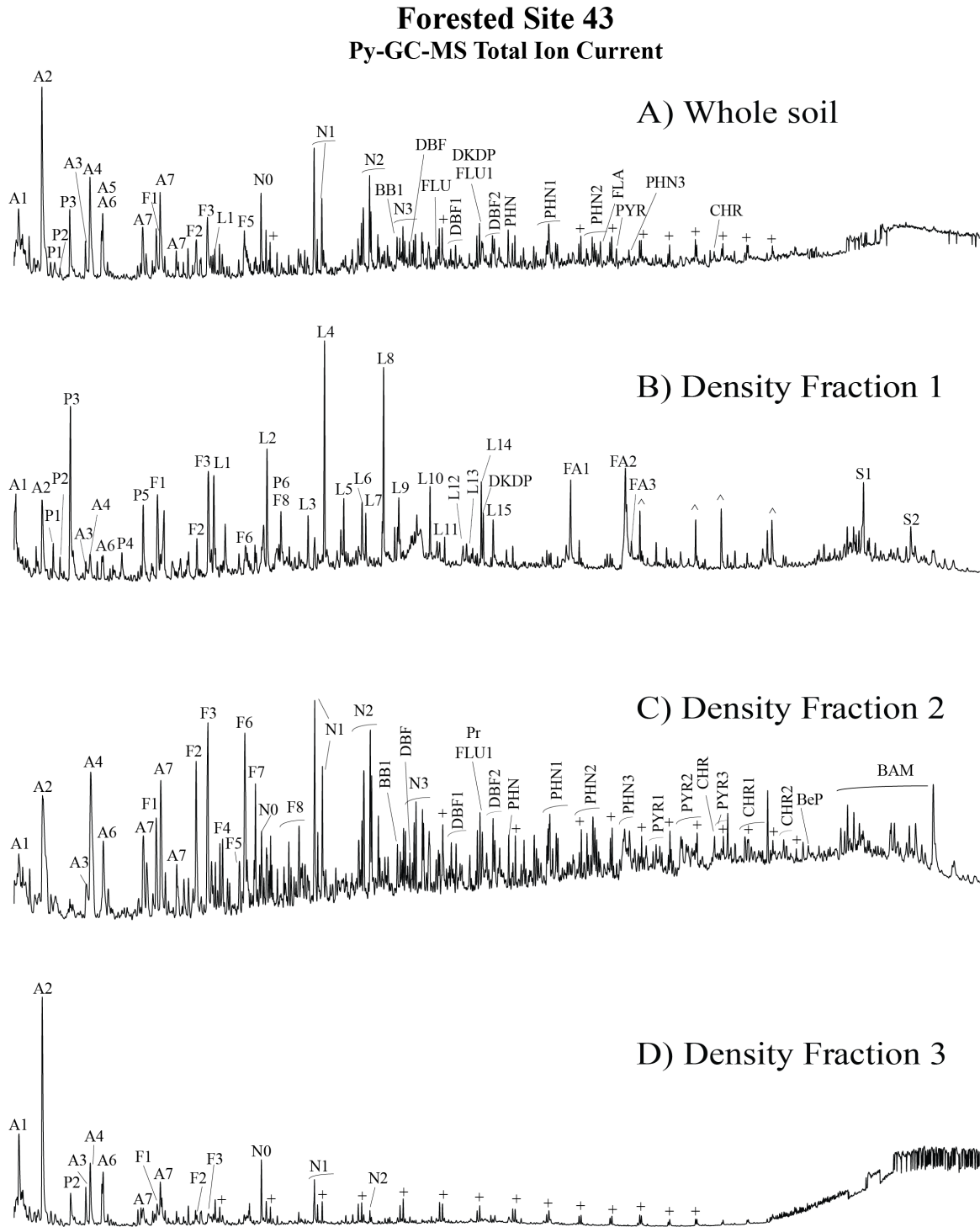


**Figure 3-9.** Py-GC-MS total ion current chromatograms. Forested LSP site 43: (A) whole soil, (B) Fraction 1 floated in DI water, (C) Fraction 2 floated in K1aq (1.6 g/mL), and (D) Fraction 3 sank in K1aq (1.6 g/mL). See Table 3-1 for peak identification.

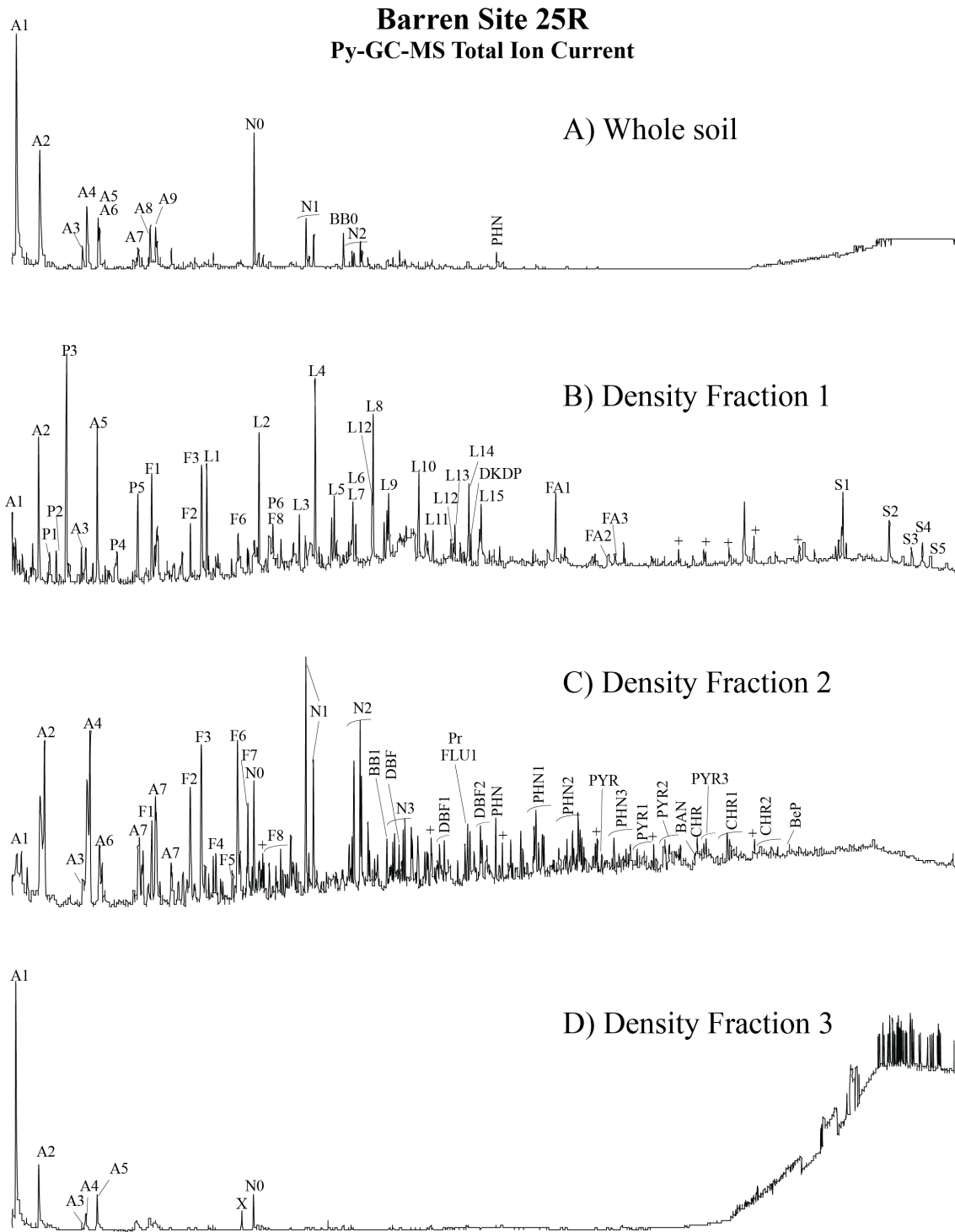


**Figure 3-10.** Py-GC-MS total ion current chromatograms. Barren LSP site 25R: (A) whole soil, (B) Fraction 1 floated in DI water, (C) Fraction 2 floated in K1aq (1.6 g/mL), and (D) Fraction 3 sank in K1aq (1.6 g/mL). See Table 3-1 for peak identification.

## Chapter 4

### **Soil microbial function and community composition along an experimentally created gradient of two contaminated soils**

#### **Abstract**

Vegetated soils can exist next to plots of land that are barren of vegetation. There are two sites that are adjacent to each other within Liberty State Park, an abandoned urban brownfield in Liberty State Park, in Jersey City, New Jersey, USA. One site is vegetated and is highly functioning, 25F, while the other is barren and is poorly-functioning, 25R and both contain PAHs and high concentrations of metal/loids. We determined whether the microbial community composition and enzyme activity of an introduced microbial community through soil inoculation was affected by an abiotic environment along an experimental gradient. We mixed these two soils in different ratios to create an experimental gradient and then we autoclaved these soil mixtures. We inoculated the different autoclaved soil mixtures with the highly functioning 25F soil. We determined the fungal and bacterial compositions of the soil mixtures along the experimental gradient after inoculation to test how the different soil environments would allow all microbial communities to establish. We found that there were some fungal classes, like Mortierellomycetes, decreased in relative abundance with increasing percent ratios (w/w) of barren 25R soil. However, there were other fungal classes that decreased. We also tested if enzyme activities of the soils inoculated with 25F soil remain the same regardless of the environment. We found that the phosphatase, cellobiohydrolase activities of inoculated soils decreased with increasing percent ratios (w/w) of barren 25R soil.

#### 4.1. Introduction

Soil microbial composition is shaped by both biotic and abiotic soil properties (Fierer and Jackson, 2006; Lauber et al., 2009; Torsvik et al., 2002; Zak et al., 2003). Bacteria and fungi play an important role in ecosystem functioning, such as mediating nutrient cycling (Bardgett et al., 2008; Singh et al., 2010; Wagg et al., 2014). Abiotic factors include pH, texture, moisture, temperature, and nutrient content. The abiotic factors referred to in this paper are the non-living soil properties, which include organic matter, moisture, and heavy metals. In contaminated soils, abiotic factors can also include heavy metals and organic contaminants, such as polycyclic aromatic compounds. The interactions between biotic and abiotic constituents in contaminated soils are complicated and can change with time (Krumins et al., 2015). Inorganic and organic contaminants can be toxic to microorganisms and therefore anthropogenic contamination can alter microbial community composition (Gadd, 2005). Contaminants can impose stress on the soil environment, acting as a filter that allows some microorganisms to thrive while others succumb to the stresses of the environment. Some microorganisms can survive in the presence of metals and organic contaminants and some degrade or use as nutrients compounds from fossil fuel contamination (Gadd and Griffiths, 1977; Johnson et al., 2004). Sites that have little plant growth as a result of contamination due to heavy metals and organic contaminants introduced by human activity are known as industrial barrens (Kozlov and Zvereva, 2007b). Even after years of abandonment these sites can remain barren due to toxic levels of metals, but certain microorganisms adapt to the contaminants (Hagmann et al., 2015; Puglisi et al., 2012).

Targeted microbial inoculation strategies are used to introduce new or different microbial communities into soil, often with the goal of altering soil functioning in a contaminated soil (Khan et al., 2000; Rajkumar et al., 2012). Soil microbial inoculations can in some cases

increase extracellular enzymatic activities (Panke-Buisse et al., 2015). Other benefits of soil inoculations can include improved plant yields, increased litter decomposition rates, and more fertile soils (Bounaffaa et al., 2018; Ouahmane et al., 2007; Rodríguez-Caballero et al., 2018; Tamayo-Vélez and Osorio, 2018). Often the soils into which new microbial communities are introduced are contaminated or poorly functioning and the goal is to speed up the degradation or transformation of contaminants. In many cases, the focus is on the identity of the microorganism that are introduced, either as a monoculture, or as a consortium of two or a few microorganisms, or in rarer cases an entire microbial community consisting of a large number of different organisms. Many unanswered questions often remain about the way in which the abiotic environment into which the microorganism/s is/are introduced impact the ability for the microorganisms to successfully establish.

Rather than just introducing soil microorganisms into one poorly-functioning soil, microorganisms can be added into a gradient of abiotic soil properties, to learn more about the relationships between the abiotic environment and the outcome of the microbial inoculation. A gradient of abiotic conditions can be created by mixing two soils with different abiotic properties in a range of ratios. The introduction of microbial inoculum into a gradient of new soil environments has the potential to elucidate the interactions between microbial communities and soil abiotic environments, providing new insights, yet this approach largely remains unexplored (Xun et al., 2015).

A site within an urban brownfield in Jersey City, New Jersey, Liberty State Park (LSP), site 25R, is an example of an industrial barren. This site has remained barren for years, despite being surrounded by other vegetated sites. LSP soils from sites including 25R and the adjacent vegetated site 25F have been investigated to further understand the reasons why 25R remains

barren despite being surrounded by large areas covered in plants and trees (Vaidya et al., 2020; Hagmann et al., 2019, *see Ch. 2*). Soils 25F and 25R are the soils used in this study. Both are contaminated with heavy metals and fossil fuel derived contaminants, including coal. Barren 25R soil contains higher concentrations of metals and has poor enzymatic function while 25F has slightly lower metal concentrations and is enzymatically active and vegetated. The well-characterized and different properties of the two adjacent soils presented an opportunity to examine the role of abiotic environment in the outcome of soil inoculation.

The goal of this study was to determine whether abiotic environment along an experimental gradient affects microbial community composition and enzyme activity of an introduced microbial community through soil inoculation. A gradient of abiotic environments/conditions was created by mixing soils from the two adjacent sites 25R and 25R in different ratios. The soil mixtures were then sterilized by autoclaving the soil with the goal to eliminate the microbial communities present in the soil. After soils were autoclaved, soil inoculum from 25F soil was added to the different ratios of 25F and 25R soils. Site 25F was used as an inoculum because it is a site in closer proximity to the barren soil 25R and has adapted to the high levels of contaminants but has higher soil function. These mixtures were incubated for about two months to let the communities establish. We asked the following questions about what happens when the microorganisms from 25F soil are introduced into a gradient of different autoclaved environments: 1) Will the microbial communities of 25F establish equally in all environments or will the microbial communities vary depending on the ratio of soils 25F and 25R and 2) Will the enzyme activities of the soils inoculated with 25F soil remain the same regardless of the environment or will enzyme activities decrease as more 25R soil is present in the mixture? To answer the first question, we characterized the fungal and

bacterial communities in the different soil mixtures. To answer the second question, we measured phosphatase, cellobiohydrolase, peroxidase activities to understand how different abiotic properties affect enzyme activities. Soil samples that had not been inoculated and soil samples that had not been autoclaved were included in the study as negative controls.

## 4.2. Methods

### 4.2.1 *Site description and soil preparation*

The soil samples were collected from two sites (25F and 25R) within a 100-ha plot within LSP in Jersey City, New Jersey (40° 42' 16 N, 74° 03' 06 W). LSP was once a rail yard, but since 1969 the 100-ha plot of land was restricted to public access, and without any human intervention a dense forest covers the abandoned site. There are both inorganic and organic contaminants present in LSP soils, which include a variety of metals and polycyclic aromatic hydrocarbons (Hagmann et al., 2019, *see Ch. 2*). The soils collected were from a barren strip of land, 25R, and a neighboring site that is covered in vegetation, 25F. Soils were collected from barren site 25R and vegetated site 25F within LSP on April 8, 2019. The soils were sieved using a 2 mm sieve and stored in a refrigerator at 4 °C.

### 4.2.2 *Experimental design*

Soils from barren site 25R were mixed with soils from vegetated site 25F to create a gradient of soils; 0 %, 25 %, 50 %, 75 %, and 100 % 25R, as illustrated in Figure 4-1. The mixtures were autoclaved (121 °C, 30 min) twice in an autoclave bag, on two consecutive days, to sterilize the soils. After autoclaving, equal weights (120 g) of the soil mixtures were added to flowerpots. To create inoculated pots, equal amounts of the autoclaved soil was removed (6 g) and non-

autoclaved 25F soil (6 g) was added in. The inoculated pots therefore contained 5% by weight of 25F soil that had not been autoclaved. To ensure that the inoculated and non-inoculated experiments were otherwise similar, equal amounts of the autoclaved soil was removed (6 g) but this time non-autoclaved 25F soil (6 g) was added into the pots. The non-inoculated pots were created to serve as controls, allowing us to determine if any contamination, such as possible input from microbes in the air, entered the pots. The percent ratios (w/w) of 25R soil in both inoculated and non-inoculated treatments were 0 %, 23.8 %, 47.6 %, 71.4 % and 95.2% 25R. The rest of the soil was 25F soil. The experimental conditions will be referred to as 0 % 25R, 25 % 25R, 50 % 25R, 75 % 25R, and 100 % 25R for simplicity. For example, the ratio labeled as 25 % 25R actually consisted of 23.8% 25R and 76.2% 25F soils (w/w) after the inoculation. In addition to the inoculated and non-inoculated soils described above, fresh soils 0 % 25R and 100 % 25R served as a baseline comparison for the treatments. Fresh soils 0 % 25R and 100 % 25R were not autoclaved nor inoculated, as seen in Figure 4-1.

Figure 4-1

There were five replicates for each treatment: inoculated (autoclaved soil mixtures + 25F inoculation), non-inoculated (autoclaved soil mixtures + autoclaved 25F soil), and fresh soils (non-autoclaved 0 % 25R and 100 % 25R). All pots were placed in a growth chamber. Sterilized tap water was added to each pot to maintain the moisture of the soil throughout the course of the experiment. The moisture was maintained by maintaining the same weight as the initial weight that was determined at the beginning of the experiment. The initial time point samples were collected the day the soils were potted, and were stored in a refrigerator at 4 °C.

The final time point samples were collected after incubation in the growth chamber, 67 days from the start of the incubation. Moisture of the soil was determined for each treatment and the extracellular soil phosphatase, cellobiohydrolase and peroxidase activities were measured for soil samples collected at the initial and final time points.

#### 4.2.3 *Phosphatase and cellobiohydrolase assays*

Both phosphatase and cellobiohydrolase enzyme activities were measured for each sample as described in (Hagmann et al., 2015). Briefly, 0.5 g of moist soil was combined with 0.1 M MES buffer (100 mL, pH 6.0) and then sonicated for 3 min at 25W. The continuously stirred soil slurry was added to the well (160  $\mu$ L) in a 96-well black plate. 4-MUB-phosphate, for phosphatase, was added (40  $\mu$ L) to three different wells (350  $\mu$ M in the well). 4-Methylumbelliferyl  $\beta$ -D-cellobioside, for cellobiohydrolase, was added (40  $\mu$ L) to three different wells (650  $\mu$ M in the well). A standard curve was created by combining a fluorescent product, (40  $\mu$ L of 4-MUB, at different concentrations with a soil slurry (160  $\mu$ L), that resulted in the following concentrations of product (0, 100, 1000, 1500 and 2500 pmols). Time points were collected on a microplate reader at 30 °C every 7.5 minutes for 3 hours to measure fluorescence intensity (320 nm ex./450 nm em.).

#### 4.2.4 *Peroxidase assay*

The peroxidase activity was measured for each sample. Briefly, 1 g of moist soil, was combined with 50 mM sodium acetate buffer (125mL, pH 6.1) then sonicated for 3 min at 25W. The continuously stirred soil slurry was added to the well (200  $\mu$ L) in a 96-well black plate. The substrate L-3,4-dihydroxyphenylalanine (L-DOPA) was added (50  $\mu$ L) to the sample wells. In

addition to the soil slurry, sample wells also contained 0.3% H<sub>2</sub>O<sub>2</sub> (10 µL), and of 25 mM L-DOPA (50 µL). To correct for the substrate background, blank wells containing 0.3 % H<sub>2</sub>O<sub>2</sub> (10 µL), 50 mM acetate buffer (200 µL), and 25 mM L-DOPA (50 µL) were used. To correct for the sample background, negative control wells containing soil slurry (200 µL), 0.3 % H<sub>2</sub>O<sub>2</sub> (10 µL), 50 mM acetate buffer (50 µL) were used. Absorbance values measured at 460 nm were obtained using a microplate reader running for 3 hours, with readings after every 7.5 minutes.

#### 4.2.5 *Microbial community analysis*

An ITS rRNA amplicon survey was performed on soils that were sampled from the final time point, after the non-inoculated, inoculated and fresh soils were incubated for 67 days. The DNA was extracted from 0.25 g of soil using the Qiagen DNeasy PowerSoil Pro DNA extraction kit following the manufacturer's instructions. Four replicates were examined for each treatment. After extraction, the samples were stored in a freezer at – 20 °C prior to sequencing. The fungal ribosomal rDNA was amplified using primer sets ITS1. Paired-end sequencing (2 x 150 bp) was carried out on an Illumina MiSeq sequencer. The trimmed sequences obtained were analyzed using DADA2 (Callahan et al., 2016). DADA2 was used for quality filtering, where only quality scores above 20 were used. Due to the low overlap between forward and reverse reads, only the forward read was used. In addition, DADA2 was used for chimera removal.

#### 4.2.6 *Data analysis*

An analysis of variance (ANOVA) was conducted between the different percent ratio (w/w) of soils 25F and 25R and soil properties (organic matter and moisture percentages) for non-

inoculated and inoculated treatments with a significance cut-off value of  $p < 0.05$ . We conducted a post-hoc test (Tukey's HSD) where significant effects were found.

We used a non-metric multidimension scaling (NMDS) analysis to observe differences among treatments and soil mixtures using the phyloseq package (McMurdie and Holmes, 2013). A PERMANOVA was used to determine statistically significant differences between the microbial communities of the different treatments (non-inoculated, inoculated and fresh soils) and the different soil mixtures using the *adonis* function from the vegan package (Oksanen, 2011). For visual representation of the relative abundance of fungal classes, ggplot2 package in R was used (Ginestet, 2011). All statistics were performed using R (version 3.6.2).

### 4.3. Results and discussion

#### 4.3.1 *Soil properties of bulk soils*

The properties of the two soils, 25F and 25R, prior to autoclaving or mixing, have been well documented. Both soils have high metal loads and similar organic contaminant profiles (Hagmann et al., 2019a). Data in Figure 4-2B show that soil 25F, collected from the vegetated site, had higher organic matter content ( $35 \pm 0.4$  %) compared to soil 25R, which had an organic matter content of  $5.5 \pm 0.2$  % (Fig. 4-2B). The percent moisture of soil 25F ( $45 \pm 0.67$  %) was higher than the percent moisture of soil 25R ( $2.8 \pm 0.41$  %) (Fig. 4-2A). Since vegetated, soil 25F has input from plant debris, which can explain the higher amounts of soil organic matter compared to soil 25R. The small amount of organic matter in site 25R consists of anthropogenic contaminants, including coal (Hagmann et al., 2019a).

Figure 4-2

The initial phosphatase, cellobiohydrolase, and peroxidase activities of fresh soil 0 % 25R were higher than fresh soil 100 % 25R: Phosphatase activities of 0 % 25R and 100 % 25R were  $3.4 \pm 0.3 \mu\text{mol} \cdot \text{g}^{-1} \cdot \text{hr}^{-1}$  and  $0.003 \pm 0.001 \mu\text{mol} \cdot \text{g}^{-1} \cdot \text{hr}^{-1}$ , respectively. Cellobiohydrolase activity of 25F was  $0.10 \pm 0.01 \mu\text{mol} \cdot \text{g}^{-1} \cdot \text{hr}^{-1}$  while the activity of 25R was below detection limit (BDL). Peroxidase activity was also higher at 25F ( $10. \pm 2.0 \mu\text{mol} \cdot \text{g}^{-1} \cdot \text{hr}^{-1}$ ) compared to 25R ( $3.3 \pm 0.31 \mu\text{mol} \cdot \text{g}^{-1} \cdot \text{hr}^{-1}$ ). As was observed here, the phosphatase, cellobiohydrolase, and peroxidase activities of soils from vegetated site 25F (fresh soil 0 % 25R) have been previously been found to be higher compared to soil from barren site 25R (fresh soil 100 % 25R) (Hagmann et al., 2019).

#### 4.3.2 *Soil properties of non-inoculated and inoculated soils*

A gradient of abiotic properties was created by mixing 25F and 25R soils in different ratios even after autoclaving and 67 days of incubation. The percent moisture and organic matter were determined for non-inoculated and inoculated. As one might expect, percent moisture and organic matter decreased systematically with increasing percent ratios (w/w) of 25R soil for both non-inoculated and inoculated soils (Fig. 4-3A-B). These results agreed with those found in other studies where the metal concentrations, organic matter content, and aggregate particle size distribution were consistent with the proportions of two soils that had been mixed together to create a gradient (Don et al., 2017; O'Brien et al., 2017; Vaidya et al., 2020a). Percent moisture or organic matter were not found to be significantly different between non-inoculated and inoculated soils ( $P > 0.05$ ) (Fig. 4-3). This is likely due to the same amount of 25F soil was

added to both non-inoculated and inoculated soils. These data suggest that inoculation had little effect on soil abiotic properties.

Figure 4-3

Vaidya and co-workers measured metal/metalloid concentrations across an experimental gradient of two different soils and found that the concentrations were proportional to ratios of the two soils in the mixtures (Vaidya et al., 2020). Sites 25F and 25R are adjacent to each other and both have high metal concentrations, but there are several metals (Cd, Cr, Co, As, Cu, Zn, Pb, and Na) that are present at 2 to 5 times higher concentrations in 25R soil compared to 25F soil (Hagmann et al., 2019, Table 4-1). Therefore, by creating mixtures with different percentage ratios (w/w) of 25R soil, we created a gradient of heavy metal concentrations as shown in Table 4-1.

Table 4-1

#### 4.3.3 *Fungal and bacterial community analysis*

An NMDS displayed evidence the different treatments (non-inoculated, inoculated and fresh soils) did not cluster together at the genus level (Fig. 4-4). A PERMANOVA analysis revealed a significant difference in fungal community compositions between all three groups (non-inoculated, inoculated and fresh soils) for both fungi (pseudo F = 32.6,  $p < 0.001$ ) and bacteria (pseudo F = 15.2,  $p < 0.001$ ). In addition, a significant difference was observed among different soil mixtures for fungi (pseudo F = 6.8,  $p < 0.001$ ) and bacteria (pseudo F = 2.0,  $p < 0.05$ ). A

statistically significant interaction was observed between inoculum and soil mixture for fungi (pseudo  $F = 4.3$ ,  $p < 0.001$ ) and bacteria (pseudo  $F = 4.3$ ,  $p < 0.01$ ). The interaction effect between inoculum and soil mixture indicates it was not just the inoculation driving the fungal and bacterial community composition, but it was also the different percent ratios (w/w) of 25F and 25R soils that influences the microbial composition.

Fig. 4-4

The relative abundance of some fungal classes gradually changes along a gradient of percent ratio (w/w) of soils 25F and 25R (Fig. 4-5). When microbial communities are introduced into new environments, some groups of organisms will perish, while others may prosper (Trabelsi and Mhamdi, 2013). For inoculated soils, the introduction of fungal communities through inoculation of 25F soil are influenced by abiotic factors. Pearson correlation analysis showed a significant negative relationship between the relative abundance of Mortierellomycetes and increasing percent ratios (w/w) of 25R ( $r = -0.976$ ,  $p < 0.01$ , Fig. 4-6). Mortierellomycetes was more successful in establishing in soils that contained more 25F soils (67 %) and decreased with increasing percent ratios (w/w) of 25R). One study found Mortierellomycetes were sensitive to Zn pollution, where the relative abundance of Mortierellomycetes decreased compared to their control soil, which was unpolluted soil (Guarino et al., 2020). This supports the decrease in relative abundance of Mortierellomycetes, since in this study, the Zn concentration were found to be about 2.9 times higher in 25R soil than in 25F.

Fig. 4-5

Fig. 4-6

A Spearman correlation analysis showed a significant positive relationship between the relative abundance of Sordariomycetes and increasing percent ratios (w/w) of 25R ( $r = 1$ ,  $p < 0.05$ , Fig. 4-6). Sordariomycetes have been found to be adaptable to different environments and resistant to environmental stress since they are present in both contaminated and uncontaminated soils (Thion et al., 2012; Ventrino et al., 2016; Ventrino et al., 2019). One possible explanation that Sordariomycetes were able to survive in 25R soil, is their ability to metabolize PAHs (Marchand et al., 2017; Ventrino et al., 2019). It is also possible that Sordariomycetes are able to outcompete other fungal classes in the barren 25R soil. This implies the fungal compositions of the inoculated treatments were driven by abiotic factors in a concentration dependent fashion.

Visual inspection of Figure 4-6 suggested that the fungal community compositions were qualitatively similar between non-inoculated and inoculated 100 % 25R soils. This indicates that the barren 25R soil was unable to be successfully colonized by the fungal communities from 25F soil. This implies that the abiotic environment in 25R did not support the establishment of all fungal classes that were introduced. Soil abiotic factors have previously been found in several studies to influence microbial composition (Brockett et al., 2012; Buyer et al., 2010; Fierer and Jackson, 2006; Haack et al., 1995; Zhou et al., 2002). The abiotic factors, including metal concentrations, percent moisture and organic matter, of 25F and 25R soils are different (Table 4-1, Fig 4-3). Therefore, due to the difference in abiotic factors, some fungi may not establish, including possible metal stress. This finding has implications for experiments where the goal was to introduce a new microbial community into a soil for remediation purposes.

Fungal community compositions at the class level for the two fresh soils (0% 25R and 100% 25R) were not different (Fig. 4-5). However, there were different relative abundances for a few fungal classes. For example, Sordariomycetes was the most abundant taxa in fresh soil 100% 25R (60.2 %) while it was less abundant in fresh soil 0% 25R (20.1 %) (Fig. 4-5). This is not surprising because (Singh et al., 2019b) also observed a different fungal community composition between these two sites. Within LSP 25R, Singh and co-workers (2019b) found the relative abundance of Sordariomycetes to be 19.3%. However, we found the relative abundance of Sordariomycetes to be much higher, 60.2 %. One possible explanation for the variation Within this study, to encourage establishment of the whole microbial community into the soil mixtures, the inoculum of 25F was introduced as unautoclaved 25F soil. The fungal diversity of fresh soils was higher compared to the inoculated soils, most likely due to the disturbance caused by autoclaving the soils before inoculation with 25F soil for the inoculated soils (Appendix-B Fig. A1). The fungal communities of 100% 25R were also similar for the fresh soil and inoculated soils. The fungal class Sordariomycetes was the most abundant class in both the fresh soil and inoculated soils. It is possible that this fungal class was able to survive autoclaving.

The changes in bacterial communities along the soil gradient were less distinct than the fungal communities for the inoculated soils (Fig. 4-5). Note that previous work studying 25R soil determined that the bacterial communities were different compared to other LSP sites including site 25F (Singh et al., 2019b). While upon visual inspection of the bacterial community composition of the various inoculated soil mixtures, the relative abundance of the top 15 bacterial classes were similar (Fig. 4-5). For example, the relative abundance of the bacterial class Alphaproteobacteria ranged between 13.2 % (75 % 25R soil) and 14.9 % (100 % 25R soil)

for the inoculated soils (Fig. 4-5). It is possible that the bacterial communities present in each soil mixture may be able to revert to the original state, with a similar composition to those of the fresh soil after inoculation and incubation for 67 days (Mawarda et al., 2020). Indeed, the relative abundances of the top 15 bacterial classes appear similar to the inoculum (25F). Therefore, the inoculation appears to be successful for bacterial community composition.

The non-inoculated soils were autoclaved twice, but even after two months of incubation in a growth chamber both the fungal and bacterial communities were not entirely eliminated as shown by the presence of both fungal and bacteria classes (Fig. 4-5). Yet, there were a few fungal and bacterial classes that did not survive autoclaving. For example, the non-inoculated soils lacked Mortierellomycetes for all soil mixtures, where the relative abundance of Mortierellomycetes was less than 0.02 %. There were fewer bacterial classes present in the non-inoculated soils compared to both the inoculated and fresh soils (Fig. 4-5). The diversity of the non-inoculated soils were less compared to the inoculated soils (Appendix-B Figs. A1 and A2). For example, non-inoculated 100 % 25R soil had 5 bacterial classes that dominated the bacterial composition, compared the inoculated 100 % 25R soil that had 15 bacterial classes. Within non-inoculated soils, both fungal and bacterial community compositions appeared to be scattered with increasing percent ratio (w/w) of 25R soils and not necessarily dependent on the soil mixture (Fig. 4-5 A-B).

#### 4.3.3 *Effect of percent ratio (w/w) of soils on enzyme activity*

Phosphatase activity had a negative relationship with increasing percent ratios (w/w) of 25R for non-inoculated ( $y = -0.009x + 0.78$ ,  $R^2_{\text{adj}} = 0.84$ ,  $P < 0.001$ ) and inoculated soils ( $y = -0.0082x + 0.77$ ,  $R^2_{\text{adj}} = 0.78$ ,  $P < 0.001$ ) (Fig. 4-7 A-B). A similar negative trend was seen in the

relationship between cellobiohydrolase activity and increasing percent ratios (w/w) of 25R for both non-inoculated and inoculated soils (Fig. 4-7 C-D). For peroxidase activity there was also a negative relationship increasing percent ratios (w/w) of 25R for inoculated soils ( $y = -0.102x + 11.9$ ,  $R^2_{\text{adj}} = -0.54$ ,  $p < 0.001$ ) (Fig. 4-7 F). Conversely, for non-inoculated soils there was no relationship between peroxidase activity did not vary with increasing percent ratios (w/w) of 25R soil (Fig. 4-7 E).

Figure 4-7

Overall, the non-inoculated and inoculated had similar phosphatase, cellobiohydrolase activities. For example, the soil mixture 0 % 25R which had the highest phosphatase activity of various soil mixtures 0 % 25R was similar for both non-inoculated ( $0.93 \pm 0.05 \mu\text{mol} \cdot \text{g}_{\text{dry}}^{-1} \cdot \text{hr}^{-1}$ ) and inoculated soils ( $0.89 \pm 0.13 \mu\text{mol} \cdot \text{g}_{\text{dry}}^{-1} \cdot \text{hr}^{-1}$ ) ( $P > 0.05$ ). In addition, the soil mixture 100 % 25R had similar cellobiohydrolase activities for both non-inoculated ( $0.0094 \pm 0.0014 \mu\text{mol} \cdot \text{g}_{\text{dry}}^{-1} \cdot \text{hr}^{-1}$ ) and inoculated soils ( $0.0029 \pm 0.0015 \mu\text{mol} \cdot \text{g}_{\text{dry}}^{-1} \cdot \text{hr}^{-1}$ ) ( $P > 0.05$ ). Microbial communities can influence soil enzyme activities (Gallo et al., 2004a; Schneckner et al., 2015; Waldrop et al., 2000). Even though inoculated 100 % 25R soil were introduced with microorganisms from a high functioning soil through soil inoculation, the fungal community composition of the non-inoculated and inoculated soils was similar. This might explain the low phosphatase and cellobiohydrolase activities of 100 % 25R soil, but both the bacterial and fungal composition were different between the non-inoculated and inoculated soils for all soil mixtures. The non-inoculated soils despite being autoclaved still contained both fungi and bacteria that could release extracellular enzymes into the soil. This suggests that the extracellular enzymes

regardless of inoculation could be limited by the abiotic environment. Phosphatase and cellobiohydrolase activities are influenced by soil properties, such as organic matter, metal concentration and moisture, which are different between sites 25F and 25R (Narendrula-Kotha and Nkongolo, 2017).

Bacteria and fungi produce extracellular peroxidases, enzymes that use a secondary oxidant, like  $H_2O_2$ , to degrade aromatic compounds, like lignin and humus (Sinsabaugh, 2010; Sinsabaugh et al., 2008; Tian and Shi, 2014). The soil mixtures containing higher percent ratios (w/w) of 25R soil, which originates from a barren site, might provide poor habitats for these organisms that are found to be more abundant in soils that have high lignin concentrations (Sinsabaugh, 2010; Sinsabaugh et al., 2008). This supports a decrease in peroxidase activity in inoculated soils, since the barren site lacks vegetation. Peroxidase activities have also been found to increase with increasing metal concentrations. However, 25R soil has lower peroxidase activity compared to 25F soil. One possible explanation for peroxidase activity not decreasing with increasing percent ratio (w/w) of 25R soil is the scattered differences in the non-inoculated fungal and bacterial communities (Fig. 4-5). It is possible that the peroxidase activities were influenced by the microbial communities more than by the abiotic properties. Yet, for both non-inoculated and inoculated treatments, phosphatase and cellobiohydrolase activities decreased with increasing percent ratios (w/w) of 25R soil (Fig. 4-7 A-D). Since both non-inoculated and inoculated fungal and bacterial community compositions did not decrease with increasing percent ratios (w/w) of 25R soils, it is more likely phosphatase and cellobiohydrolase activities were influenced by the abiotic properties more than by the microbial communities. This data support previous findings that abiotic properties present in the soil limited enzyme activity (Singh et al., 2019a; Vaidya et al., 2020a).

#### 4.4. Conclusion

The introduction of soil microbial communities through soil inoculation from 25F soil varied depending on the ratio of soils 25F and 25R. The relative abundance of some fungal classes increased while other fungal classes decreased with increased percent ratio (w/w) of 25R soils. Introduction of 25F microbial communities into the barren 25R soil (100 % 25R) was unsuccessful as demonstrated by the similarities in fungal community compositions found for non-inoculated and inoculated soils. Singh and co-workers (2019a) found that fungal communities were driven by inoculation. However, we found that fungal community compositions of inoculated soils were driven by abiotic properties. Phosphatase, cellobiohydrolase and peroxidase activities decreased with increasing percent ratios (w/w) of 25R soil for inoculated soils. If enzyme activities were increased in the barren soil, 25R, then the degradation of organic matter can increase. An increase of organic matter in contaminated soils can help retain metals in the soil, which can reduce their bioavailability to plants and microorganisms. However, we found in the inoculated treatment that abiotic properties present in 25R soil limited phosphatase, cellobiohydrolase and peroxidase activities. Inorganic contaminants, moisture content and organic matter content are a few soil properties that could explain the differences in both microbial community composition and enzyme activity. Introducing microbial inoculum into a gradient of increasing percent ratios (w/w) of 25R provided insights into how microbial communities and different abiotic environments interact, which may explain the inability for certain microorganisms to survive. There may be other barren sites like 25R that create an environment that are inhospitable to introduced microbial communities.

### References

- Bardgett R.D., Freeman C., Ostle N.J., 2008. Microbial contributions to climate change through carbon cycle feedbacks. *The ISME Journal*; 2: 805-814.
- Bounaffaa M., Florio A., Le Roux X., Jayet P.-A., 2018. Economic and Environmental Analysis of Maize Inoculation by Plant Growth Promoting Rhizobacteria in the French Rhône-Alpes Region. *Ecological Economics*; 146: 334-346.
- Brockett B.F.T., Prescott C.E., Grayston S.J., 2012. Soil moisture is the major factor influencing microbial community structure and enzyme activities across seven biogeoclimatic zones in western Canada. *Soil Biology and Biochemistry*; 44: 9-20.
- Buyer J.S., Teasdale J.R., Roberts D.P., Zasada I.A., Maul J.E., 2010. Factors affecting soil microbial community structure in tomato cropping systems. *Soil Biology and Biochemistry*; 42: 831-841.
- Callahan B.J., McMurdie P.J., Rosen M.J., Han A.W., Johnson A.J.A., Holmes S.P., 2016. DADA2: High-resolution sample inference from Illumina amplicon data. *Nature Methods*; 13: 581-583.
- Don A., Böhme I.H., Dohrmann A.B., Poeplau C., Tebbe C.C., 2017. Microbial community composition affects soil organic carbon turnover in mineral soils. *Biology and fertility of soils*; 53: 445-456.
- Fierer N., Jackson R.B., 2006. The diversity and biogeography of soil bacterial communities. *Proceedings of the National Academy of Sciences*; 103: 626-631.
- Gadd G.M., 2005. Microorganisms in toxic metal-polluted soils. *Microorganisms in soils: roles in genesis and functions*. Springer, pp. 325-356.

- Gadd G.M., Griffiths A.J., 1977. Microorganisms and heavy metal toxicity. *Microbial ecology*; 4: 303-317.
- Gallo M., Amonette R., Lauber C., Sinsabaugh R., Zak D., 2004. Microbial community structure and oxidative enzyme activity in nitrogen-amended north temperate forest soils. *Microbial ecology*; 48: 218-229.
- Ginestet C., 2011. *ggplot2: elegant graphics for data analysis*. Wiley Online Library.
- Guarino F., Improta G., Triassi M., Cicatelli A., Castiglione S., 2020. Effects of Zinc Pollution and Compost Amendment on the Root Microbiome of a Metal Tolerant Poplar Clone. *Frontiers in Microbiology*; 11.
- Haack S.K., Garchow H., Klug M.J., Forney L.J., 1995. Analysis of factors affecting the accuracy, reproducibility, and interpretation of microbial community carbon source utilization patterns. *Applied and Environmental Microbiology*; 61: 1458-1468.
- Hagmann D.F., Goodey N.M., Mathieu C., Evans J., Aronson M.F.J., Gallagher F., et al., 2015. Effect of metal contamination on microbial enzymatic activity in soil. *Soil Biol. Biochem.*; 91: 291-297.
- Hagmann D.F., Krüge M.A., Cheung M., Mastalerz M., Gallego J.L.R., Singh J.P., et al., 2019. Environmental forensic characterization of former rail yard soils located adjacent to the Statue of Liberty in the New York/New Jersey harbor. *Sci. Total Environ.*; 690: 1019-1034.
- Johnson D.L., Maguire K.L., Anderson D.R., McGrath S.P., 2004. Enhanced dissipation of chrysene in planted soil: the impact of a rhizobial inoculum. *Soil Biology and Biochemistry*; 36: 33-38.

- Khan A.G., Kuek C., Chaudhry T.M., Khoo C.S., Hayes W.J., 2000. Role of plants, mycorrhizae and phytochelators in heavy metal contaminated land remediation. *Chemosphere*; 41: 197-207.
- Kozlov M.V., Zvereva E.L., 2007. Industrial barrens: extreme habitats created by non-ferrous metallurgy. *Reviews in Environmental Science and Bio/Technology*; 6: 231-259.
- Krumins J.A., Goodey N.M., Gallagher F., 2015. Plant–soil interactions in metal contaminated soils. *Soil Biology and Biochemistry*; 80: 224-231.
- Lauber C.L., Hamady M., Knight R., Fierer N., 2009. Pyrosequencing-based assessment of soil pH as a predictor of soil bacterial community structure at the continental scale. *Applied and environmental microbiology*; 75: 5111-5120.
- Marchand C., St-Arnaud M., Hogland W., Bell T.H., Hijri M., 2017. Petroleum biodegradation capacity of bacteria and fungi isolated from petroleum-contaminated soil. *International Biodeterioration & Biodegradation*; 116: 48-57.
- Mawarda P.C., Le Roux X., Dirk van Elsas J., Salles J.F., 2020. Deliberate introduction of invisible invaders: A critical appraisal of the impact of microbial inoculants on soil microbial communities. *Soil Biology and Biochemistry*; 148: 107874.
- McMurdie P.J., Holmes S., 2013. phyloseq: an R package for reproducible interactive analysis and graphics of microbiome census data. *PloS one*; 8: e61217.
- Narendrula-Kotha R., Nkongolo K.K., 2017. Changes in enzymatic activities in metal contaminated and reclaimed lands in Northern Ontario (Canada). *Ecotoxicology and Environmental Safety*; 140: 241-248.

- O'Brien P.L., DeSutter T.M., Ritter S.S., Casey F.X.M., Wick A.F., Khan E., et al., 2017. A large-scale soil-mixing process for reclamation of heavily disturbed soils. *Ecological Engineering*; 109: 84-91.
- Oksanen J., 2011. *vegan: Community Ecology Package*. R package version 1.17-9. <http://cran.r-project.org/package=vegan>.
- Ouahmane L., Thioulouse J., Hafidi M., Prin Y., Ducousso M., Galiana A., et al., 2007. Soil functional diversity and P solubilization from rock phosphate after inoculation with native or allochthonous arbuscular mycorrhizal fungi. *Forest Ecology and Management*; 241: 200-208.
- Panke-Buisse K., Poole A.C., Goodrich J.K., Ley R.E., Kao-Kniffin J., 2015. Selection on soil microbiomes reveals reproducible impacts on plant function. *The ISME Journal*; 9: 980-989.
- Puglisi E., Hamon R., Vasileiadis S., Coppolecchia D., Trevisan M., 2012. Adaptation of Soil Microorganisms to Trace Element Contamination: A Review of Mechanisms, Methodologies, and Consequences for Risk Assessment and Remediation. *Critical Reviews in Environmental Science and Technology*; 42: 2435-2470.
- Rajkumar M., Sandhya S., Prasad M.N.V., Freitas H., 2012. Perspectives of plant-associated microbes in heavy metal phytoremediation. *Biotechnology Advances*; 30: 1562-1574.
- Rodríguez-Caballero E., Castro A.J., Chamizo S., Quintas-Soriano C., Garcia-Llorente M., Cantón Y., et al., 2018. Ecosystem services provided by biocrusts: From ecosystem functions to social values. *Journal of Arid Environments*; 159: 45-53.

- Schnecker J., Wild B., Takriti M., Eloy Alves R.J., Gentsch N., Gittel A., et al., 2015. Microbial community composition shapes enzyme patterns in topsoil and subsoil horizons along a latitudinal transect in Western Siberia. *Soil Biology and Biochemistry*; 83: 106-115.
- Singh B.K., Bardgett R.D., Smith P., Reay D.S., 2010. Microorganisms and climate change: terrestrial feedbacks and mitigation options. *Nature Reviews Microbiology*; 8: 779-790.
- Singh J.P., Ojinnaka E.U., Krumins J.A., Goodey N.M., 2019a. Abiotic factors determine functional outcomes of microbial inoculation of soils from a metal contaminated brownfield. *Ecotoxicol. Environ. Saf.*; 168: 450-456.
- Singh J.P., Vaidya B.P., Goodey N.M., Krumins J.A., 2019b. Soil microbial response to metal contamination in a vegetated and urban brownfield. *J. Environ. Manage.*; 244: 313-319.
- Sinsabaugh R.L., 2010. Phenol oxidase, peroxidase and organic matter dynamics of soil. *Soil Biol. Biochem.*; 42: 391-404.
- Sinsabaugh R.L., Lauber C.L., Weintraub M.N., Ahmed B., Allison S.D., Crenshaw C., et al., 2008. Stoichiometry of soil enzyme activity at global scale. *Ecology Letters*; 11: 1252-1264.
- Tamayo-Vélez Á., Osorio N.W., 2018. Soil Fertility Improvement by Litter Decomposition and Inoculation with the Fungus *Mortierella* sp. in Avocado Plantations of Colombia. *Communications in Soil Science and Plant Analysis*; 49: 139-147.
- Thion C., Cébron A., Beguiristain T., Leyval C., 2012. Long-term in situ dynamics of the fungal communities in a multi-contaminated soil are mainly driven by plants. *FEMS Microbiology Ecology*; 82: 169-181.

- Tian L., Shi W., 2014. Soil peroxidase regulates organic matter decomposition through improving the accessibility of reducing sugars and amino acids. *Biology and Fertility of Soils*; 50: 785-794.
- Torsvik V., Øvreås L., Thingstad T.F., 2002. Prokaryotic diversity--magnitude, dynamics, and controlling factors. *Science*; 296: 1064-1066.
- Trabelsi D., Mhamdi R., 2013. Microbial Inoculants and Their Impact on Soil Microbial Communities: A Review. *BioMed Research International*; 2013: 863240.
- Vaidya B.P., Hagemann D.F., Balacco J., Passchier S., Krumins J.A., Goodey N.M., 2020. Plants mitigate restrictions to phosphatase activity in metal contaminated soils. *Environ. Pollut.*: 114801.
- Ventorino V., Parillo R., Testa A., Viscardi S., Espresso F., Pepe O., 2016. Chestnut green waste composting for sustainable forest management: Microbiota dynamics and impact on plant disease control. *Journal of Environmental Management*; 166: 168-177.
- Ventorino V., Pascale A., Fagnano M., Adamo P., Faraco V., Rocco C., et al., 2019. Soil tillage and compost amendment promote bioremediation and biofertility of polluted area. *Journal of Cleaner Production*; 239: 118087.
- Wagg C., Bender S.F., Widmer F., van der Heijden M.G.A., 2014. Soil biodiversity and soil community composition determine ecosystem multifunctionality. *Proceedings of the National Academy of Sciences*; 111: 5266-5270.
- Waldrop M.P., Balser T.C., Firestone M.K., 2000. Linking microbial community composition to function in a tropical soil. *Soil Biology and Biochemistry*; 32: 1837-1846.
- Xun W., Huang T., Zhao J., Ran W., Wang B., Shen Q., et al., 2015. Environmental conditions rather than microbial inoculum composition determine the bacterial composition,

microbial biomass and enzymatic activity of reconstructed soil microbial communities.

Soil Biology and Biochemistry; 90: 10-18.

Zak D.R., Holmes W.E., White D.C., Peacock A.D., Tilman D., 2003. Plant diversity, soil microbial communities, and ecosystem function: are there any links? Ecology; 84: 2042-2050.

Zhou J., Xia B., Treves D.S., Wu L.-Y., Marsh T.L., O'Neill R.V., et al., 2002. Spatial and Resource Factors Influencing High Microbial Diversity in Soil. Applied and Environmental Microbiology; 68: 326-334.

## TABLES

**Table 4-1.** Concentrations of Cd, Cr, Co, As, Cu, Zn, Pb, and Na (mg/kg) in soil from LSP sites 25F and 25R. Concentrations of soils 100% 25F and 100% 25R were reported in Hagmann et al., 2019. The concentrations of the other soil mixtures (25 % 25R, 50 % 25R, and 75 % 25R) were calculated based on experimentally determined amounts of soils that were mixed and were indicated by †.

mg/kg	[Cd]	[Cr]	[Co]	[As]	[Cu]	[Zn]	[Pb]	[Na]
0% 25R	3.88 ± 0.63	79.2 ± 3.2	257 ± 47	630 ± 187	2,256 ± 320	14,435 ± 2,845	7,145 ± 1351	873 ± 129
25% 25R†	4.85 ± 0.90	100.7 ± 7.8	410 ± 80	763 ± 192	3,483 ± 618	21,144 ± 4,265	10,434 ± 2,065	1,753 ± 264
50% 25R†	5.81 ± 1.17	122.2 ± 12.4	563 ± 113	896 ± 197	4,711 ± 916	27,853 ± 5,685	13,724 ± 2,777	2,633 ± 399
75% 25R†	6.77 ± 1.45	143.7 ± 17.1	716 ± 146	1,029 ± 202	5,938 ± 1214	34,562 ± 7,106	17,013 ± 3,490	3,513 ± 534
100% 25R	7.74 ± 2.91	165.2 ± 21.7	869 ± 179	1,162 ± 207	7,165 ± 1512	41,271 ± 8,526	20,302 ± 4,203	4,393 ± 669

## FIGURES

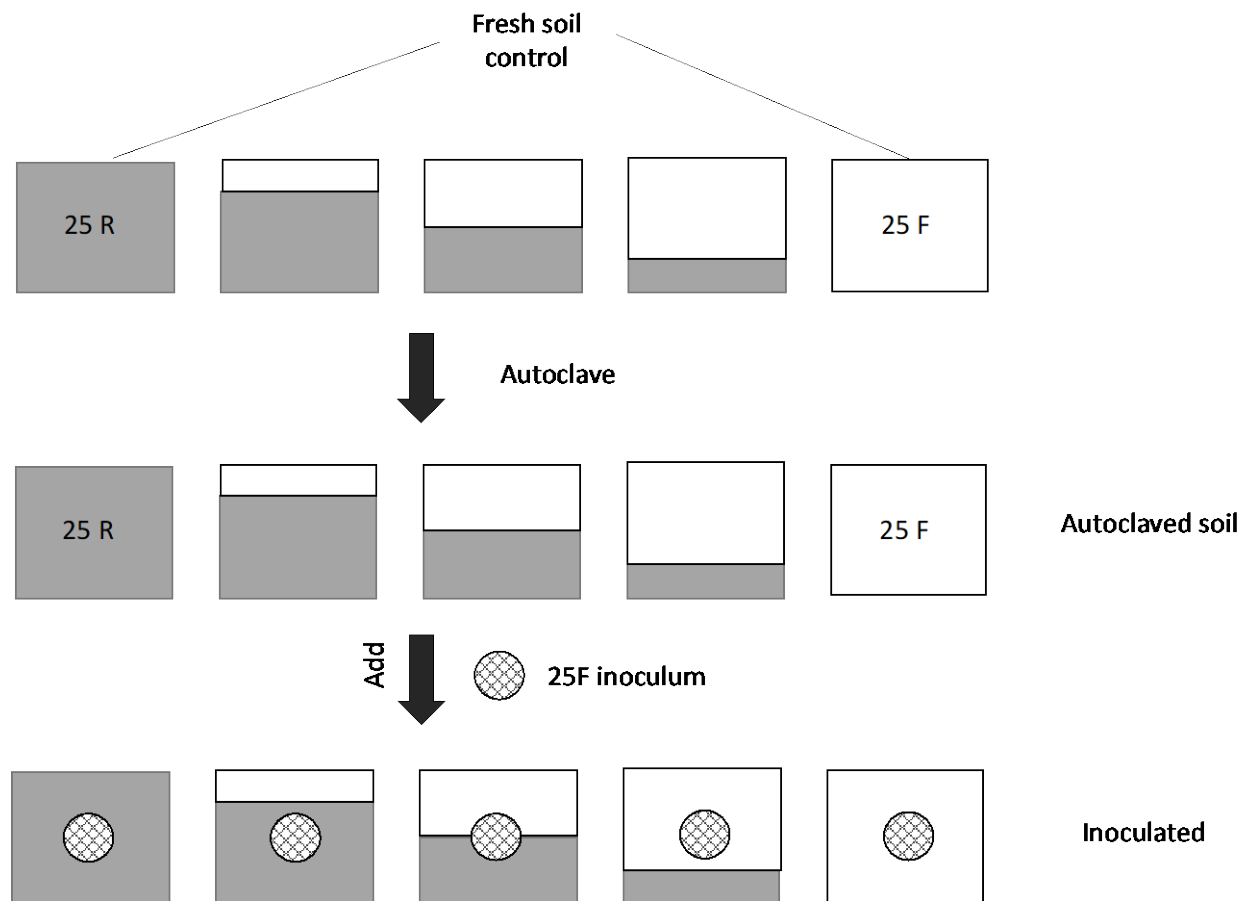


**Fig. 4-1.** Experimental design for the inoculation of 25F soils into an experimentally created gradient of different soil mixtures. Soil mixtures included 0 % 25R, 25 % 25R, 50 % 25R, 75 % 25R, and 100 % 25R. The non-inoculated treatment were autoclaved soil mixtures with 5 % autoclaved 25F soil. The inoculated treatment were autoclaved soil mixtures that were inoculated with 25F soil. Fresh soils were non-autoclaved 0 % 25R and 100 % 25R soils.

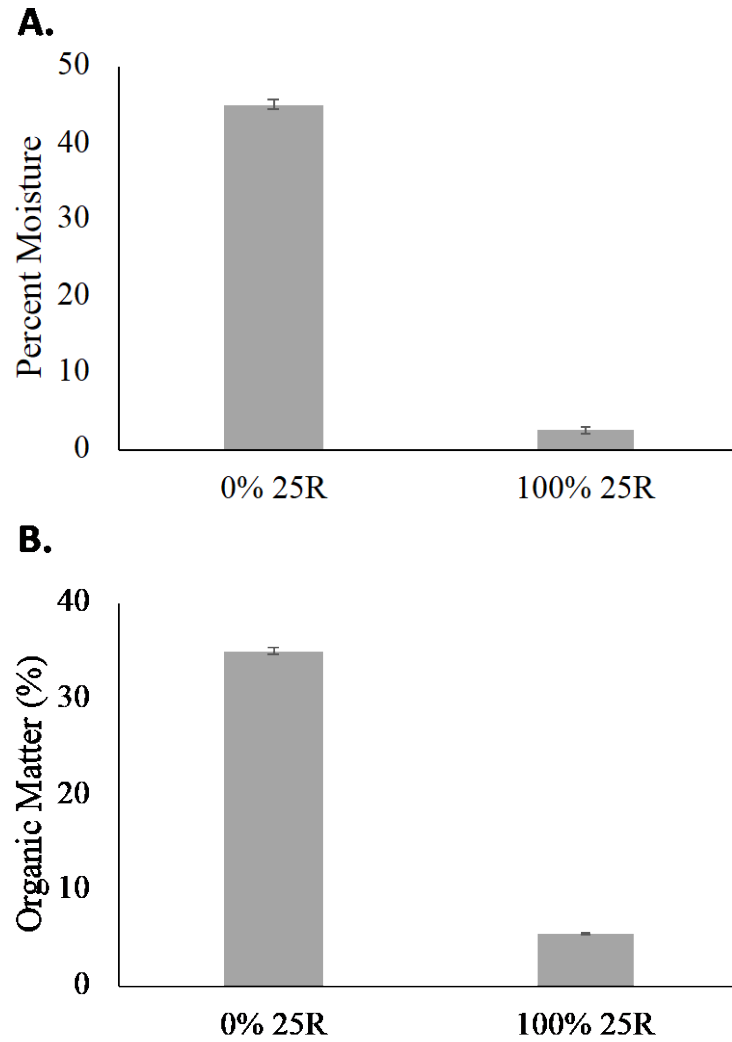


**Fig 4-2.** Moisture (A) and organic matter (B) percentages (w/w) of fresh soils (non-autoclaved) from sites 25F and 25R. Soil samples collected from 25F had higher percentages of moisture and organic matter. Bars represent the average of five replicates ( $n = 5$ ) with standard errors shown.

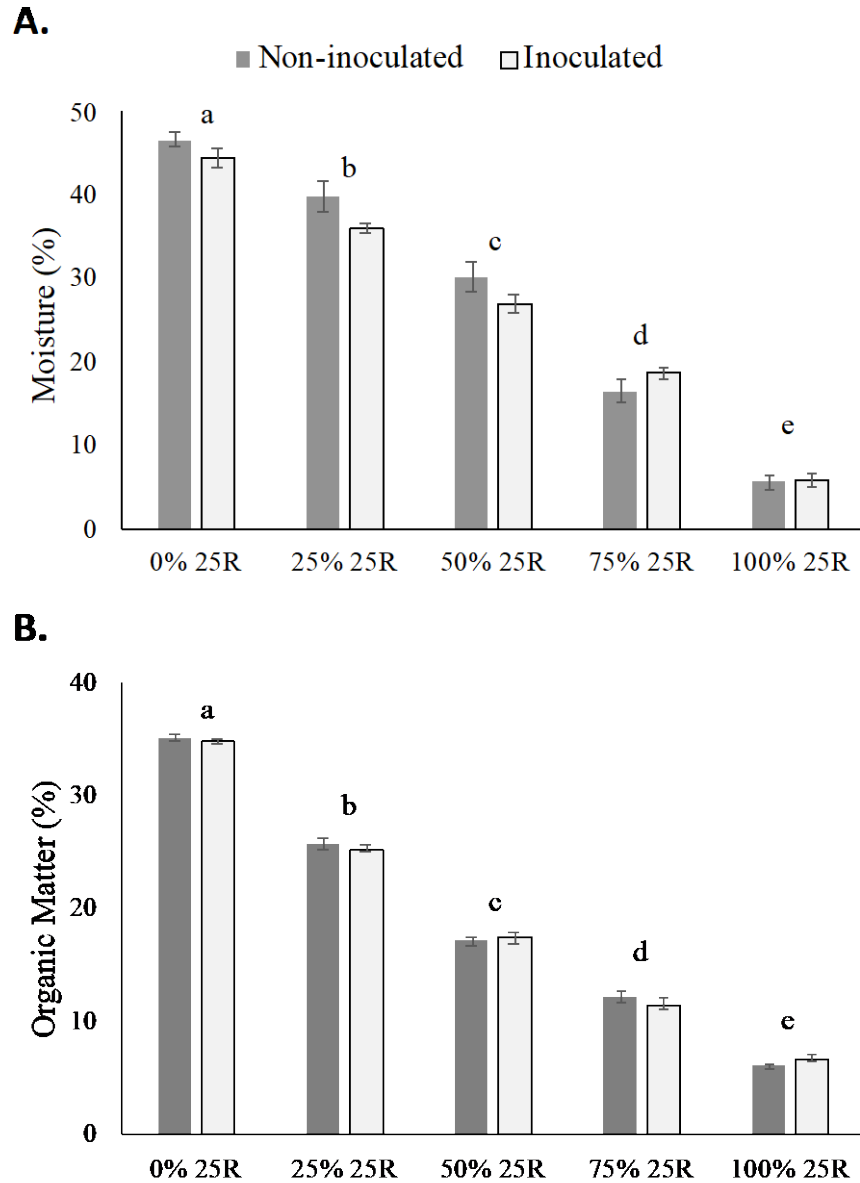


**Fig 4-3.** Moisture (A) and organic matter (B) of different percent ratio (w/w) of soils 25F and 25R for non-inoculated (dark gray) and inoculated (light gray) soils after 67 days in a growth chamber. No statistically significant differences in moisture or organic matter were found between non-inoculated and inoculated soils. Increasing percent ratios (w/w) of 25R soil corresponded to decreased percent moisture and organic matter. Bars represent the averages of

five replicates ( $n = 5$ ) with standard errors shown. Letters (a-e) over bars indicate significant differences among the means of the different soil mixtures (Tukey test,  $p < 0.05$ ).

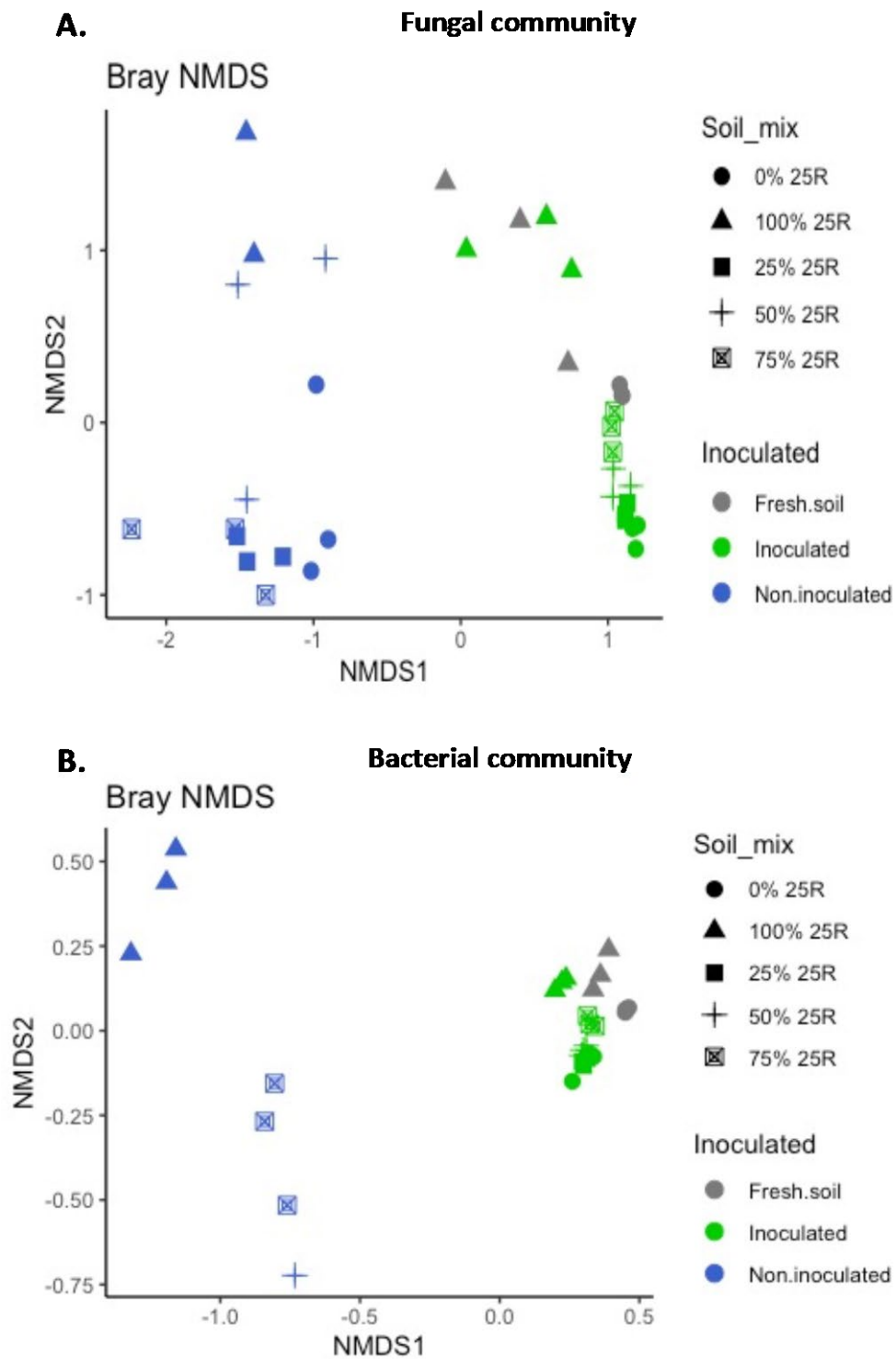


**Fig. 4-4.** NMDS of fungal genus (A) and bacterial genus (B) across the different treatments (non-inoculated, inoculated and fresh soil). Both soil mixtures and treatments (non-inoculated, inoculated and fresh soils) had a significant impact on fungal and bacterial communities.

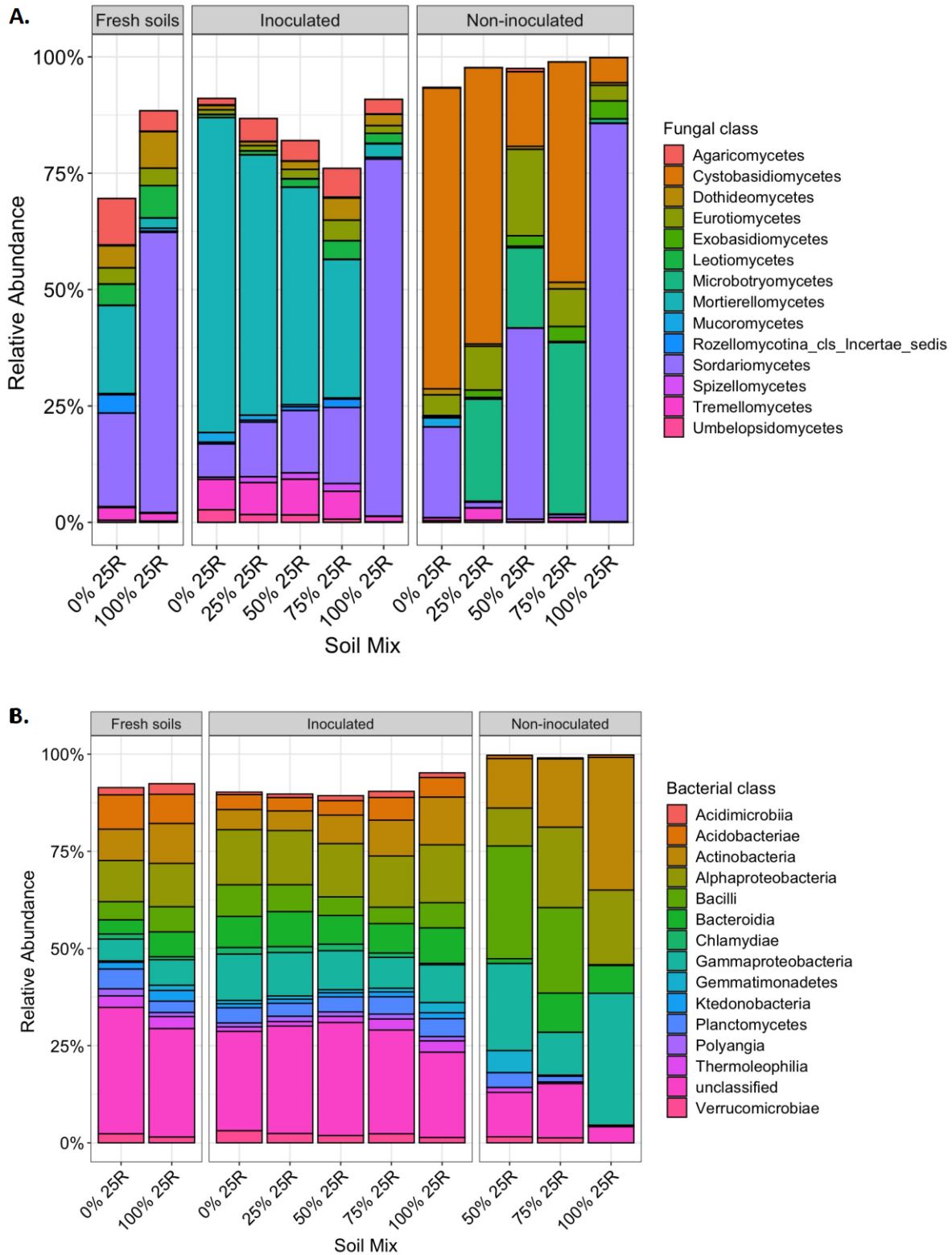


**Fig. 4-5.** Relative abundances of the top 15 fungal classes (A) and bacterial classes (B) across different soil mixtures for non-inoculated, inoculated and fresh soils.

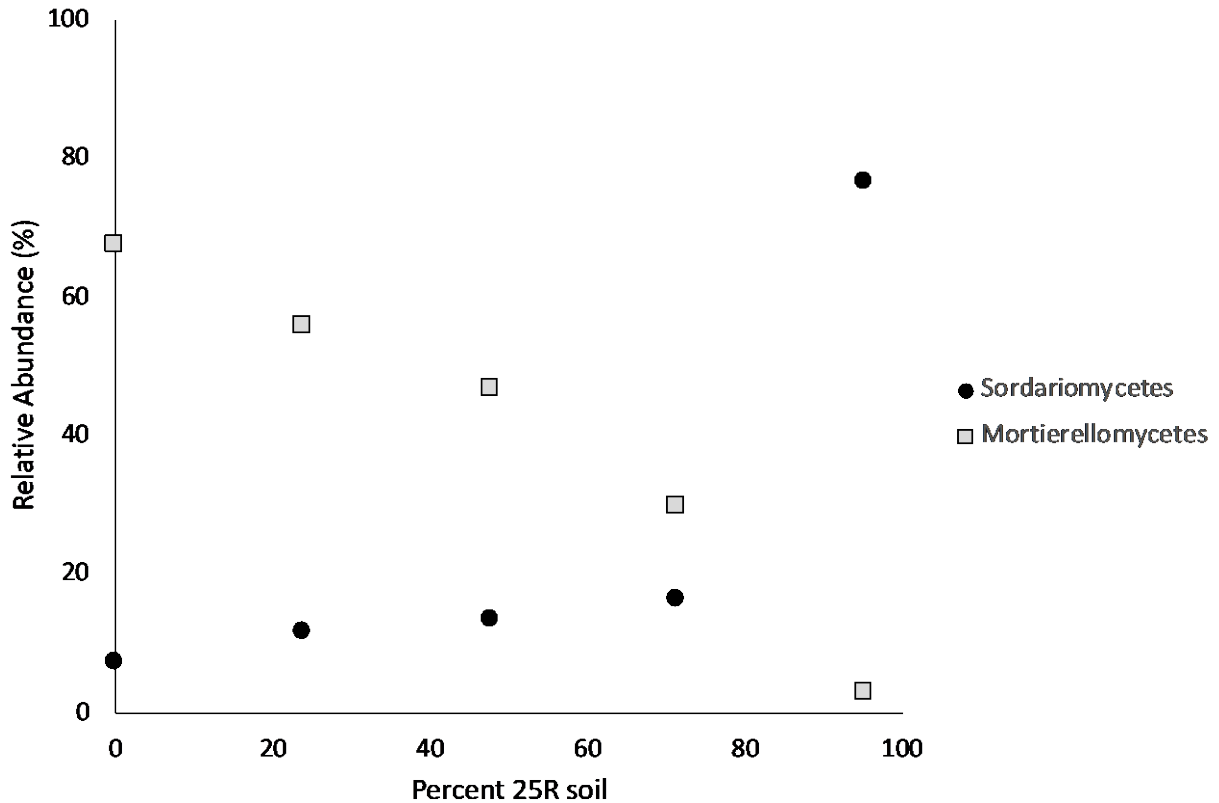


**Fig. 4-6.** Correlations of relative abundance of fungal classes Mortierellomycetes (A) and Sordariomycetes (B) across the ratios of soil mixtures containing increasing percent ratios (w/w) of 25R soil for inoculated soils. There was a significant negative relationship between the relative abundance of Mortierellomycetes and the percent ratio (w/w) of soil mixtures (A) ( $r = -0.976$ ,  $p < 0.01$ , Pearson). There was significant positive relationship between the relative abundance of Sordariomycetes and the ratios of soil mixtures (B) with increasing amounts of 25R ( $r = 1$ ,  $p < 0.05$ , Spearman).

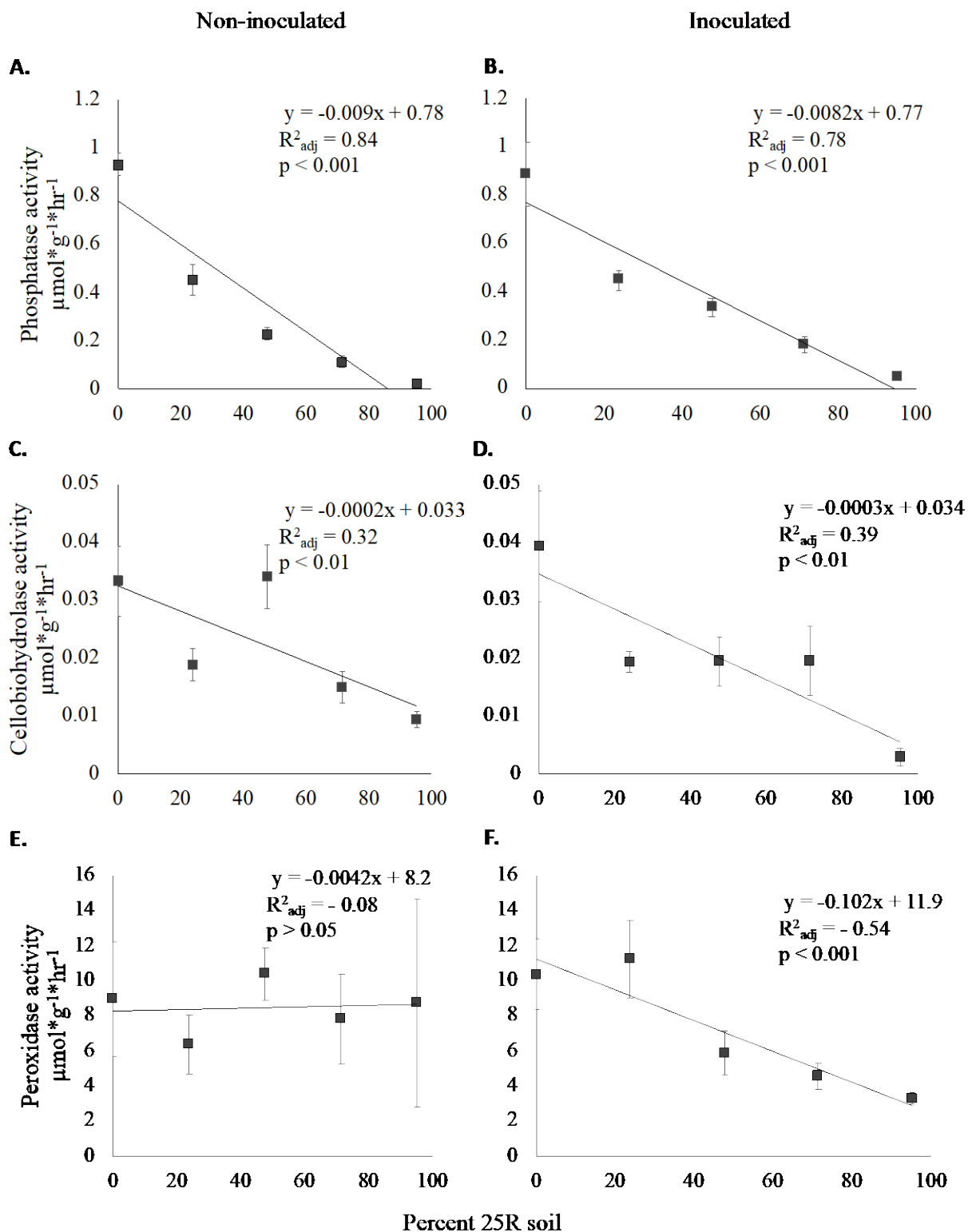


**Fig. 4-7.** Relationship between enzyme activities with the increasing percent ratios (w/w) of 25R soils (0 %, 25 %, 50 %, 75 %, and 100% 25R), for both non-inoculated and inoculated treatments

after incubation for 67 days in a growth chamber. The data were fitted to a Linear equation.

Phosphatase (A, B), cellobiohydrolase (C, D) and peroxidase (E, F) activities are shown.

Phosphatase and cellobiohydrolase activities decreased with increasing percent ratios (w/w) of 25R soil for both non-inoculated and inoculated soils for phosphatase and cellobiohydrolase activities. Peroxidase activity did not decrease with increasing percent ratios (w/w) of 25R soil. However, peroxidase activity did not decrease with increasing percent ratios (w/w) of 25R soil for the non-inoculated soil. The error bars indicate the standard errors with a minimum of 3 replicates ( $n = 3$ ).

## Chapter 5

### Revitalizing soil function through different combinations of artificial root exudates

#### Abstract

In vegetated soils, roots release exudates, impacting rhizosphere microbiome composition and function. The change in composition of low molecular weight compounds present in root exudates can change soil function (Strickland et al., 2015). However, unvegetated industrial barrens and contaminated brownfields cannot capitalize on this ecosystem service when conditions are too restrictive to support plant growth. We test this idea in soils from a barren site within an abandoned brownfield that is contaminated with heavy metals and organic pollutants, Liberty State Park, located in Jersey City, New Jersey, USA. Specifically, we tested the effects of adding different combinations of artificial root exudates including sugars, organic acids, and amino acids on soil enzymatic activities in otherwise barren and inactive soil. We measured three soil enzymatic activities over several time points over 120 days. The combination of sugars, organic acids, and amino acids increased phosphatase ( $1.26 \pm 0.12 \mu\text{mol} \cdot \text{g}_{\text{dry}}^{-1} \cdot \text{hr}^{-1}$ ), cellobiohydrolase ( $0.02 \pm 0.002 \mu\text{mol} \cdot \text{g}_{\text{dry}}^{-1} \cdot \text{hr}^{-1}$ ), and L-leucine aminopeptidase ( $0.15 \pm 0.036 \mu\text{mol} \cdot \text{g}_{\text{dry}}^{-1} \cdot \text{hr}^{-1}$ ) activities to a greater degree than other combinations. Phosphatase activity increased by a greater factor than the other enzyme activities regardless of the root exudate combination added. The addition of exudate combinations that included amino acids led to the greatest increase in L-leucine aminopeptidase. Our results indicate that the different enzyme activities depend on the different components of root exudates (*ie* sugars organic acids and amino acids).

### 5.1. Introduction

Roots secrete a wide range of compounds (root exudates) into the surrounding rhizosphere soils, including amino acids, organic acids, sugars and secondary metabolites (Rovira, 1969; Steinauer et al., 2016). The quality and quantity of root exudates depends on the plant species, age of an individual plant, and soil biotic and abiotic factors (Badri and Vivanco, 2009; Hertenberger et al., 2002; Jones et al., 2004). The effect of root exudates on soil function is influenced by the soil's nutrient availability, including concentrations and substrate stoichiometry of C, N and P (Girkin et al., 2018). Here, substrate stoichiometry is defined as the ratio of C, N, and P required by organisms and how it affects nutrient cycling (Hessen et al., 2004). Priming effects result from the input of labile C and/or N through amendments like artificial root exudates that cause strong short-term changes in microbial decomposition of soil organic matter (Kuzyakov et al., 2000). Artificial root exudates are solutions that mimic the composition of naturally occurring root exudate mixtures can be prepared and usually comprise of a synthetic mixture of sugars, organic acids and amino acids.

Root exudate composition can change extracellular enzyme activity (Kreyling et al., 2008; Strickland et al., 2015). It is possible for extracellular enzyme activity to increase, decrease or have no change. There can be an increase in enzyme activity in response to root exudates, which may stimulate microbial demand for nutrients (Cheng and Kuzyakov, 2005). Labile root exudate compounds can serve as co-metabolites where they provide easily assimilated carbon, which can induce increase in enzyme activity and enzyme production (Fontaine et al., 2003; Keiluweit et al., 2015; Kuzyakov et al., 2000). Sugars have been found to be the most prominent fraction of root exudates present in agricultural plants such as maize and perennial ryegrass (Baudoin et al., 2003; Benizri et al., 2002; Henry et al., 2008; Paterson et al.,

2007). Conversely, organic acids have been found to a more significant component in root exudates from forest trees (Hodge et al., 1996; Smith, 1976). Various combinations of sugars, organic acids and amino acids are all exuded into the soil. Yet, it is also important to investigate how each variation of the different components of root exudates influences extracellular enzyme activity. For example, if sugars dominate and small amounts of amino acids are exuded, then will the enzyme activity reflect only the addition of sugars or the combination of the two individual components. One question arises, since the composition of root exudates can vary, will enzyme activity be reflective of the different combinations.

Because different plant species release different quantities and varieties of low molecular weight organic compounds, it is expected that a greater diversity of plant species will lead to a more diverse composition of root exudates in the soil (Steinauer et al., 2016). It has been found that soil microbial communities and function are connected with plant diversity, which can alter soil enzyme activities (Chung et al., 2007; Steinauer et al., 2015). There has been speculation that the quantity and diversity of root exudates can influence the effects of plant diversity on microbial communities (Eisenhauer et al., 2017). Therefore, if plant diversity can affect microbial communities, then will soil function change. High diversity treatment of root exudates is defined here as a greater number of different compounds present in the exudate solution compared to low diversity treatment (Steinauer et al., 2016).

Postindustrial barren and contaminated sites globally require strategies for revitalizing soil microbial function. Contamination, including heavy metal presence, can have negative effects on enzyme activities (Khan et al., 2010; Yang et al., 2006). A previous study showed that by establishing conditions that allowed plant growth in a contaminated, poorly-functioning, previously barren soil within Liberty State Park (LSP), an increase in soil phosphatase activity

was observed (Vaidya et al., 2020b). The poorly-functioning, barren soil from LSP, is site 25R. Instead of growing plants, addition of organic amendments, such as artificial exudates, can potentially overcome the adverse effect of the contaminant/s by boosting microbial activity (Gianfreda and Ruggiero, 2006; Nannipieri, 1994; Nannipieri et al., 2012). For example, Vaidya and co-workers found phosphatase activity increased by 351-fold change compared to the control where no exudates were added with the addition several root exudates, which included the combination of sugars, organic acids and amino acids, to a poorly-functioning LSP 25R (Vaidya et al., *submitted*). Root exudates that include a combination of sugars, organic acids and amino acids provide both C and N sources into the soil. Since enzyme activities are indicator of microbial nutrient demand, then different nutrient cycling enzymes, such as cellobiohydrolase might not result in such a large increase due to the different inputs of nutrients (Caldwell, 2005; Moorhead and Sinsabaugh, 2006; Schimel and Weintraub, 2003).

The aim of this experiment was to determine the impacts of different combinations of artificial root exudates on the enzymatic function of a contaminated, barren, poorly functioning soil. Specifically, we hypothesized that the addition of a combination of sugars, organic acids and amino acids would yield a higher enzyme activity than the individual components alone. We also determined whether phosphatase, cellobiohydrolase, and L-leucine aminopeptidase activities would respond to artificial exudate treatments in the same way and to the same extent or whether the responses were different among the enzyme activities studied. Selected combinations of artificial exudate groups (sugars, organic acids and amino acids) were added to low functioning soil LSP 25R, and phosphatase, cellobiohydrolase, and L-leucine aminopeptidase activities were measured over 120 days. The other aim of this study was to determine how the diversity of the composition of root exudates affects soil function in a contaminated poorly-functioning soil. We

added low and high diversity artificial root exudates to LSP 25R and measured phosphatase activity over 60 days.

## **5.2. Methods**

### *5.2.1 Study site and soil collection*

The soil samples were collected from a 100-ha plot within LSP in Jersey City, New Jersey (40° 42' 16 N, 74° 03' 06 W). This plot of land has restricted access from the public since 1969, and a naturally occurring mixed plant community (primarily temperate deciduous forest and ephemeral wetlands) has assembled across much of the site. LSP has been investigated in several recent studies that have characterized both the inorganic and organic contaminants present in the soil (Hagmann et al., 2019, *see Ch. 2*). There are a variety of heavy metals in the soil that are not evenly distributed within the restricted 100 ha brownfield (Gallagher et al., 2008). In addition to the heavy metals, there is also presence of fossil fuel derived compounds, like polycyclic aromatic hydrocarbons, in the soil (Hagmann et al., 2019, *see Ch. 2*). The soils collected for each experiment described below were from a barren strip of land, 25R, that has never supported vegetation. Soils were collected from barren site 25R within LSP on April 8, 2019. The soils were sieved and stored in a refrigerator at 4 °C.

### *5.2.2 Experimental design of different combinations of artificial root exudates*

Consistent amounts of sieved soil (< 2 mm, ~ 120 g) were added to pots. These soils were placed in a climate-controlled chamber that maintained a temperature of 24 °C with the relative humidity maintained at 65 % during the day and a temperature of 19 °C with the relative humidity maintained at 55 % during the evening. Artificial root exudates solutions prepared

consist of low molecular weight compounds that include sugars (S-), organic acids (O-) and amino acids (A-), which will be in this manuscript referred to as exudate groups. Each exudate group is comprised of different numbers of individual synthetic compounds as listed in Table 5-1 (top three rows). The specific compounds were chosen based on a previous study by (Steinauer et al., 2016), but the concentrations of artificial exudates were 2.5x higher. Eight combinations of compounds belonging to one or more exudate groups were examined: 1) sugars (S-), 2) organic acids (O-), 3) amino acids (A-), 4) 'sugars + organic acids' (S-O), 5) 'organic acids + amino acids' (O-A), 6) 'sugars + amino acids' (S-A), 7) 'sugars + organic acids + amino acids' (S-O-A) and 8) a control that had only sterilized tap water added (No exudates). The artificial exudates for each factor were added to LSP 25R, every other day (3 days a week), for a total of 15 mL each week. Sterilized tap water was added to each pot as needed to maintain soil moisture. We implemented four replicates for each combination of exudates.

Table 5-1

Soil for each combination and replicate were analyzed for three different soil extracellular enzyme activities, phosphatase, cellobiohydrolase, and L-leucine aminopeptidase; which are representative of P-, C- and N-cycling respectively. These three enzyme activities were determined using methods described in detail below. The experiment lasted four months with soils collected at six time points; 1, 15, 30, 60, 90, and 120 days. Collected soil from each time point was used for analysis of enzyme activity

### 5.2.3 *Experimental design of low vs. high diversity treatments of artificial root exudates*

Constant weights of sieved soil (< 4 mm, ~ 100 g) were added to small flowerpots and placed in a greenhouse. This experiment used a high compound diversity treatment, which is made up of more compounds compared to the low compound diversity treatment, these will be referred to as low and high diversity treatments throughout the manuscript. For example, for the exudate group S-, there are four compounds in the high diversity treatment compared to two compounds in the low diversity treatment. The combination of exudate groups (S-O, O-A, S-A and S-O-A) were examined for both low and high diversity treatments. A total of three replicates were made for each combination of exudates for both diversity treatments. The artificial exudate mixtures for each combination of exudates were added every other day (3 days a week), for a total of 20 mL each week. Sterilized tap water was added to each pot as needed to maintain moisture. The control pots had only sterilized tap water added to the soil. After 30 and 60 days, the soil was harvested to analyze for phosphatase activity.

### 5.2.4 Enzymatic assays

Phosphatase, cellobiohydrolase and L-leucine aminopeptidase activities were measured for the six time points (1, 15, 30, 60, 90, and 120 days) of each combination of exudates (S, O, A, S-O, O-A, S-A and S-O-A) for understanding the effect on soil function for different artificial exudate combinations. In the second experiment, phosphatase activity was measured at days 30 and 60 to understand the effect of different number of compounds with low and high diversity of treatments for P- cycling. All assays follow protocols described here and in detail previously in Hagmann et al. (2015).

*Phosphatase, cellobiohydrolase and L-Leucine aminopeptidase assays*

Briefly, moist soil, 0.1 g for phosphatase and cellobiohydrolase and 0.5 g for L-Leucine aminopeptidase, was added to 100 mL of 0.1 M MES buffer (pH 6.0) and then sonicated for 3 min at 25W. The continuously stirred soil slurry was added (160  $\mu$ L) to the wells of a 96-well black plate. For the phosphatase assay, 4-MUB-phosphate was added (40  $\mu$ L) to three different wells (350  $\mu$ M in the well). For the cellobiohydrolase assay, 4-Methylumbelliferyl  $\beta$ -D-cellobioside was added (40  $\mu$ L) to three different wells (650  $\mu$ M in the well). For the L-Leucine aminopeptidase, L-Leucine-7-amido-4-methylcoumarin hydrochloride was added (40  $\mu$ L) to three different wells (400  $\mu$ M in the well). To determine the concentration of the fluorescent product produced, a standard curve was created with the additions (40  $\mu$ L) of different concentrations of a fluorescent product (4-MUB for phosphatase and cellobiohydrolase assays, and 7-MUC for L-Leucine aminopeptidase) combined with 160  $\mu$ L of soil slurry. For phosphatase and cellobiohydrolase assays, the combination of 4-MUB with a soil slurry combined to yield concentrations 0, 500, 1000, 1500 and 2500 pmols of product in different wells. The standard curve for L-Leucine aminopeptidase used four different concentrations 0, 500, 750, 1125 and 1500 pmols of product using 7-MUC. Time points were collected on a microplate reader at 30 °C every 7.5 minutes for 3 hours to measure fluorescence intensity (320 nm ex./450 nm em.) for both phosphatase and cellobiohydrolase assays and (350 nm ex./440 nm em.) for L-Leucine aminopeptidase.

### 5.2.5 Data Analysis

To fully appreciate the impact of the exudate combinations, the changes in enzyme activities were expressed as fold changes. The fold change was calculated by dividing the enzyme activity

of a soil treated with an artificial exudate factor by the mean enzyme activity of the corresponding control soil (No exudates). This was done for data obtained at each time point and the fold change values were averaged over time excluding the initial time point. An analysis of variance (ANOVA) was conducted between different combinations of artificial exudates to compare fold changes within a given enzymatic activity with a significance cut-off value of  $p < 0.05$ . Each enzyme activity was analyzed separately. Prior to analysis, the fold changes of each enzyme activity were natural log-transformed to help meet assumptions of normality. In addition, an ANOVA was conducted between low and high diversity treatments for different combinations of artificial exudates to compare phosphatase activity with a significance cut-off value of  $p < 0.05$ . We conducted a post-hoc test (Tukey's HSD) where significant effects were found. All statistics were performed using R (version 3.6.2).

### 5-3. Results

The three enzyme activities, phosphatase, cellobiohydrolase and L-leucine aminopeptidase, that were measured increased over the course of the experiment (120 days) when artificial exudates were added to LSP 25R. For example, with the addition of SOA, phosphatase activity increased from  $0.03 \pm 0.01$  to  $1.26 \pm 0.12 \mu\text{mol} \cdot \text{g}_{\text{dry}}^{-1} \cdot \text{hr}^{-1}$  from day 1 to day 120, cellobiohydrolase activity from  $0.001 \pm 0.0009$  to  $0.02 \pm 0.002 \mu\text{mol} \cdot \text{g}_{\text{dry}}^{-1} \cdot \text{hr}^{-1}$ , and L-leucine aminopeptidase activity from  $0.01 \pm 0.002$  to  $0.15 \pm 0.036 \mu\text{mol} \cdot \text{g}_{\text{dry}}^{-1} \cdot \text{hr}^{-1}$  (Appendix-C Figs A1, A2, A3). The increases from day 1 to day 120 were statistically significant for phosphatase ( $F_{5,18} = 37.46$ ,  $p < 0.001$ ), cellobiohydrolase ( $F_{5,18} = 32.15$ ,  $p < 0.001$ ), and L-leucine aminopeptidase ( $F_{5,18} = 26.76$ ,  $p < 0.001$ ) activities.

Phosphatase, cellobiohydrolase, and L-leucine aminopeptidase activities in soil 25R responded differently to the addition artificial exudate combinations. For example, SOA addition yielded a larger fold increase in phosphatase activity ( $136 \pm 38$  fold increase) compared to cellobiohydrolase activity ( $2.3 \pm 0.27$  fold increase ) and L-leucine aminopeptidase activity ( $8.0 \pm 0.91$  fold increase), which changed less in response to the exudates (Fig 5-1A-C). Phosphatase activity fold changes varied widely and ranged from  $9.7 \pm 2.6$  (A) to  $136 \pm 37.7$  (S-O-A), depending on the exudate combination (Fig. 5-1A). Conversely, the effects of different artificial exudate combinations on cellobiohydrolase activity fold change were similar to each other and only ranged between  $1.1 \pm 0.06$  (A) and  $2.3 \pm 0.27$  (SOA) (Fig. 5-1B). Only the combination SOA resulted in a cellobiohydrolase activity fold change that was significantly larger than those observed for the other combinations (Fig. 5-1B,  $p < 0.05$ , Tukey). Similar to phosphatase activity, L-Leucine aminopeptidase activity fold changes also varied widely depending on the exudate combination. The fold changes for L-leucine aminopeptidase activity ranged between  $0.38 \pm 0.39$  (SO) and  $8.0 \pm 0.91$  (SOA) (Fig. 5-1 C). Interestingly, for L-Leucine aminopeptidase activity, the two exudate combinations, A and SOA, were not the low and high fold change values. Conversely for phosphatase and cellobiohydrolase activities the two exudate combinations, A and SOA resulted in the low and high fold change values respectively.

Figure 5-1

Changes in phosphatase, cellobiohydroalse, and L-leucine aminopeptidase activity depended on the specific artificial exudates combination that was added. For example, the

addition of each artificial exudate combination resulted in an increased soil phosphatase activity, but the magnitude of this increase varied depending on which combination was added. The differences between artificial exudate combinations were significantly different for the changes in phosphatase activity ( $F_{6,133} = 8.475$ ,  $p < 0.0001$ , Fig. 5-1A). For example, phosphatase fold change was greater with the addition combination the three exudate groups (S-O-A) compared to the other combinations. Similarly, the addition of S-O-A also resulted in a higher fold change in cellobiohydrolase activity compared to the addition of the other combination of exudates. The differences between artificial exudate combinations were significantly different for changes in cellobiohydrolase activity ( $F_{6,132} = 7.395$ ,  $p < 0.0001$ , Fig. 5-1B).

The fold changes for L-leucine aminopeptidase activity were significantly larger when combinations that included amino acids (A, OA, SA, and SOA) were added compared to combinations without amino acids ( $p < 0.0001$ , Fig. 5-1C). The differences in fold change for L-leucine aminopeptidase activity were significant for the various combinations ( $F_{6,119} = 28.65$ ,  $p < 0.0001$ , Fig. 5-1C). Addition of amino acids alone (A) increased L-leucine aminopeptidase activities by  $6.0 \pm 0.8$  fold, while the combinations of amino acids O-A, S-A and S-O-A increased L-leucine aminopeptidase activities by  $5.5 \pm 0.6$ ,  $5.7 \pm 0.7$ , and  $8.0 \pm 0.9$  fold change, respectively (Fig. 5-1C). In contrast, the fold change of L-leucine aminopeptidase activity with combinations that don't include A were smaller, which include the addition of S- compared to the control was  $0.7 \pm 0.2$ , the addition of O- was  $1.2 \pm 0.1$  and the addition of S-O was  $0.4 \pm 0.4$  (Fig. 5-1 C). The exudate combinations that contain A resulted in larger increases in L-leucine aminopeptidase activity.

We were interested in whether the effects of exudate additions on enzyme activities were additive or non-additive. For example, if addition of individual groups (S-, O- and A-) is

additive, then the sum of the effects would equal the effect of adding the combination SOA.

Phosphatase activities that resulted from treatments S-, O- and A- averaged over 120 days after the treatments were added were  $1.0 \pm 0.1 \mu\text{mol} \cdot \text{g}_{\text{dry soil}}^{-1} \cdot \text{hr}^{-1}$  (S-),  $0.64 \pm 0.07 \mu\text{mol} \cdot \text{g}_{\text{dry soil}}^{-1} \cdot \text{hr}^{-1}$  and  $0.57 \pm 0.04 \mu\text{mol} \cdot \text{g}_{\text{dry soil}}^{-1} \cdot \text{hr}^{-1}$  respectively. If there was an additive effect that resulted from treatment S-O-A, then the calculated phosphatase activity would be  $2.2 \pm 0.2 \mu\text{mol} \cdot \text{g}_{\text{dry soil}}^{-1} \cdot \text{hr}^{-1}$ . However, the phosphatase activity that resulted from treatment S-O-A was measured to be  $16.1 \pm 1.9 \mu\text{mol} \cdot \text{g}_{\text{dry soil}}^{-1} \cdot \text{hr}^{-1}$ , which is significantly higher than the calculated value ( $t(3) = 7.36, p < 0.01$ ).

Cellobiohydrolase activity showed a non-additive effect for the combination SA. The cellobiohydrolase activity averaged over 120 days after the treatments were added that resulted with the addition of S- was  $0.29 \pm 0.03 \mu\text{mol} \cdot \text{g}_{\text{dry soil}}^{-1} \cdot \text{hr}^{-1}$  and the activity that resulted with the addition of A- was  $0.23 \pm 0.02 \mu\text{mol} \cdot \text{g}_{\text{dry soil}}^{-1} \cdot \text{hr}^{-1}$ . If the effect was additive, the treatment S-A would have a calculated cellobiohydrolase activity of  $0.52 \pm 0.05 \mu\text{mol} \cdot \text{g}_{\text{dry soil}}^{-1} \cdot \text{hr}^{-1}$ . However, the actual cellobiohydrolase activity that resulted from the addition of S-A was measured to be  $0.31 \pm 0.03$ , which is significantly below the calculated value ( $t(3) = -8.76, p < 0.005$ ). L-leucine aminopeptidase activity also showed a non-additive effect for another combination of components, S-O. The L-leucine aminopeptidase activity averaged over 120 days after the treatments were added that resulted from the addition of S- was  $0.19 \pm 0.07 \mu\text{mol} \cdot \text{g}_{\text{dry soil}}^{-1} \cdot \text{hr}^{-1}$  and the activity that resulted from the addition of O- was  $0.30 \pm 0.03 \mu\text{mol} \cdot \text{g}_{\text{dry soil}}^{-1} \cdot \text{hr}^{-1}$ . If there was an additive effect. The actual L-leucine aminopeptidase activity that resulted from treatment S-O was  $0.11 \pm 0.03 \mu\text{mol} \cdot \text{g}_{\text{dry soil}}^{-1} \cdot \text{hr}^{-1}$ , which was significantly less than the calculated value of  $0.49 \pm 0.20 \mu\text{mol} \cdot \text{g}_{\text{dry soil}}^{-1} \cdot \text{hr}^{-1}$  ( $t(3) = -4.45, p < 0.05$ ). There were, however, some combinations of treatments that did have an additive effect.

One example is phosphatase activity for S-O ( $1.6 \pm 0.33 \mu\text{mol} \cdot \text{g}_{\text{dry soil}}^{-1} \cdot \text{hr}^{-1}$ ), which is within standard error of the calculated sum of S and O ( $1.64 \pm 0.33 \mu\text{mol} \cdot \text{g}_{\text{dry soil}}^{-1} \cdot \text{hr}^{-1}$ ,  $t(3) = 0.054$ ,  $p < 0.05$ ).

In a separate experiment, the effect of adding low and high diversity treatments of artificial exudate on phosphatase activity were compared. Interestingly, there was no significant difference in phosphatase activity that was measured after the addition of low and high diversity treatments ( $p > 0.05$ , Fig. 5-2). Similar to the previous experiment, the additions of different exudate groups, O-A, S-A, and S-O-A resulted in a greater change in phosphatase activity compared to the control. For example, the phosphatase activities of the combinations of the high diversity treatments were  $0.93 \pm 0.25 \mu\text{mol} \cdot \text{g}_{\text{dry soil}}^{-1} \cdot \text{hr}^{-1}$  (O-A),  $4.20 \pm 1.26 \mu\text{mol} \cdot \text{g}_{\text{dry soil}}^{-1} \cdot \text{hr}^{-1}$  (S-A) and  $9.89 \pm 3.64 \mu\text{mol} \cdot \text{g}_{\text{dry soil}}^{-1} \cdot \text{hr}^{-1}$  (S-O-A). There was a significant difference between the different combinations of artificial exudates added to LSP 25R soil ( $F_{3,32} = 105.49$ ,  $p < 0.0001$ , Fig. 5-2).

Figure 5-2

#### 5-4. Discussion

In this study, we found that phosphatase, cellobiohydrolase, and L-leucine aminopeptidase activities responded differently to the addition of artificial exudates. In other studies, soil extracellular enzyme activities have also shown different responses to the addition of artificial exudates depending on the specific enzyme being studied (Hernández and Hobbie, 2010; Yin et al., 2016; Zhang et al., 2019). For example, Zhang and co-workers found a greater increase in phosphatase activity with the addition of only glucose, but not with the addition of only citrate

(Zhang et al., 2019). In our study, the fold change in phosphatase activity was much greater compared to the fold changes in the other two enzyme activities, regardless of the exudate combination added. Phosphatase has been previously found to be the most sensitive enzyme to the addition of artificial exudates (Zhang et al., 2019). Several studies have found that artificial exudates, no matter the composition, increased phosphatase activity (Lv et al., 2013; Renella et al., 2007; Zhang et al., 2019). However, Yin and co-workers found that exudates that did not contain N resulted in a decrease in phosphatase activity (Yin et al., 2016).

Additionally, here we found that within a given enzyme the addition of different artificial exudate combinations resulted in varying enzyme activities. Adding different root exudates to the soil increases the C and N availability, thus resulting in different effects on enzyme activities as likely explained by substrate stoichiometry (Carreiro et al., 2000; Gallo et al., 2004b; Nannipieri et al., 2012; Sinsabaugh et al., 2008; Waldrop and Firestone, 2006; Wild et al., 2014). Both sugars and organic acids only add labile C to the soil, while amino acids can act as both a C and N source. The resource allocation theory can explain the differences in enzyme activity between the varying root exudate combinations, stating that microorganisms produce more enzymes that are related to the limiting nutrient (Allison et al., 2011). Studies have found that the addition of either a nitrogen and/or carbon source increases the demand for P, thus resulting in an increase in phosphatase activity (Allison and Vitousek, 2005; Elfstrand et al., 2007; Hernández and Hobbie, 2010; Keeler et al., 2009; Olander and Vitousek, 2000; Spohn et al., 2013; Zhang et al., 2019). The amount of P present in LSP 25R is low, 4.5 ppm (data not shown). A higher phosphatase activity has been found to relate with P limitation (Allison et al., 2007). The addition of root exudates can contribute to the mobilization of P, which can increase phosphatase activity (Lagomarsino et al., 2009; Romanyà et al., 2017). Phosphatase is needed to

catalyze the hydrolysis of phosphate bonds found in nucleic acids, phospholipids, and release phosphates (P) into the soil (Jian et al., 2016; Nannipieri et al., 2011; Sinsabaugh et al., 2008). Knowing this we now understand that the high phosphatase activity that resulted with the addition of different combinations of artificial exudates was due to both the limitation of P in 25R and possible mobilization P into the soil,

In this study, there was no difference when sugars or amino acids alone were added compared to the control in cellobiohydrolase activity. Since the additions of labile C, via additions of sugars did not increase cellobiohydrolase activity suggests that the barren soil at LSP, 25R, might not be C-limited. Note that site 25R is barren and but contains coal particles, which can act as a potential C source. Soils from site 25R have a C:N ratio of 62.9, which support that these soils are not C-limited. The cellobiohydrolase activity only increased when S-O-A was added. Steinauer and coworkers also found an increase in cellobiohydrolase activity with the additions of sugars, organic acids and amino acids, which had a composition of root exudates similar to our S-O-A (Steinauer et al., 2016).

In our study, L-leucine aminopeptidase activity in was stimulated by the addition of amino acids. Several studies have found that an amendment with N increased L-leucine aminopeptidase (Hernández and Hobbie, 2010; Lagomarsino et al., 2009), while others have found a decrease in activity (Ramirez et al., 2012; Shi et al., 2018). L-leucine aminopeptidase hydrolyzes amino acids from the N-terminus (Sinsabaugh et al., 2008). By adding the product to the soil, it is surprising that there was an increase in L-leucine aminopeptidase activities. This is surprising because the addition a product or N source would result in a decrease or no change in L-leucine aminopeptidase activity (Hernández and Hobbie, 2010). However, the exact explanation for this is not fully understood.

In order to understand the impact with the addition of a N source to the soil, several studies have used inorganic forms of N, such as  $\text{NH}_4\text{Cl}$  or  $\text{NH}_4\text{NO}_3$  (Lagomarsino et al., 2009; Ramirez et al., 2012; Yin et al., 2016). The impact on soil function through the addition of a N source via amino acids is complicated by the simultaneous addition of both C and N components. The reason we chose amino acids in our artificial root exudate composition is because they are naturally constituents of root exudates. Organic N has been found to increase several extracellular enzyme activities more than inorganic N additions (Yin et al., 2016).

There are limited studies analyzing the additive effects of individual components of root exudates on enzyme activities. The addition of all three exudate groups (S-O-A) led to the greatest increase in phosphatase and cellobiohydrolase activities, especially compared to the individual exudate groups. Conversely, L-leucine aminopeptidase activities depended on one of the individual exudates, amino acids. Drake and coworkers found the combination of C and N exudates led to a greater enzymatic response compared to C exudates alone (Drake et al., 2013). They suggested that since their soil was N-limited, the addition N containing compounds would result in a greater response in enzyme activity (Drake et al., 2013). In our study, S-O-A resulted in a non-additive effect, which could potentially be the interplay between these various groups that led to the greater increase in phosphatase and cellobiohydrolase activities when the exudate groups are combined.

The composition of artificial exudates is not the only factor that regulates enzyme production, but enzyme activity can also be altered by the quantity of individual artificial exudates (Hernández and Hobbie, 2010; Kreyling et al., 2008; Steinauer et al., 2016). A higher plant diversity has more diverse root exudate compounds present in the soil, which can influence soil function (Chung et al., 2007; Steinauer et al., 2015). Steinauer and co-workers (2016) found

that cellobiohydrolase activity was significantly higher in the high diversity treatment compared to the low diversity exudate treatments (Steinauer et al., 2016). Conversely, we found that the effects of low and high diversity treatments were the same. This infers that phosphatase activities are driven by the composition of artificial exudates, which contains C and N sources and not the diversity of compounds. The effect of these low and high diversity treatments may have varying effects on different enzymes.

### **5-5. Conclusion**

Within LSP, the barren strip of land 25R has high concentrations of heavy metals and barely detectable enzyme activities and presents a unique opportunity to examine the role of artificial exudates on soil functioning and revitalization. Despite having poor soil function, this barren soil contained measurable counts of bacteria (Hagmann et al., 2019, *see Ch. 2*). It is possible that microbes in the barren soil are dormant and the addition of artificial root exudates allows these microbes to leave the dormant state and again produce more enzymes, which are responsible for soil function. Indeed, this is what we show here. A complex mixture of sugars, amino acids and organic acids can enhance enzymatic activity in this otherwise poorly-functioning soils. However, not all enzyme activities studied responded the same, and the composition of the exudates but not the diversity significantly affected enzymatic activities. For instance, phosphatase activity increased more than cellobiohydrolase or L-leucine aminopeptidase when exudates were added, but specifically, L-leucine aminopeptidase increased only when the combination of exudates included amino acids. There are both ecological mechanisms that may explain our results and remediation implications. Ecologically, these soils are barren and nutrient limitation likely operates in conjunction with metal toxicity and microbial growth under the

sudden pulse of nutrients. With respect to remediation, our results show that dormant soils can be brought back to life by artificially priming the soil to mimic the benefits of rooted plants. Further research will inform the long term benefits of a quick pulse of nutrients as opposed to a long term pulse for primary production and plant community development. A reduced set of artificial exudate compounds that achieve similar effects on enzyme activity could revitalize the soil in a more economical and efficient manner if other enzyme activities have a similar response to phosphatase activity.

### References

- Allison S.D., Vitousek P.M., 2005. Responses of extracellular enzymes to simple and complex nutrient inputs. *Soil Biology and Biochemistry*; 37: 937-944.
- Allison S.D., Weintraub M.N., Gartner T.B., Waldrop M.P., 2011. Evolutionary-Economic Principles as Regulators of Soil Enzyme Production and Ecosystem Function. In: Shukla G, Varma A, editors. *Soil Enzymology*. Springer Berlin Heidelberg, Berlin, Heidelberg, pp. 229-243.
- Allison V.J., Condon L.M., Peltzer D.A., Richardson S.J., Turner B.L., 2007. Changes in enzyme activities and soil microbial community composition along carbon and nutrient gradients at the Franz Josef chronosequence, New Zealand. *Soil Biology and Biochemistry*; 39: 1770-1781.
- Badri D.V., Vivanco J.M., 2009. Regulation and function of root exudates. *Plant, Cell & Environment*; 32: 666-681.
- Baudoin E., Benizri E., Guckert A., 2003. Impact of artificial root exudates on the bacterial community structure in bulk soil and maize rhizosphere. *Soil Biology and Biochemistry*; 35: 1183-1192.
- Benizri E., Dedourge O., Dibattista-Leboeuf C., Piutti S., Nguyen C., Guckert A., 2002. Effect of maize rhizodeposits on soil microbial community structure. *Applied Soil Ecology*; 21: 261-265.
- Caldwell B.A., 2005. Enzyme activities as a component of soil biodiversity: A review. *Pedobiologia*; 49: 637-644.

- Carreiro M.M., Sinsabaugh R.L., Repert D.A., Parkhurst D.F., 2000. Microbial Enzyme Shifts Explain Litter Decay Responses To Simulated Nitrogen Deposition. *Ecology*; 81: 2359-2365.
- Cheng W., Kuzyakov Y., 2005. Root Effects on Soil Organic Matter Decomposition. *Roots and Soil Management: Interactions between Roots and the Soil*, pp. 119-143.
- Chung H., Zak D.R., Reich P.B., Ellsworth D.S., 2007. Plant species richness, elevated CO<sub>2</sub>, and atmospheric nitrogen deposition alter soil microbial community composition and function. *Global Change Biology*; 13: 980-989.
- Drake J.E., Darby B.A., Giasson M.A., Kramer M.A., Phillips R.P., Finzi A.C., 2013. Stoichiometry constrains microbial response to root exudation- insights from a model and a field experiment in a temperate forest. *Biogeosciences*; 10: 821-838.
- Eisenhauer N., Lanoue A., Strecker T., Scheu S., Steinauer K., Thakur M.P., et al., 2017. Root biomass and exudates link plant diversity with soil bacterial and fungal biomass. *Scientific Reports*; 7: 44641.
- Elfstrand S., Hedlund K., Mårtensson A., 2007. Soil enzyme activities, microbial community composition and function after 47 years of continuous green manuring. *Applied Soil Ecology*; 35: 610-621.
- Fontaine S., Mariotti A., Abbadie L., 2003. The priming effect of organic matter: a question of microbial competition? *Soil Biology and Biochemistry*; 35: 837-843.
- Gallagher F.J., Pechmann I., Bogden J.D., Grabosky J., Weis P., 2008. Soil metal concentrations and vegetative assemblage structure in an urban brownfield. *Environmental Pollution*; 153: 351-361.

- Gallo M., Amonette R., Lauber C., Sinsabaugh R.L., Zak D.R., 2004. Microbial Community Structure and Oxidative Enzyme Activity in Nitrogen-Amended North Temperate Forest Soils. *Microbial Ecology*; 48: 218-229.
- Gianfreda L., Ruggiero P., 2006. Enzyme Activities in Soil. In: Nannipieri P, Smalla K, editors. *Nucleic Acids and Proteins in Soil*. Springer Berlin Heidelberg, Berlin, Heidelberg, pp. 257-311.
- Girkin N.T., Turner B.L., Ostle N., Craigon J., Sjögersten S., 2018. Root exudate analogues accelerate CO<sub>2</sub> and CH<sub>4</sub> production in tropical peat. *Soil Biology and Biochemistry*; 117: 48-55.
- Hagmann D.F., Kruge M.A., Cheung M., Mastalerz M., Gallego J.L.R., Singh J.P., et al., 2019. Environmental forensic characterization of former rail yard soils located adjacent to the Statue of Liberty in the New York/New Jersey harbor. *Science of The Total Environment*; 690: 1019-1034.
- Henry S., Texier S., Hallet S., Bru D., Dambreville C., Chèneby D., et al., 2008. Disentangling the rhizosphere effect on nitrate reducers and denitrifiers: insight into the role of root exudates. *Environmental Microbiology*; 10: 3082-3092.
- Hernández D.L., Hobbie S.E., 2010. The effects of substrate composition, quantity, and diversity on microbial activity. *Plant and Soil*; 335: 397-411.
- Hertenberger G., Zampach P., Bachmann G., 2002. Plant species affect the concentration of free sugars and free amino acids in different types of soil. *Journal of Plant Nutrition and Soil Science*; 165: 557-565.
- Hessen D.O., Ågren G.I., Anderson T.R., Elser J.J., de Ruiter P.C., 2004. Carbon Sequestration In Ecosystems: The Role of Stoichiometry *Ecology*; 85: 1179-1192.

- Hodge A., Grayston S.J., Ord B.G., 1996. A novel method for characterisation and quantification of plant root exudates. *Plant and Soil*; 184: 97-104.
- Jian S., Li J., Chen J., Wang G., Mayes M.A., Dzantor K.E., et al., 2016. Soil extracellular enzyme activities, soil carbon and nitrogen storage under nitrogen fertilization: A meta-analysis. *Soil Biology and Biochemistry*; 101: 32-43.
- Jones D.L., Hodge A., Kuzyakov Y., 2004. Plant and mycorrhizal regulation of rhizodeposition. *New Phytologist*; 163: 459-480.
- Keeler B.L., Hobbie S.E., Kellogg L.E., 2009. Effects of Long-Term Nitrogen Addition on Microbial Enzyme Activity in Eight Forested and Grassland Sites: Implications for Litter and Soil Organic Matter Decomposition. *Ecosystems*; 12: 1-15.
- Keiluweit M., Bougoure J.J., Nico P.S., Pett-Ridge J., Weber P.K., Kleber M., 2015. Mineral protection of soil carbon counteracted by root exudates. *Nature Climate Change*; 5: 588-595.
- Khan S., El-Latif Hesham A., Qiao M., Rehman S., He J.-Z., 2010. Effects of Cd and Pb on soil microbial community structure and activities. *Environmental Science and Pollution Research*; 17: 288-296.
- Kreyling J., Beierkuhnlein C., Elmer M., Pritsch K., Radovski M., Schloter M., et al., 2008. Soil biotic processes remain remarkably stable after 100-year extreme weather events in experimental grassland and heath. *Plant and Soil*; 308: 175.
- Kuzyakov Y., Friedel J.K., Stahr K., 2000. Review of mechanisms and quantification of priming effects. *Soil Biology and Biochemistry*; 32: 1485-1498.

- Lagomarsino A., Grego S., Marhan S., Moscatelli M.C., Kandeler E., 2009. Soil management modifies micro-scale abundance and function of soil microorganisms in a Mediterranean ecosystem. *European Journal of Soil Science*; 60: 2-12.
- Lv Y., Wang C., Wang F., Zhao G., Pu G., Ma X., et al., 2013. Effects of nitrogen addition on litter decomposition, soil microbial biomass, and enzyme activities between leguminous and non-leguminous forests. *Ecological Research*; 28: 793-800.
- Moorhead D.L., Sinsabaugh R.L., 2006. A Theoretical Model Of Litter Decay And Microbial Interaction. *Ecological Monographs*; 76: 151-174.
- Nannipieri P., 1994. The potential use of soil enzymes as indicators of productivity, sustainability and pollution. CSIRO Publications, East Melbourne, pp. 238-244.
- Nannipieri P., Giagnoni L., Landi L., Renella G., 2011. Role of Phosphatase Enzymes in Soil. In: Bünemann E, Oberson A, Frossard E, editors. *Phosphorus in Action: Biological Processes in Soil Phosphorus Cycling*. Springer Berlin Heidelberg, Berlin, Heidelberg, pp. 215-243.
- Nannipieri P., Giagnoni L., Renella G., Puglisi E., Ceccanti B., Masciandaro G., et al., 2012. Soil enzymology: classical and molecular approaches. *Biology and Fertility of Soils*; 48: 743-762.
- Olander L.P., Vitousek P.M., 2000. Regulation of soil phosphatase and chitinase activity by N and P availability. *Biogeochemistry*; 49: 175-191.
- Paterson E., Gebbing T., Abel C., Sim A., Telfer G., 2007. Rhizodeposition shapes rhizosphere microbial community structure in organic soil. *New Phytologist*; 173: 600-610.

- Ramirez K.S., Craine J.M., Fierer N., 2012. Consistent effects of nitrogen amendments on soil microbial communities and processes across biomes. *Global Change Biology*; 18: 1918-1927.
- Renella G., Landi L., Valori F., Nannipieri P., 2007. Microbial and hydrolase activity after release of low molecular weight organic compounds by a model root surface in a clayey and a sandy soil. *Applied Soil Ecology*; 36: 124-129.
- Romanyà J., Blanco-Moreno J.M., Sans F.X., 2017. Phosphorus mobilization in low-P arable soils may involve soil organic C depletion. *Soil Biology and Biochemistry*; 113: 250-259.
- Rovira A.D., 1969. Plant root exudates. *The Botanical Review*; 35: 35-57.
- Schimel J.P., Weintraub M.N., 2003. The implications of exoenzyme activity on microbial carbon and nitrogen limitation in soil: a theoretical model. *Soil Biology and Biochemistry*; 35: 549-563.
- Shi B., Zhang J., Wang C., Ma J., Sun W., 2018. Responses of hydrolytic enzyme activities in saline-alkaline soil to mixed inorganic and organic nitrogen addition. *Scientific Reports*; 8: 4543.
- Sinsabaugh R.L., Lauber C.L., Weintraub M.N., Ahmed B., Allison S.D., Crenshaw C., et al., 2008. Stoichiometry of soil enzyme activity at global scale. *Ecology Letters*; 11: 1252-1264.
- Smith W.H., 1976. Character and Significance of Forest Tree Root Exudates. *Ecology*; 57: 324-331.
- Spohn M., Ermak A., Kuzyakov Y., 2013. Microbial gross organic phosphorus mineralization can be stimulated by root exudates – A <sup>33</sup>P isotopic dilution study. *Soil Biology and Biochemistry*; 65: 254-263.

- Steinauer K., Chatzinotas A., Eisenhauer N., 2016. Root exudate cocktails: the link between plant diversity and soil microorganisms? *Ecology and Evolution*; 6: 7387-7396.
- Steinauer K., Tilman D., Wragg P.D., Cesarz S., Cowles J.M., Pritsch K., et al., 2015. Plant diversity effects on soil microbial functions and enzymes are stronger than warming in a grassland experiment. *Ecology*; 96: 99-112.
- Strickland M.S., McCulley R.L., Nelson J.A., Bradford M.A., 2015. Compositional differences in simulated root exudates elicit a limited functional and compositional response in soil microbial communities. *Frontiers in Microbiology*; 6.
- Vaidya B.P., Hagemann D.F., Balacco J., Passchier S., Krumins J.A., Goodey N.M., 2020. Plants mitigate restrictions to phosphatase activity in metal contaminated soils. *Environmental Pollution*; 265: 114801.
- Waldrop M.P., Firestone M.K., 2006. Response of Microbial Community Composition and Function to Soil Climate Change. *Microbial Ecology*; 52: 716-724.
- Wild B., Schneckler J., Alves R.J.E., Barsukov P., Bárta J., Čapek P., et al., 2014. Input of easily available organic C and N stimulates microbial decomposition of soil organic matter in arctic permafrost soil. *Soil Biology and Biochemistry*; 75: 143-151.
- Yang Y., Campbell C.D., Clark L., Cameron C.M., Paterson E., 2006. Microbial indicators of heavy metal contamination in urban and rural soils. *Chemosphere*; 63: 1942-1952.
- Yin H., Phillips R.P., Liang R., Xu Z., Liu Q., 2016. Resource stoichiometry mediates soil C loss and nutrient transformations in forest soils. *Applied Soil Ecology*; 108: 248-257.
- Zhang X., Dippold M.A., Kuzyakov Y., Razavi B.S., 2019. Spatial pattern of enzyme activities depends on root exudate composition. *Soil Biology and Biochemistry*; 133: 83-93.

## TABLES

**Table 5-1.** Composition of artificial root exudates for high and low diversity treatments. Low and high diversity treatments were comprised of a different number of exudate compounds.

These treatments were applied to barren soil from LSP site 25R.

<b>Exudate Diversity</b>	<b>Exudate composition</b>	<b>Exudate Compounds</b>	<b>Amount added each week (mmol)</b>
High compound diversity	Sugars (S)	Glucose, Fructose, Sucrose, Maltose	0.5 each
	Organic Acids (O)	Acetic acid, Citric acid, Lactic acid, Malic acid, Succinic acid	0.2 each
	Amino Acids (A)	Alanine, Arginine, Asparagine, Glutamic acid, Glycine, Histidine, Leucine, Tyrosine	0.063 each
Low compound diversity	Sugars (S)	Glucose, Sucrose	1.0 each
	Organic Acids (O)	Acetic acid, Succinic acid	0.5 each
	Amino Acids (A)	Alanine, Glutamic acid, Glycine	0.167 each

## FIGURES

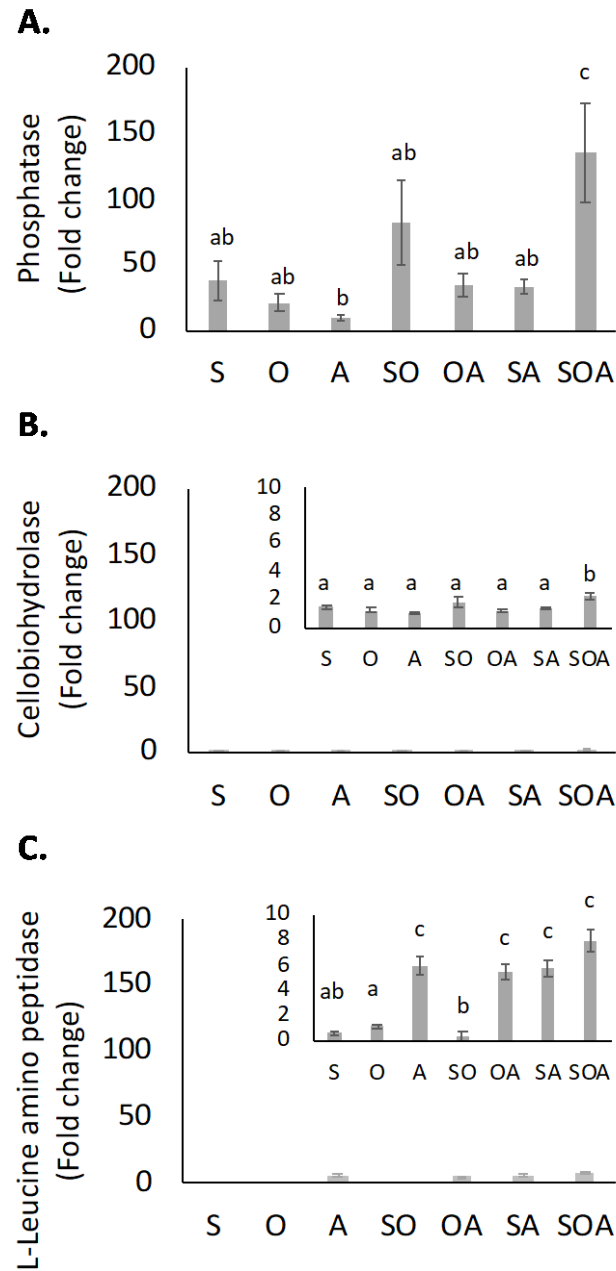


**Figure 5-1.** Enzyme activity fold changes of barren soil LSP 25R are shown for each artificial exudate factor for phosphatase (A), cellobiohydrolase (B), and L-leucine amino peptidase (C).

The values shown represent the averages of five time points. The data are shown for seven different treatments, (S-, O-, A-, S\_O, O\_A, S\_A, S\_O\_A). Bars represent the averages of four

replicates (n=4) with standard errors shown. Significant differences among the means are indicated by letters a, b, c, (Tukey test,  $p < 0.05$ ).

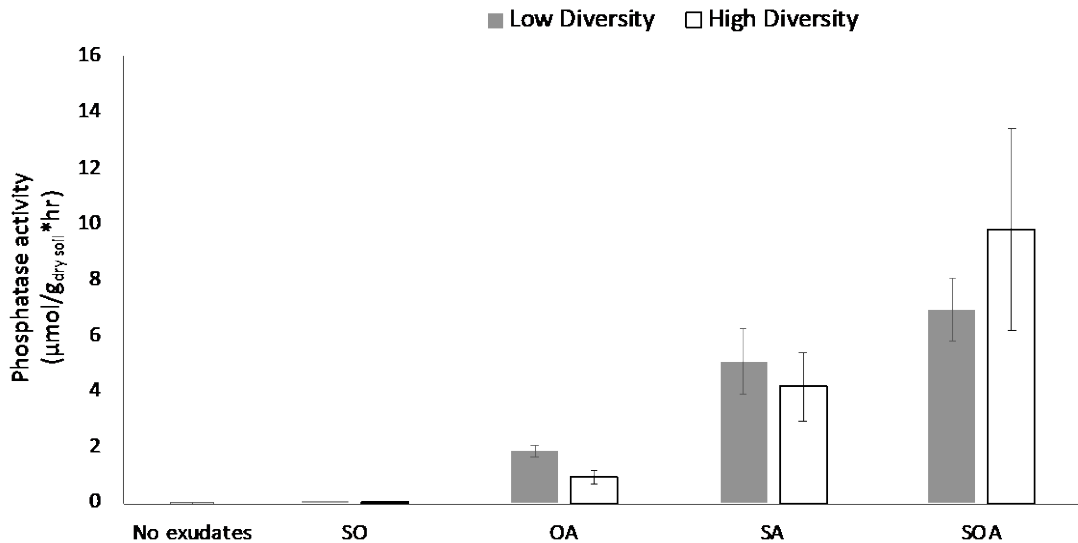


**Figure 5-2.** Effect of low and high diversity treatments added to 25R soil on phosphatase activity ( $\mu\text{mol} \cdot \text{g}^{-1} \cdot \text{hr}^{-1}$ ) for four different combinations of artificial exudates (SO, OA, SA, and SOA) averaged over two times points (30 and 60 days). Dark grey and white bars represent low and high diversity treatments respectively. The difference between phosphatase activities where the soil was treated with low and high diversity treatments were not significant. Bars represent the average of three replicates (n = 3) of each enzyme activity with standard errors shown.

### Dissertation Summary

The overall goal of this dissertation was to understand the impacts of both abiotic and biotic properties on soil function. First, the inorganic and organic compounds present within the urban brownfield Liberty State Park, LSP were characterized. Inorganic compounds, such as heavy metals, and organic contaminants, such as polycyclic aromatic compounds (PAHs), pose threats to the environment due to their persistence in the soil. The combination of heavy metals and PAHs can have adverse effects on vegetation (Maliszewska-Kordybach and Smreczak, 2003; Shen et al., 2005). We found that the heavy metal/loid concentrations of soils from several sites (43, 146, 25F and 25R) within LSP were much higher compared to an uncontaminated reference site, Hutcheson Memorial Forest (HMF). HMF has similar metal/loid concentrations compared to northeastern NJ (“urban Piedmont”) soils (Sanders 2003). We also found that all the sites within LSP 25R contained PAHs. A further investigation of the extracted aromatic fraction determined that 25R had a similar fingerprint of PAHs compared to the other sites. It was possible the concentration of the organic compounds, specifically PAHs, could explain the lack of vegetation. However, the extract yields from 25R were much lower compared to the other LSP sites which implies that the organic compounds present in 25R are not responsible low soil function compared to the other sites at LSP.

The PAHs in the soil suggested fossil fuel contamination, which is not surprising since LSP was once a rail yard. We further investigated the coal particles, which can potentially introduce PAHs into the soil. The PAHs, which pose concerns to the vegetation and microorganisms, might not be bioavailable. Most of the coal present in LSP are anthracite and higher rank (medium volatile) bituminous, which was revealed by optical microscopy analyses.

It has been found that extractable PAH content decreases with increasing coal rank (Stout and Emsbo-Mattingly, 2008; Laumann et al., 2011). The hand selected coals from site 43 support these findings, where the anthracite coal consisted of primarily of alkylated benzenes, while bituminous coal consisted of both alkylated benzenes and a variety of PAHs. Bituminous coals are less abundant at LSP compared to anthracite, so there is a reduced environmental concern.

We found that sites 25F and 25R, which are adjacent to each other had some metals (Na, Co, Cu, Zn, As, and Pb) were about 2-5 times higher compared to an adjacent vegetated site, 25F. The differences in heavy metal concentration are not the only differences between sites 25F and 25R. Soils from site 25F have higher organic matter and moisture content compared to 25R soils. By mixing 25F and 25R in different proportions, an experimental gradient was created. After autoclaving these different soil mixtures, both the moisture and organic matter content were proportionate to the ratio of the two soils. Introducing communities from 25F soil, which is highly-functioning soil, into an experimental gradient of increasing ratios of 25R provided some insights into a possible reason why 25R is poorly-functioning. The abiotic factors present in the soil were found to adversely affect phosphatase, cellobiohydrolase and peroxidase activities of the inoculated soils. The microbial communities of the introduced microbial community (25F) were also altered by abiotic factors systematically across the gradient, where some fungal classes increased while others decreased.

A previous study found that by growing plants in the poorly-functioning 25R soil that enzyme activity increased over time (Vaidya et al., 2020). Artificial root exudates mimic the low molecular weight compounds that are the excreted by plants (Cite). The phosphatase activity at site 25R is below our limit of detection, yet there are measurable bacterial counts, which indicate the presence of bacteria. If these microbes in 25R soils are present but lying dormant, perhaps

by adding different combinations of artificial root exudates will revive some of the microbes and subsequently improve overall soil function. We found that not all enzyme activities studied (phosphatase, cellobiohydrolase, L-leucine aminopeptidase) responded the same. Phosphatase activity increased the most for any combination of artificial exudate compared to cellobiohydrolase or L-leucine aminopeptidase. For a given enzyme, it depended on the specific artificial exudates combination that was added, for example when the combination of exudates includes amino acids then L-leucine aminopeptidase activity increases. Determining the optimal combination of artificial exudates added to the soil suggests a potential strategy that can be used to improve soil function of other poorly-functioning contaminated soils. Similar studies of the impact of artificial exudate combinations added to contaminated soils from other brownfield sites would be interesting.

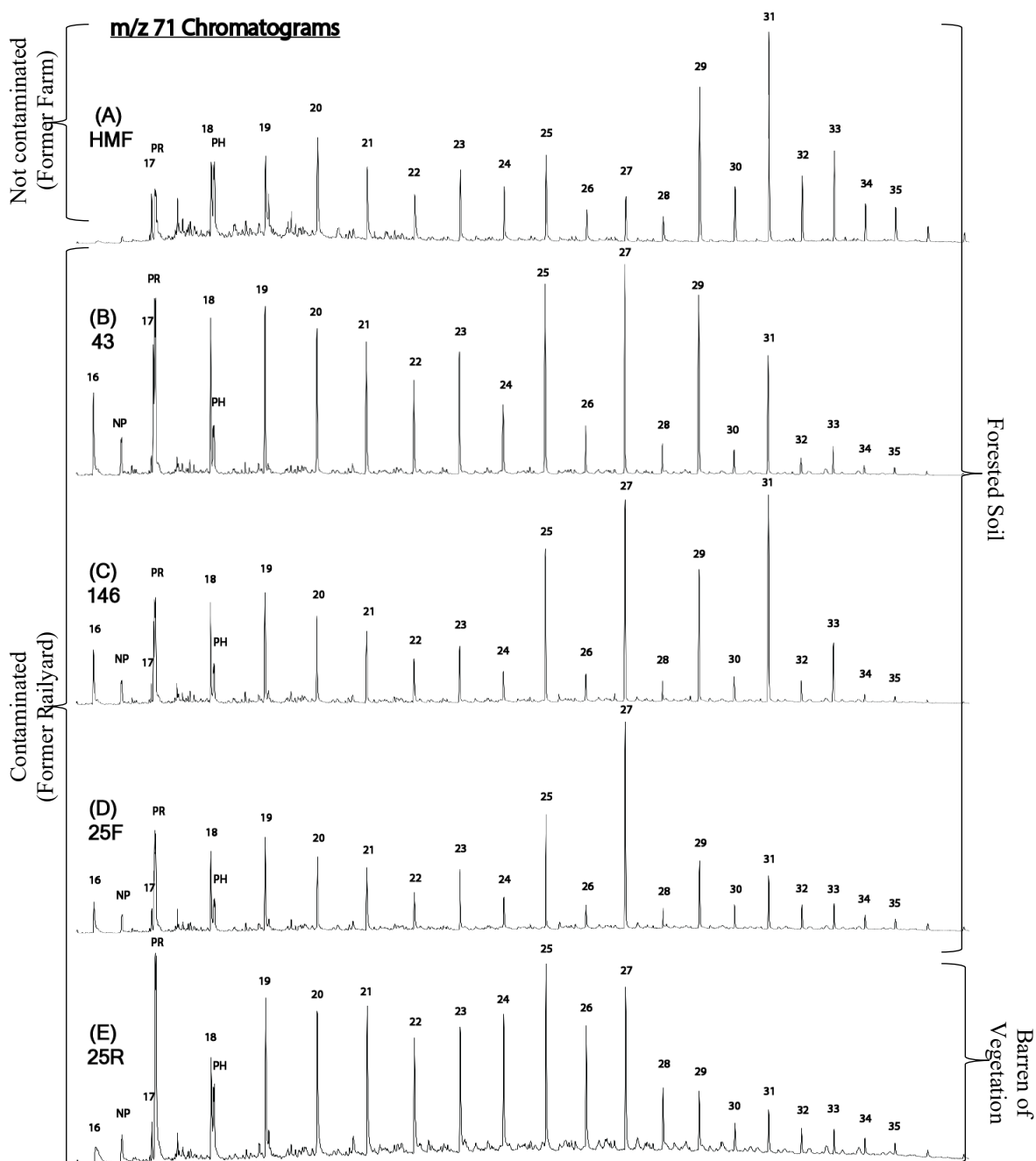
Improving soil function as a step towards remediation, including allowing plants to flourish, involves exploring different strategies, which is especially beneficial for barren soils. Plants can help remove (phytoextraction) or stabilize (phytostabilization) the contaminants within the soil (Cheraghi et al., 2011; Yang et al., 2014). One of these strategies examined in this dissertation showed that the introduced microorganisms from a highly functioning soil (25F) did not fully establish in the barren 25R soil. Thus, while introducing presumably beneficial microorganisms into the soil could improve soil function. Instead, we found that they failed to establish and improve soil function in the barren soil. Another strategy includes adding certain combinations of artificial exudates, which seems to improve soil function at least over a short duration.

### References

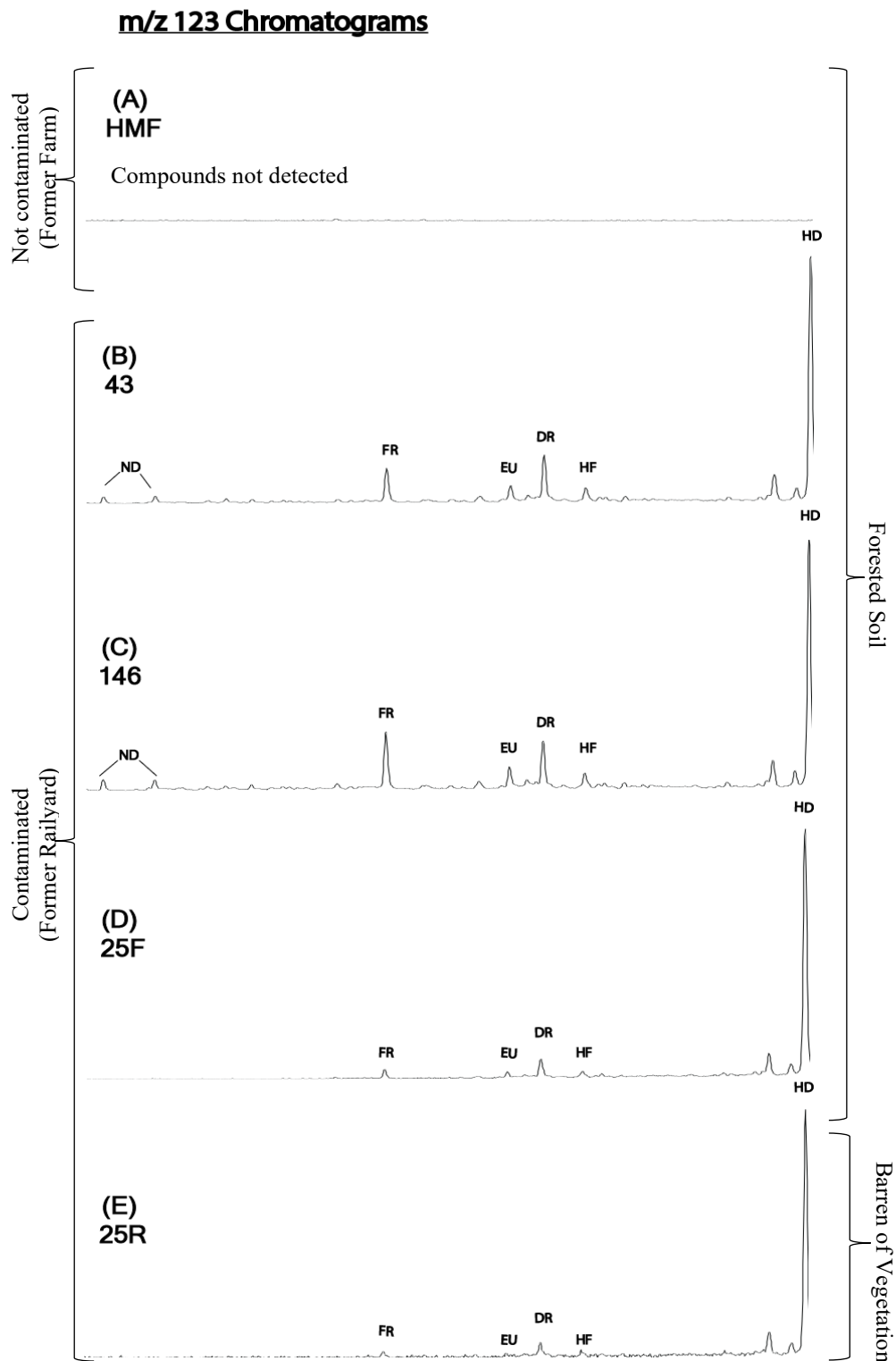
- Cheraghi, M., Lorestani, B., Khorasani, N., Yousefi, N., & Karami, M. (2011). Findings on the phytoextraction and phytostabilization of soils contaminated with heavy metals. *Biological Trace Element Research*, *144*(1), 1133-1141.
- Laumann S., Micić V., Krüge M.A., Achten C., Sachsenhofer R.F., Schwarzbauer J., et al., 2011. Variations in concentrations and compositions of polycyclic aromatic hydrocarbons (PAHs) in coals related to the coal rank and origin. *Environ. Pollut.*; *159*: 2690-2697.
- Maliszewska-Kordybach B., Smreczak B., 2003. Habitat function of agricultural soils as affected by heavy metals and polycyclic aromatic hydrocarbons contamination. *Environ. Int.*; *28*: 719-728.
- Sanders P.F., 2003. Ambient levels of metals in New Jersey soils. Environmental Assessment and Risk Analysis Element Research Project Summary. New Jersey Dept. of Environmental Protection, Division of Science, Research & Technology, Trenton, N.J.
- Shen, G., Lu, Y., Zhou, Q., & Hong, J. (2005). Interaction of polycyclic aromatic hydrocarbons and heavy metals on soil enzyme. *Chemosphere*, *61*(8), 1175-1182.
- Stout S.A., Emsbo-Mattingly S.D., 2008. Concentration and character of PAHs and other hydrocarbons in coals of varying rank – Implications for environmental studies of soils and sediments containing particulate coal. *Org. Geochem.*; *39*: 801-819.
- Vaidya B.P., Hagmann D.F., Balacco J., Passchier S., Krumins J.A., Goodey N.M., 2020. Plants mitigate restrictions to phosphatase activity in metal contaminated soils. *Environ. Pollut.*: 114801.
- Yang, S., Liang, S., Yi, L., Xu, B., Cao, J., Guo, Y., & Zhou, Y. (2014). Heavy metal accumulation and phytostabilization potential of dominant plant species growing on

manganese mine tailings. *Frontiers of Environmental Science & Engineering*, 8(3), 394-404.

## APPENDIX-A

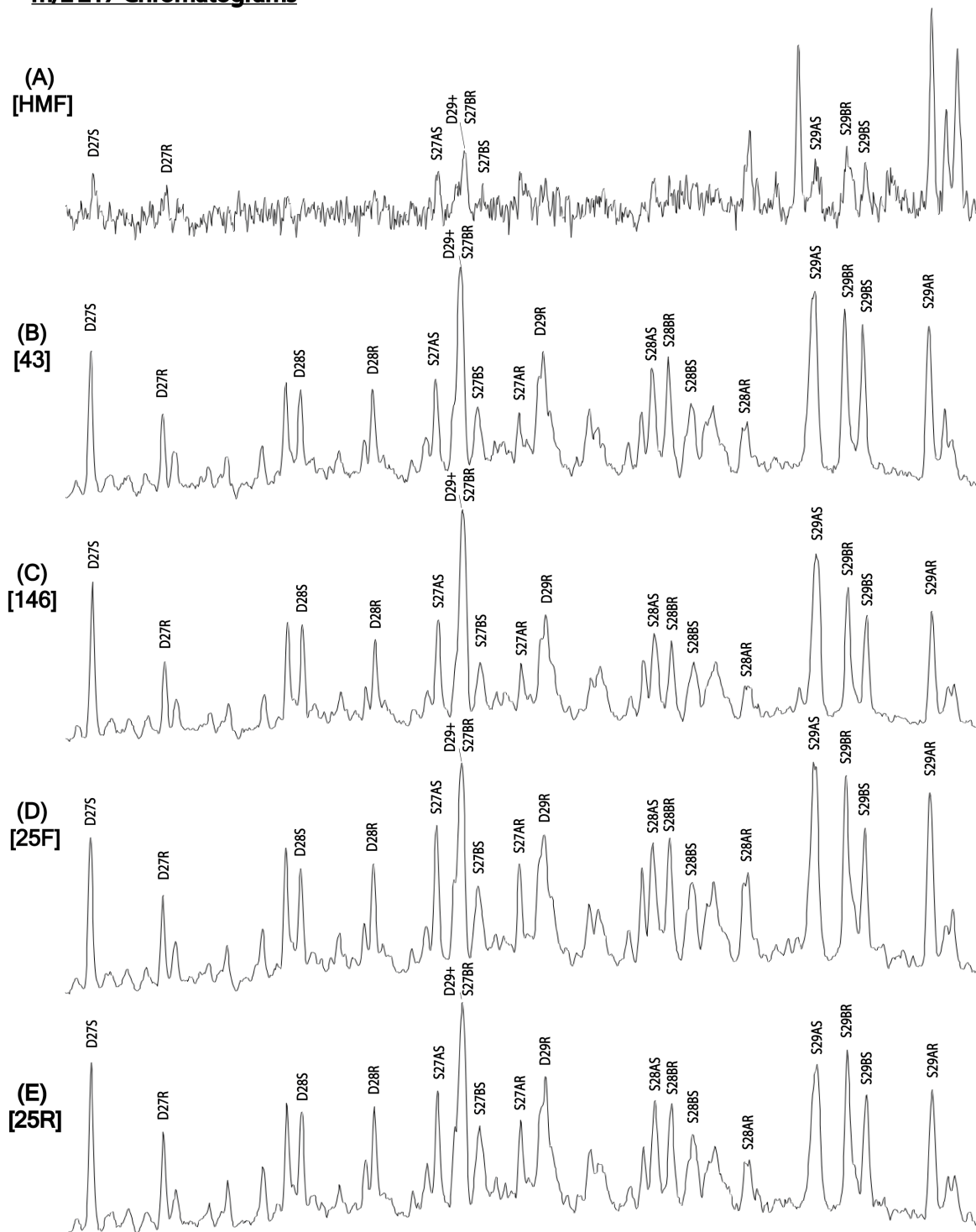


**Appendix-A Figure A1.** Mass chromatograph (m/z 71) for all five samples (HMF, 146, 43, 25F, 25R), showing extracted normal alkanes with some isoprenoid compounds. See Table 2-1 for compound symbols.



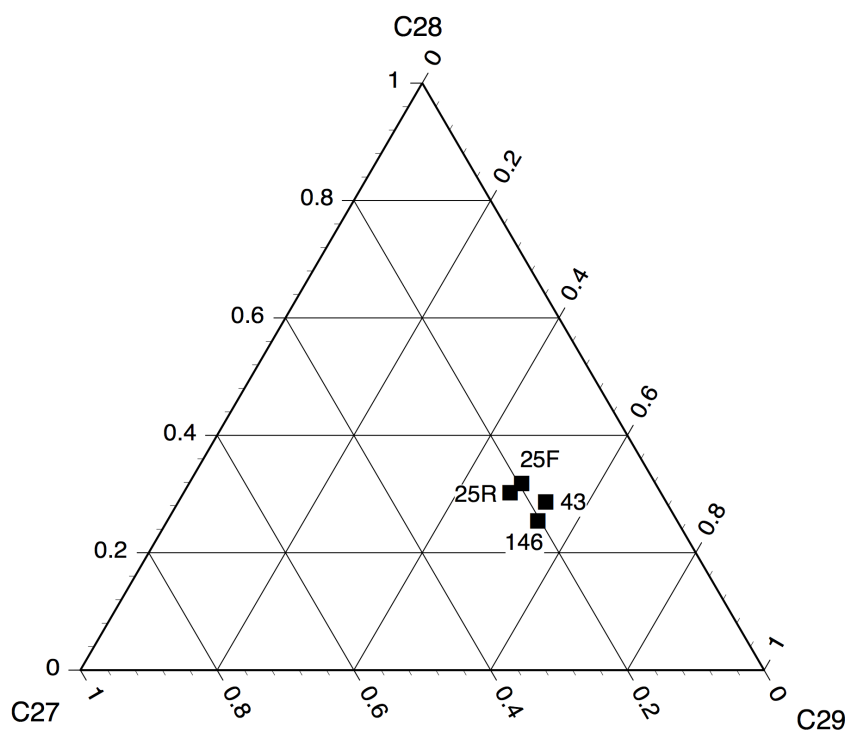
**Appendix-A Figure A2.** Mass chromatogram (m/z 123), showing sesquiterpanes in all sample sites (HMF, 146, 43, 25F, and 25R); an indication of fossilized higher plant biomass. They are

bicyclic compounds and the building components for triterpenoids. The compound symbols are as follows: nor-drimane (ND), farnesane (FR), 4A(H)-eudesmane (EU), 8B(H)-drimane (DR), homofarnesane (HF), 8B(H)-homodrimane (HD). Sesquiterpanes were not detected in HMF.

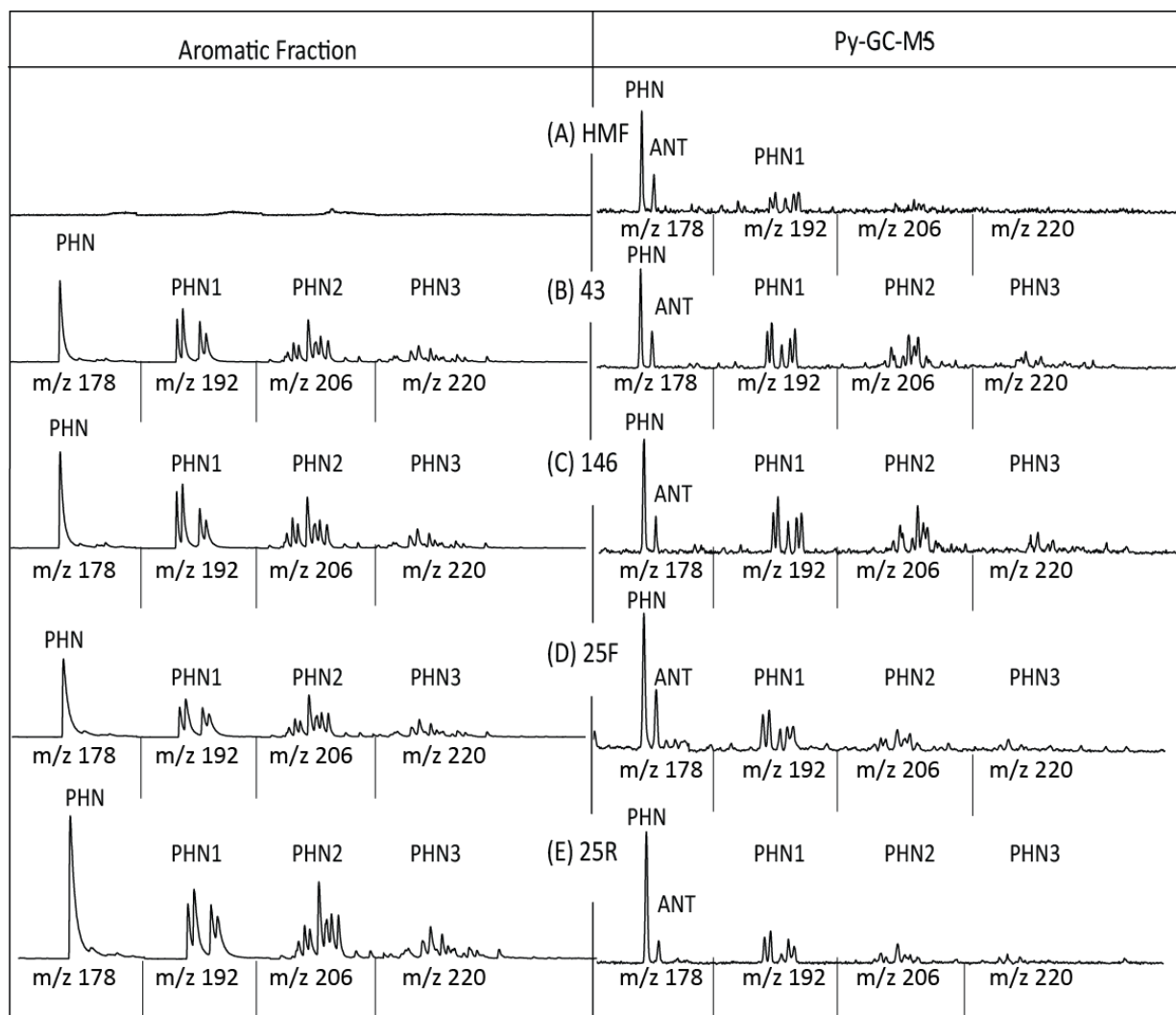
**m/z 217 Chromatograms**

**Appendix-A Figure A3.** Mass chromatogram ( $m/z$  217), showing steranes, which are indicators of fossil fuels in sample sites (HMF, 146, 43, 25F, and 25R). The compound symbols are as follows:  $C_{28}$  20S-13 $\beta$ (H),17 $\alpha$ (H)-diasterane (D28S),  $C_{28}$  20R-13 $\beta$ (H),17 $\alpha$ (H)-diasterane (D28R),

C<sub>27</sub> 20*S*-5α(H),14α(H),17α(H)-cholestane (S27AS), C<sub>29</sub> 20*S*-13β(H),17α(H)-diasterane (D29+), C<sub>27</sub> 20*R*-5α(H),14β(H),17β(H)-cholestane (S27BR), C<sub>27</sub> 20*S*-5α(H),14β(H),17β(H)-cholestane (S27BS), C<sub>27</sub> 20*R*-5α(H),14α(H),17α(H)-cholestane (S27AR), C<sub>29</sub> 20*R*-13β(H),17α(H)-diasterane (D29R), C<sub>28</sub> 20*S*-5α(H),14α(H),17α(H)-ergostane (S28AS), C<sub>28</sub> 20*R*-5α(H),14β(H),17β(H)-ergostane (S28BR), C<sub>28</sub> 20*S*-5α(H),14β(H),17β(H)-ergostane (S28BS), C<sub>28</sub> 20*R*-5α(H),14α(H),17α(H)-ergostane (S28AR), C<sub>29</sub> 20*S*-5α(H),14α(H),17α(H)-stigmastane (S29AS), C<sub>29</sub> 20*R*-5α(H),14β(H),17β(H)-stigmastane (S29BR), C<sub>29</sub> 20*S*-5α(H),14β(H),17β(H)-stigmastane (S29BS), C<sub>29</sub> 20*R*-5α(H),14α(H),17α(H)-stigmastane (S29AR).



**Appendix-A Figure S4.** Ternary diagram showing the relative abundance of C<sub>27</sub>, C<sub>28</sub>, and C<sub>29</sub> regular steranes in Fraction 1 of LSP sites 43, 146, 25F and 25R.



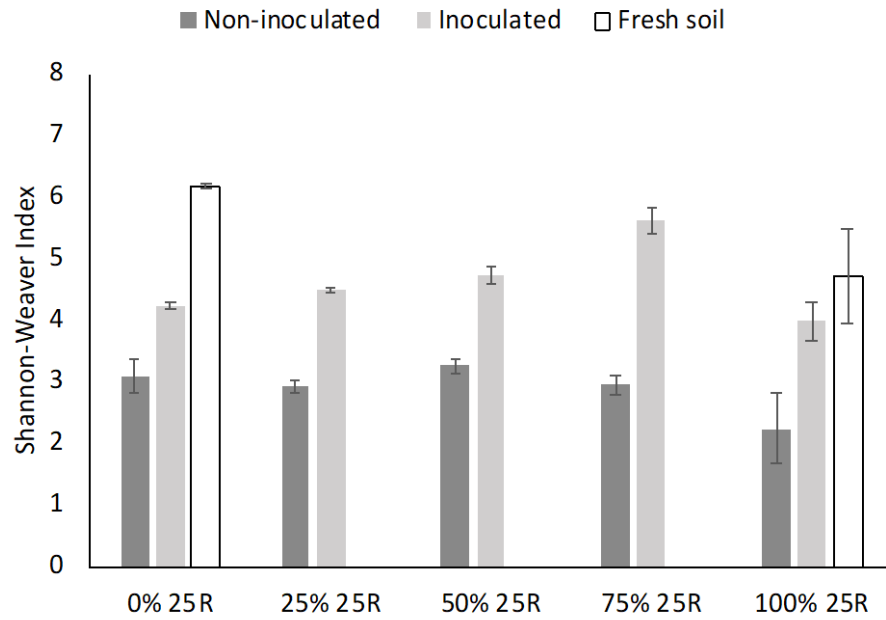
**Appendix-A Figure S5.** Mass chromatograms ( $m/z$  178, 192, 206, 220) showing the distribution of phenanthrene and methylated phenanthrenes in the aromatic fractions (on left) and Py-GC-MS (on right) of soil samples from HMF and LSP sites 43, 146, 25F and 25R. See Table 1 for compound symbols.

	43	146	25F	25R	HMF	Urban NJ Piedmont
mg/kg	Average $\pm$ standard error	Median				
Li	7.7 $\pm$ 0.8	5.4 $\pm$ 0.7	24.1 $\pm$ 4.07	40.7 $\pm$ 12.4	23.8 $\pm$ 0.6	
Na	99 $\pm$ 8	218 $\pm$ 12	873 $\pm$ 129	4393 $\pm$ 669	47 $\pm$ 3	90.1
Mg	1240 $\pm$ 129	1477 $\pm$ 106	3132 $\pm$ 411	6213 $\pm$ 1819	3153 $\pm$ 60	2190
Al	4980 $\pm$ 325	5563 $\pm$ 1195	16132 $\pm$ 1519	20470 $\pm$ 4194	20527 $\pm$ 249	10500
P	429 $\pm$ 17	690 $\pm$ 14	684 $\pm$ 14	789 $\pm$ 49	534 $\pm$ 48	
K	839 $\pm$ 80	686 $\pm$ 16	1737 $\pm$ 113	2697 $\pm$ 404	1927 $\pm$ 78	693
Ca	1948 $\pm$ 164	4065 $\pm$ 775	8228 $\pm$ 1402	10068 $\pm$ 1685	1542 $\pm$ 107	1425
Sc	2.06 $\pm$ 0.13	2.82 $\pm$ 0.25	2.40 $\pm$ 0.24	3.43 $\pm$ 0.48	3.06 $\pm$ 0.02	
V	32.9 $\pm$ 0.9	164 $\pm$ 8.3	70.7 $\pm$ 9.5	77.3 $\pm$ 11.8	30.1 $\pm$ 0.1	29.6
Cr	24.8 $\pm$ 0.7	118.0 $\pm$ 2.1	79.2 $\pm$ 3.2	165.2 $\pm$ 21.7	21.0 $\pm$ 0.3	18.5
Mn	159 $\pm$ 10	127 $\pm$ 4	460 $\pm$ 32	1042 $\pm$ 141	674 $\pm$ 56	311
Fe	34061 $\pm$ 1819	17520 $\pm$ 1491	179062 $\pm$ 22211	266653 $\pm$ 59863	18722 $\pm$ 1540	14600
Co	5.5 $\pm$ 0.4	6.2 $\pm$ 0.3	256.5 $\pm$ 46.5	868.7 $\pm$ 178.8	6.0 $\pm$ 0.1	6.3
Ni	21.1 $\pm$ 1.4	46.7 $\pm$ 0.9	121.4 $\pm$ 13.8	317.4 $\pm$ 62.5	18.5 $\pm$ 0.3	12.4
Cu	79 $\pm$ 4	93 $\pm$ 3	2256 $\pm$ 320	7165 $\pm$ 1512	18 $\pm$ 2	29.5
Zn	89 $\pm$ 4	180 $\pm$ 24	14435 $\pm$ 2845	41271 $\pm$ 8526	78 $\pm$ 4	75.3
As	17.8 $\pm$ 1.0	37.4 $\pm$ 4.5	630 $\pm$ 187	1162 $\pm$ 207	5.3 $\pm$ 0.1	5.2
Mo	3.5 $\pm$ 0.1	4.7 $\pm$ 0.4	29.3 $\pm$ 1.6	63.1 $\pm$ 10.1	1.6 $\pm$ 0.1	
Ag	0.42 $\pm$ 0.02	0.97 $\pm$ 0.01	3.80 $\pm$ 0.07	7.04 $\pm$ 0.79	0.58 $\pm$ 0.01	< D.L.
Cd	0.20 $\pm$ 0.01	0.63 $\pm$ 0.06	3.88 $\pm$ 0.63	7.74 $\pm$	0.30 $\pm$ 0.02	< D.L.
Ba	88 $\pm$ 3	181 $\pm$ 15	533 $\pm$ 53	1467 $\pm$ 267	139 $\pm$ 4	80.6
Pb	215 $\pm$ 9	355 $\pm$ 18	7145 $\pm$ 1351	20302 $\pm$ 4203	28 $\pm$ 1	111

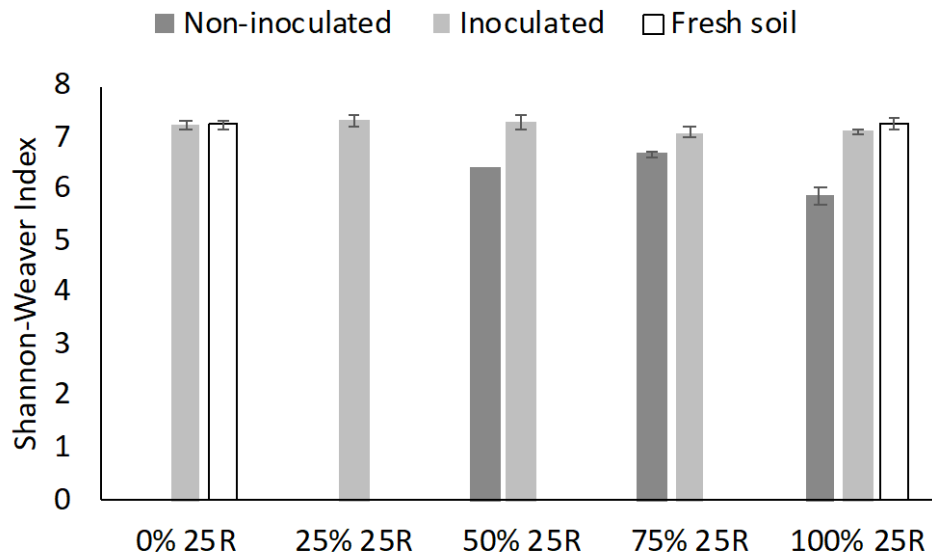
**Appendix-A Table A1.** Concentrations ( $\mu\text{g/g}$ ) of elements listed in order of atomic weight for the average of HMF, 43, 146, 25F and 25R of three replicates. ( $1 \pm \text{S.E.}$ ). Urban NJ Piedmont is

from Sanders 2003, where values indicated are the median concentration (mg/kg). < D.L. is below detection limit, which is Ag = 0.2 and Cd = 0.4 mg/kg.

## APPENDIX-B

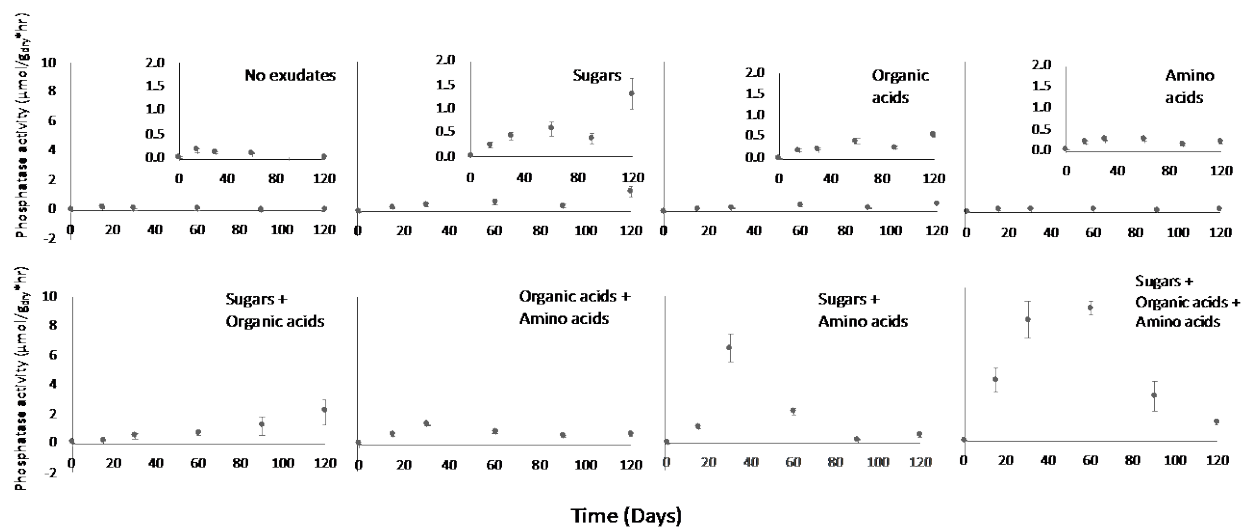


**Appendix-B Figure A1.** Shannon-Weaver diversity index of Fungal genus. Bars represent the average of three replicates ( $n = 3$ ) with standard errors shown.

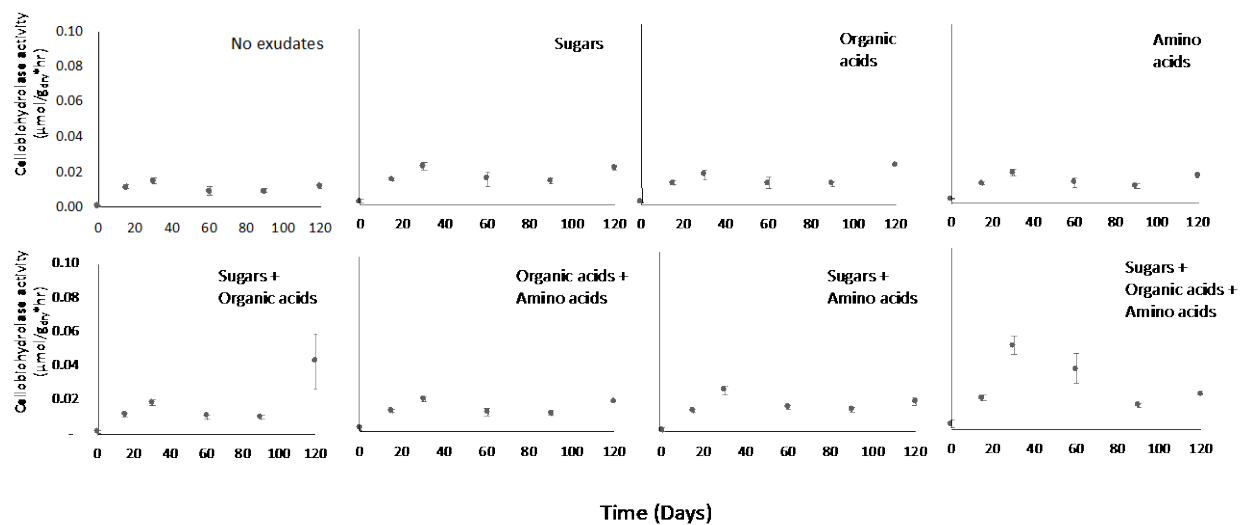


**Appendix-B Figure A2.** Shannon-Weaver diversity index of Bacterial genus. Data is missing due to low reads. Bars represent the average of three replicates ( $n = 3$ ) with standard errors shown.

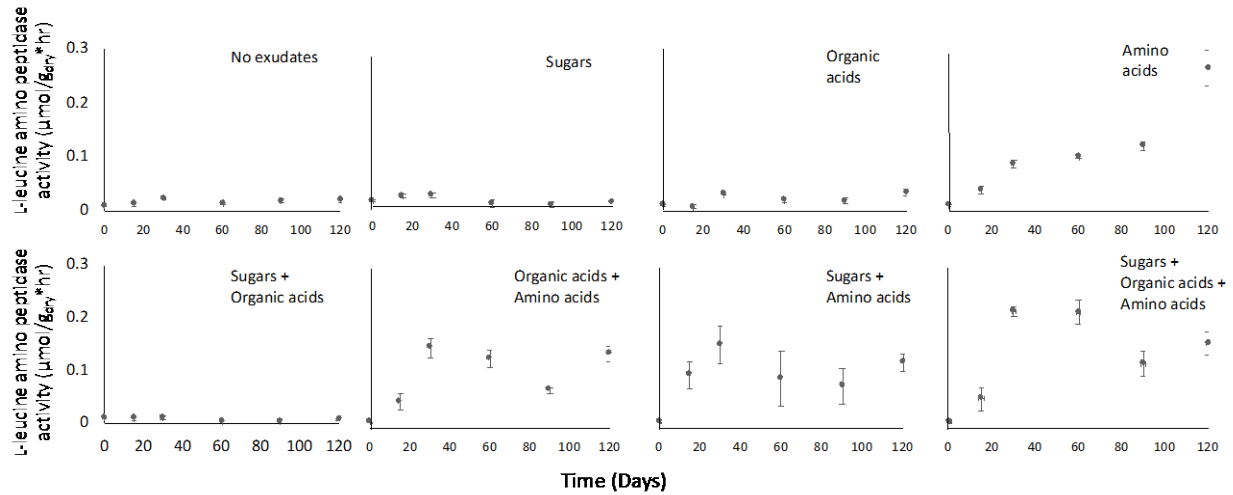
## APPENDIX-C



**Appendix-C Fig. A1.** Phosphatase activity ( $\mu\text{mol} \cdot \text{g}_{\text{dry}}^{-1} \cdot \text{hr}^{-1}$ ) of LSP 25R soil for the different combinations of exudates and the control, where no exudates were added. Phosphatase activities were measured at days 1, 15, 30, 60 and 90.



**Appendix-C. Fig. A2.** Cellobiohydrolase activity ( $\mu\text{mol} \cdot \text{g}_{\text{dry}}^{-1} \cdot \text{hr}^{-1}$ ) of LSP 25R soil for the different combinations of exudates and the control, where no exudates were added. Cellobiohydrolase activities were measured at days 1, 15, 30, and 60.



**Appendix-C Fig. A3.** L-leucine aminopeptidase activity ( $\mu\text{mol} \cdot \text{g}_{\text{dry}}^{-1} \cdot \text{hr}^{-1}$ ) of LSP 25R soil for the different combinations of exudates and the control, where no exudates were added. L-leucine aminopeptidase activities were measured at days 1, 15, 30, and 90.